TÉCNICO LISBOA

A comparative study of Geostatistical History Matching of Watt Field Reservoir at Different Scales

Kelechi Wisdom Chukwuemeka

Thesis to obtain the Master of Science Degree in

Petroleum Engineering

Supervisor: Prof. Doutor Leonardo Azevedo Guerra Raposo Pereira

Examination Committee

Chairperson: Prof. Doutora Maria João Correia Colunas Pereira

Supervisor: Prof. Doutor Leonardo Azevedo Guerra Raposo Pereira

Members of Committee: Prof. Doutor Gustavo André Paneiro

November 2019

Declaration

I declare that this document is an original work of my own authorship and that it fulfils all the requirements of the Code of Conduct and Good Practices of the Universidade de Lisboa.

Acknowledgements

Firstly, I would like to thank God for His guidance and protection throughout the period of undertaking this work.

Secondly, I express my gratitude to Professor Leonardo Azevedo for the immense supervision of this work. Your patience and guidance through this work, has been a great help to me. Your time spent on this thesis have gone a long way to add quality to it.

I want to thank to CERENA for the support and working conditions as well as to providing the necessary data sets to test and implement this thesis algorithm.

I also would like to thank to IST MSc students and PhD students for making this journey easier, encouraging me and being next to me in difficult moments of study, work and fun. Thank you

Finally, I would like to appreciate my parents, my siblings and my friends for their support throughout my master degree program.

Abstract

In the petroleum industry, field development decisions are based on three-dimensional reservoir models. These reservoir models in turn depend on a good history match between observed and simulated production to forecast reservoirs' behavior. Human knowledge of any reservoir is limited and as a result proposed models have large uncertainties. During production, observations from reservoir like production rate, bottom hole pressure provide us crucial information about the subsurface fluid flow. History matching aims to model the reservoir properties by perturbing model parameters and then use these updated models to predict future behaviour of reservoir. This thesis compares geostatistical history matching of a semi synthetic reservoir - the Watt Field – at two scales. Stochastic sequential simulation and co-simulation were used as model perturbation technique. An upscaling procedure was also carried out on the reservoir to have different grids sizes so as to aid comparison. The upscaling showed good results which was validated by production curves after flow simulation. The results from geostatistical history matching, showed that the fine scale produced a better match quality over the coarse scale. It represented the general pattern more than the coarse scale and had more production curves closer to the history data than the coarse scale. One disadvantage of the fine scale is the computational processing time which took 39h11m as compared to the coarse scale which was 09h17m.

Keywords

History Matching, Geostatistics, Direct Sequential Simulation, Upscaling.

Resumo

Na indústria petrolífera, as decisões de desenvolvimento de campo são baseadas em modelos tridimensionais de reservatórios. Esses modelos, por sua vez, dependem de uma boa correspondência histórica entre a produção observada e a simulação para prever o comportamento dos reservatórios. O conhecimento humano de qualquer reservatório é limitado e, como resultado, os modelos propostos apresentam grandes incertezas. Durante a produção, as observações do reservatório fornecem informações cruciais sobre o fluxo de fluido subterrâneo. A correspondência do histórico visa modelar as propriedades do reservatório perturbando os parâmetros do modelo e, em seguida, usar esses modelos atualizados para prever o comportamento futuro do reservatório. Esta tese compara a correspondência geoestatística da história de um reservatório semi-sintético - o Campo Watt - em duas escalas. Simulação sequencial estocástica e co-simulação, estas foram utilizadas como técnica de perturbação do modelo. Também foi realizado um procedimento de aumento de escala no reservatório para ter diferentes tamanhos de grades, a fim de ajudar na comparação. O upscaling mostrou bons resultados que foram validados pelas curvas de produção após a simulação do fluxo. Os resultados da correspondência da história geoestatística mostraram que a escala fina produzia uma melhor qualidade de correspondência em relação à escala grossa. Representava o padrão geral mais do que a escala grossa e tinha mais curvas de produção mais próximas dos dados do histórico do que a escala grossa. Uma desvantagem da escala fina é o tempo de processamento computacional que levou 39h11m em comparação com a escala grossa que foi 09h17m.

Palavras-chave

Correspondência de histórico, Geoestatística, Simulação eqüencial Direta, Upscaling.

Table of Contents

List of Figures

List of Tables

List of Acronyms

cdf – Cumulative Distribution Function

Co–DSS – Direct Sequential Co–Simulation

DSS – Direct Sequential Simulation

FOPR – Field Oil Production Rate

FOPT – Field Oil Production Total

FWPR – Field Water Production Rate

FPR – Field Average Pressure

GHM – Geostatistical History Matching

GRV – Gross Rock Volume

RFT- Repeat formation test

k – Permeability

M – Misfit Value

OWC – Oil Water Contact

WBHP – Well Bottom whole Pressure

WOPR – Well Oil Production Rate

WOC – Water oil Contact

WWPR – Well Water Production Rate

γ – Variogram

σ – Sigma

φ – Porosity

1. INTRODUCTION

1.1 Motivation

Oil and gas reservoirs are complex geological structures with uncertainties. These uncertainties most times arise from models being used without detailed knowledge of all-important parameters. When dealing with reservoir simulation, rock parameters, such as porosity or permeability, are very important, but are not well known. In almost every case, natural systems are way too complex to describe properly on a conceptual model level.

For many years, scientists have been studying and bringing up different methods to solve this ever-occurring problem. The methods are divided into two major groups. The first being the deterministic models and the other the stochastic models. Deterministic models work by claiming all processes, parameters, boundary and initial conditions to be known. As a result, deterministic models claim their results to be true, or assume that a single best prediction is sufficient. Stochastic models on the other hand, admit the inherent uncertainty, and hence provide a range of possible predictions, with probabilities assigned to them (Heimhuber, 2012). By assessing the uncertainty of these models it is possible to assess the risk level and consequently costs related with a given hydrocarbon reservoir, allowing better management decisions, such as the definition of the number and the location of new wells, the amount of existing oil and predict the economic return generated by the same (Caers, 2011; Azevedo, 2013).

The economic viability of oilfield development projects is greatly influenced by the reservoir's performance under the current and future operation conditions (Rwechungura et al., 2011). During the course of a field development, the information available increases over time. The well-log data, the rock core measurement among others, allow the estimation of the spatial distribution of the petrophysical properties in the near well-bore region as well as an indication of the reservoir productivity (Barrela, 2016). To achieve an efficient reservoir management process, it is essential to evaluate the past and present reservoir performance to forecast its future. A technique for handling this is *history matching*. History matching is the act of adjusting a model of a reservoir until it closely reproduces the past behavior of a reservoir. It is a phase in the modelling and simulation process and the main objective of history matching is to build reservoir models capable of predicting the future performance of the reservoir accurately.

Over the years, different methods have been proposed for history matching and extensive works have been carried out. This thesis is focused on comparing of geostatistical history matching at different scales. Here, coarse models will be generated from the fine scale and will be tuned to match the observed production data. This approach uses a Direct Sequential Simulation (DSS) as model perturbation technique (Mata-Lima, 2008). The method is applied to a semi-synthetic reservoir called "Watt Field" developed by the Herriot Watt Uncertainty Quantification Group (Arnold et al., 2013).

This thesis proposal is being developed from my internship at the CERENA (Centro de Recursos

Naturais e Ambiente), Instituto Superior Tecnico, Lisbon Portugal. It is a continuation of my Petroleum Engineering Internship from this semester, where I focused on upscaling the Watt field reservoir in order to carry out a geostatistical history matching. The simulation will be carried out and the differences between results will be observed and discussed and further works will be suggested.

1.2 Objectives

This thesis intends to address a relevant problem of the oil and gas industry related with reservoirs modelling and characterization:

- To assess how to upscale a reservoir model preserve the geologic conceptual model and the internal reservoir properties consistency;
- To use an iterative algorithm that integrates production data into stochastic models (permeability and porosity models), using Direct Sequential Simulation as convergence process for HM;
- To minimize petrophysical modifications (permeability, porosity) during the HM exercise;

1.3 Thesis Structure

This thesis comprises of five chapters:

Chapter one (1) introduces the thesis topic and the challenges addressed by this work. The reader will understand what the motivation behind the thesis is and the importance of the study in the industry.

Chapter two (2) is about the theoretical background and literature review of past and recent developments on history matching. Details about the concepts as well as algorithms used for this work are explained.

Chapter three (3) explains the method(s) used for the development of this work, providing details about the algorithms integrated to attain the thesis objective.

Chapter four (4) introduces the case study; the results and discusses them.

Chapter five (5) is the final chapter and discusses the main take away from the project. It will also introduces recommendations for further works.

2. LITERATURE REVIEW

This literature review begins with a brief discussion about history matching, upscaling, geostatistical history matching. These are the theories and methods in which this work was done.

2.1 History Matching

History matching can be defined as the process of conditioning reservoir simulation models to dynamic data (Aanonsen, 2005). The goal of history matching is to get better reservoir models, with simulation results closer to the observed data, so that future reservoir prediction based on these models are more reliable and accurate. It is a difficult and time-consuming process. For a model to be well matched, it should honour all data both static and dynamic, as well as be consistent with the priori geological knowledge (Aanonsen, 2006).

The importance of history matching during the development and management of a petroleum reservoir cannot be downplayed because these models are used to support the decision-making process. It also helps to characterize a reservoir more accurately.

History matching is mathematically defined as an inverse problem (Christie et al., 2006): we know the response of the system (production history such as flow rates and pressure) to a stimulus (production) but lack the knowledge of the variables that originate that response (parameters and descriptions of the reservoir model, such as the spatial distribution of permeability and porosity).

History matching methods require a solution of inverse problem to minimize the objective function. The main idea of the inverse problem is to find model parameters that best match to the production data. An inverse problem is said to be well-posed if stable and unique solution exists, else the problem is said to be ill-posed. Typically, history matching is an ill-posed problem for which non-unique solution exists. (Ibrahim, 2012)

The starting point for the history matching process will be formed when an acceptable characterized model is established. After the initial model is created, simulations will be done in order to perturb the model parameters to match the observed data. Table 1 shows commonly perturbed parameters during history matching process.

Table 1**:** Geological and engineering parameters commonly perturbed in history matching (Barrela, 2016)

Data Type	Data
Pore Volume	Volume Net- to-Gross (NTG) Porosity
Permeability or Transmissibility	Horizontal Vertical
Relative permeability	Curves End-points
Contact	Gas-oil contact (GOC) Oil-water contact (OWC)
Compartment	Gas-oil contact (GOC) Oil-water contact (OWC)
Fault	Location Transmissibility
Rock	compressibility
Saturation	Incredible water saturation Oil residual saturations
Aquifer	Size (affects Pore Volume) Strength (affects Permeability)

The manual history matching is a trial-and-error procedure. The production and development teams analyze the differences between simulated and observed data, such as gas-oil ratio, water cut, and bottom hole pressures, and make manual changes to the reservoir model in order to minimize the difference.

Automatic History Matching which is also called Assisted History Matching (AHM) is history matching process assisted by a computer. The computer logic adjusts the reservoir model parameters rather than humans. These algorithms are based on minimizing an objective function, such a quadratic function which measures the difference between observed and predicted measurements. The most common method to quantify an objective function is the least –square method:

$$O(m) = [g(m) - d_{obs}]^T [g(m) - d_{obs}], \quad (1)$$

where m is the model, g (m) the predicted data and d_{obs} the observed data.

Assisted history matching techniques have been proposed to use nonlinear optimization to minimize the objective function and produce the best least square fit of the historical observed data:

$$M = \sum_{t=1}^{T} \left(w(q^{obs} - q^{sim}) \right)_t^2 , \quad (2)$$

where T is number of observations, q^{sim} and q^{obs} are the simulated and observed data respectively

representing production rates, cumulative or pressure measurements from the reservoir, w is the weighting factor.

The main idea behind most history matching is to perturb the model parameter space following the next sequence of steps (Marques, 2015):

1. Knowing some data: Prior knowledge and observation from well (porosity, permeability), models from a reservoir model are created that try to describe the spatial distribution of the subsurface properties of interest;
2. Run a dynamic simulation in the previous models to obtain the simulated production history per existed well;
3. Compare the production data from this realization with the real historical production data through an objective function. The simulation that minimizes the objective function is accepted;
4. Create a perturbation in the initial model with the information obtained from the objective function and repeat all the previous steps until a minimum value to the objective function is achieved.

These steps are represented in the general framework below.

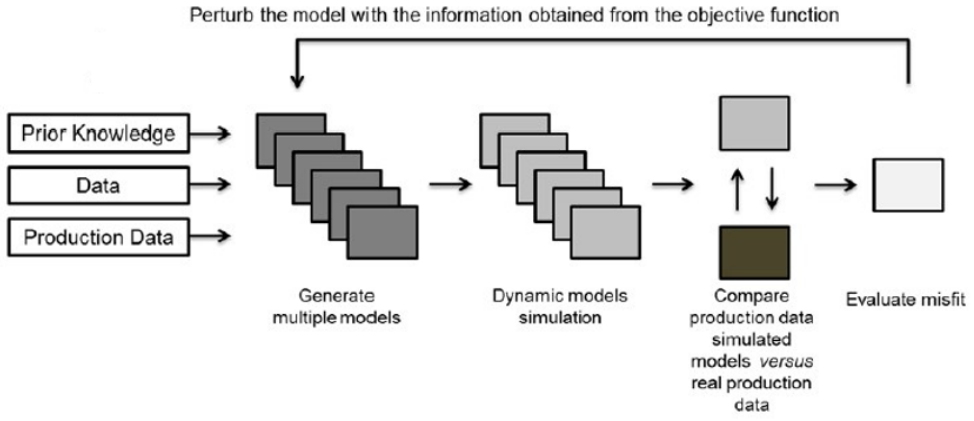

Figure 2.1: *History matching Framework (Adapted from Marques, 2015)*

During any kind of model calibration process such as this, it is important to note that

- Reservoir models are models, not reality. There are inevitable errors and approximations that: are found in any model of physical phenomena.
- The history matching process is undertaken for the purpose of decision making. History matching serves no purpose on its own.
- The model input is uncertain, and the uncertainty is almost always underestimated.
- The observable data always contains errors, however small.

2.2 Upscaling

Geological and reservoir simulation plays an important role in the design and development of oil fields. Geological models can reproduce the detailed structure of the oil fields and often contain several million cells. Therefore, calculations on the finite difference grids of geological models, even with modern computing facilities, take much time. One way to speed-up computations is to reduce the number of cells of the geological model by applying an upscaling procedure (Rodionov et al., 2012).

In reservoir simulation, the process of scaling up all properties (e.g., permeability, porosity, and fluid saturations) from a fine-grid system to equivalent properties to a coarse-grid system, such that the two systems act as most similarly as possible is defined as upscaling. Different upscaling techniques have been used to bridge the gap between these geological models and full-field reservoir simulation. The main idea of upscaling is to replace a number of heterogeneous fine grid blocks with one equivalent coarse homogeneous grid block. So, the essence of upscaling is averaging. (Qi and Hesketh 2005)

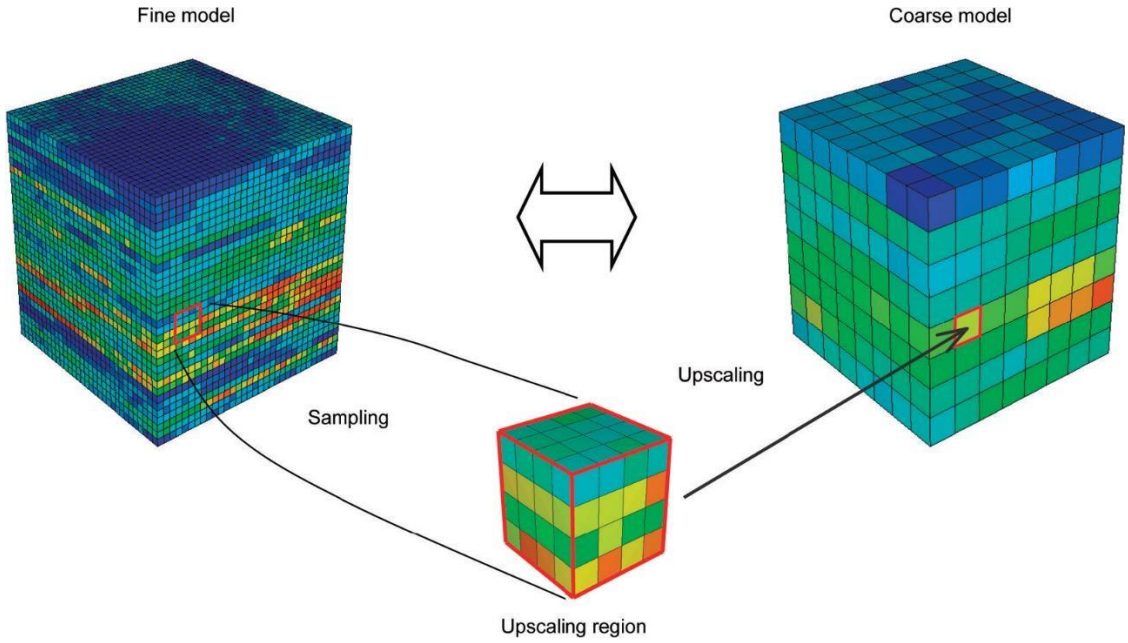

Figure 2.2**:** *Concept of upscaling (Upscaling of grid properties in reservoir simulation, 2013)*

There are different classifications methods for upscaling. Mansoori (1994) divided the upscaling methods into three types namely: numerical, analytical, and tensor. Li, (1995) made a classification of two classes, single-phase flow and multiphase flow which are dependent on different methods. Cristie, (1996) in his work provided 5 types of classification.

The most common and widely used upscaling technique is the analytical which is the power law average. This method uses average values to upscale permeability:

Arithmetic:
$$K_{arithm} = \frac{\sum_{i=1}^{n} K_i}{n}, \quad (3)$$

Geometric

$$K_{geom} = \left(\prod_{i=1}^{n} K_i \right)^{1/n}, \quad (4)$$

Or Harmonic

$$K_{harm} = n \left(\prod_{i=i}^{n} \frac{1}{K_i} \right)^{-1}, \quad (5)$$

where K_i is the permeability value of a grid block in the original grid, and the total number of grid blocks is *n.*

The average power *(w)* is constrained to lie between the upper and lower limits 1.0 and −1.0 corresponding to the arithmetic and harmonic average, respectively. The geometric average is found at $w = 0$.

The power-law averaging provides a scalar result. Although very efficient computationally, power-law averaging methods have some limitations. Specifically, the value of the power exponent is case-dependent and requires calibration.

Upscaling replaces a heterogeneous unit with an equivalent homogeneous one. As a consequence, some resultant information loss in upscaling is inevitable. The key issue is to optimize the upscaling technique and minimize the information loss. Among the main objectives of upscaling, Wang (2011) noted it is worthy to mention the following:

- ***Accuracy*****:** How accurate is the upscaling? Are the fine-scale flow behaviors from the initial model still maintained? Some of the behaviors include flow rates at given pressures and breakthrough times for fluids injection.
- ***Robustness:*** this refers to how independent the level of processing is. Can different flow processes be applied to the same coarse scale properties?
- ***Efficiency*****:** this involves the coarsening degree achieved by the upscaling algorithm. All upscaling techniques come with some costs; thus, the efficiency needs to be considered to ensure that the accuracy is not compromised.

2.3 Geostatistical History Matching

Geostatistical history matching methodologies use historical production data from well(s) to model the static properties of the reservoir.

Significant developments have taken place over the years as regards assisted history matching. (Hoffman and Caers 2003) proposed a regional perturbation method as an advancement on the global perturbation method.

Mata-lima (2008) developed a method of integrating fluid dynamic (production) data into the static model of reservoirs. He perturbed the permeability of the field model using direct sequential simulation and co-

simulation.

In 2013, (Maschio, et.,al) proposed a new frame work for geostatistical history matching using genetic algorithm with adaptive bounds. They showed the advantages of GA which included process speed up. In geostatistical history matching procedure, this perturbation step is performed with stochastic simulation and co-simulation in order to maintain the geological consistency and also honoring the wells and log data.

The convergence speed depends on the reservoir characterization that is done based on the hard data, logs and reservoir understanding, and the closer description to the real reservoir description, the more rapid convergence to the historical data match will be achieved (Gilman and Ozgen,2013). This highlight the importance of setting a solid understanding of the reservoir.

Caeiro et al., (2015) proposed a methodology that couples adaptive stochastic optimization and direct sequential simulation with local anisotropy correction as the basis of image transformation.

Marques, (2016) further developed the works of Mata-lima (2008) and proposed a multiscale geostatistical history matching using block-dss as way to speed-up the iterative process as well as the history matching procedure.

Nunes, et al., (2016) said the geological characteristics of the reservoir, porosity and permeability, are perturbed locally, using DSS and Co-DSS with multi-distribution functions and spatial continuity patterns and it is based on the method proposed by Mata-Lima (2008).

The main advantage of all the approaches above over traditional history matching is the simplicity of implementation and possibility of exploring different parameter perturbations.

3. METHODOLOGY AND WORKFLOW

The methodology for this work has been basically divided into two major stages. They are as follows:

1. Upscaling: Creation of the coarse model from the fine model using analytical method such as the Power law averaging to get the mean of fine grid properties and use it for the coarse grid properties: then, run a fluid flow simulation on the new upscaled grid to compare results from production data with the initial data;
2. Geostatistical history matching of the models (fine and coarse). The GHM methodology is based on the works of Mata-Lima (2008).

The model, a semi-synthetic case field was built borrowing reservoir conditions from an actual oil field in the North Sea. Due to the lack of real data, uncertainty is generated and propagated throughout the reservoir model (Arnold et al, 2013).

The dynamic flow simulation will be run in Schlumberger's Eclipse 300® and tNavigator® by Rock Flow Dynamics. A simplified schematic representation of the workflow described is presented in Figure 3.1.

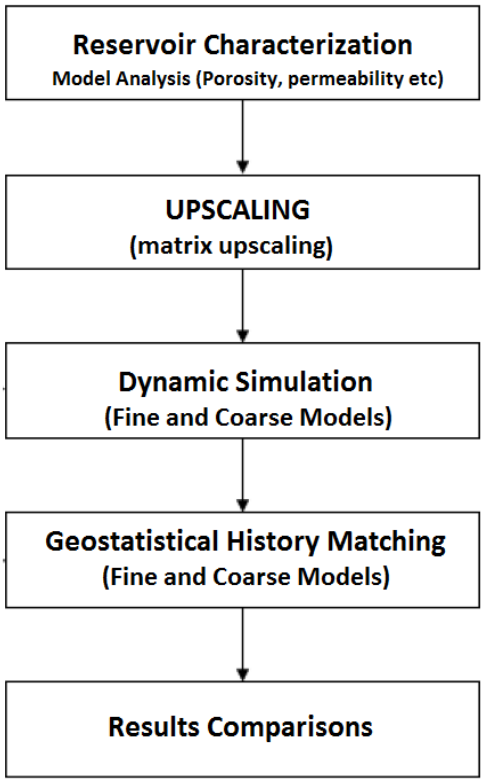

Figure 3.1: *A simplified schematic representation of the workflow used for the proposed methodology*

3.1 Upscaling workflow

The use of upscaling is of great benefit to reservoir engineers for simulating reservoir performance and optimizing oil recovery. An upscaled model can be used to identify the location of by-passed mobile oil for recompletion, placement of horizontal wells, infill drilling, and other sweep-improving measures (Qi et al., 2005)

Qi et al., (2005), divided upscaling into four stages generally.

1. Physical model investigation: to study and understand the features (heterogeneous and homogenous) of the geological model;
2. Up-gridding: to construct a coarse grid system that is compatible with the physical model;
3. Scaling up the properties: this is averaging of the heterogeneous properties.
4. Result qualification: this is to validate the results by a means of comparison.

Schlumberger's Petrel software was used in the upscaling. The sequence of steps are listed below for better understanding:

a. Firstly, import the reservoir data into the petrel software and convert to a petrel case.
b. Make Surfaces: using the horizons from the fine grid creates surface.
c. Define the fault Model using the fine model. This will ensure the faults in the fine model are also in the coarse model.
d. Pillar grid: This creates the new 3D grid. The pillar gridding option increases the size of I and J from 100m to the desired values for each block in this case 200m.
e. Next is to upscale the structure of the new grid. For this work, Arithmetic averaging was used.
f. Finally, scale up the properties.

The parameters from the flow simulation, which are used for comparison between fine and coarse grid are the field oil production total as well as rate, field average pressure, and water production rates and totals. The efficiency and accuracy of the upscaling will be validated by comparing the fuild flow simulation results obtained for the fine grid (reference model) and coarse grid.

3.2 Geostatistical History Matching Workflow

The geostatistical history matching applied under the scope of this thesis follows Marques (2015). The geostatistical history matching workflow is summarized in the following sequence of steps (Figure 3.2):

1. Create a set of stochastic models with equal probability of occurring from a reservoir property with DSS (simulate porosity then co-simulate permeability). This is conditioned to the well-log data and spatial continuity to ensure it honours the model:
2. Run a dynamic flow simulation to obtain the production history for each reservoir model simulation;

3. Evaluate the production data from the realizations with the real production data through an objective function. This objective function compares the values of each well at different times.
4. Repeat all steps again using the best composed imaged from iteration 1 as soft data and secondary variable. This continues until the minimum objective function is achieved or until the set of predefined iterations is reached.

This will be done with prior information that is, the well-log data (porosity and permeability) and the production data which will be used as reference in the misfit evaluation.

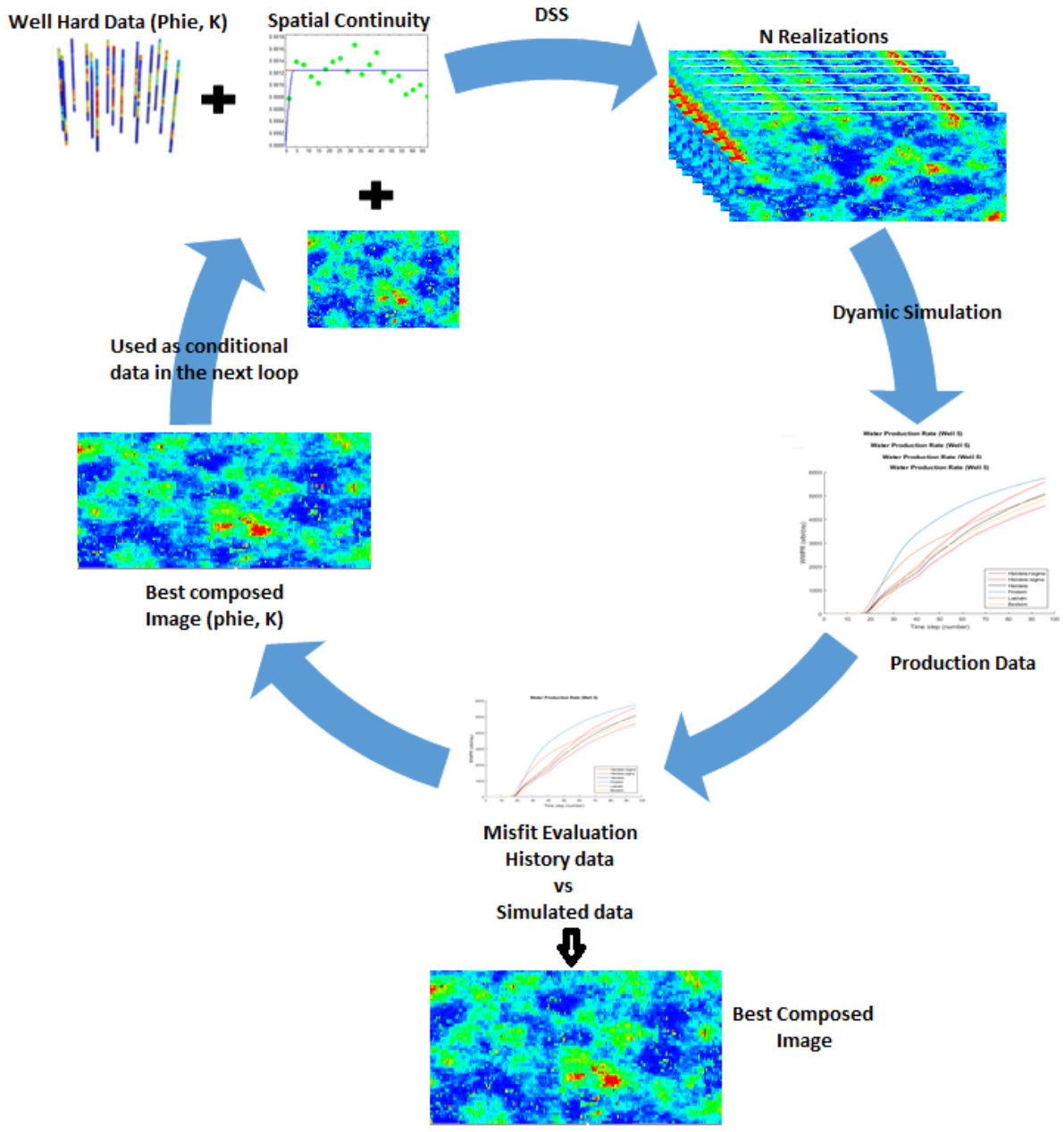

Figure 3.2: *Geostatistical history matching detailed workflow.*

This method allows us to generate multiple models. The difference between the historical production data and the simulated data decreases as the iterative process evolves and also the patterns of spatial continuity are seen in the simulated models.

3.3 Objective function and misfit value

Oliveira (2016), defined objective function as a mathematical expression that measures the match between the true observed production time and the production retrieved by the fluid flow simulation Objective function is usually the value that is minimized by the algorithm which finds a model that best fits the observed data (Christie et al., 2013).

The most applied objective function in history matching methods basis on a single number, the misfit or match quality (Mf), which is obtained by summing the least square misfits for all the quantities of interest in a history match:

$$Mf = \frac{1}{2}\sum_{t=0}^{n}\frac{(obs_t - sim_t)^2}{2{\sigma_t}^2}, \tag{6}$$

where t is the time, obs_t the observed or historical data (e.g. rate or pressure) at time t and sim_t the simulated results at time t. *n* refers to the number of measurements (the amount of time steps where the measurement was made) and σ_t the measurement error or standard deviation in the observed data.

For this thesis, a multi-variable objective function was used where different parameters are taken into account and when summed together performed as an objective function. This objective function is able to comprise targets with different scales by combining all the evaluated parameters (pressures, rates, etc.) and thereby obtaining an optimization problem which in practice is reduced to one variable:

$$Mf = \sum wells \sum wbhp, wopr, wwpr \frac{1}{2}\sum_{t=0}^{n}\frac{(obs_t - sim_t)^2}{2{\sigma_t}^2}, \tag{7}$$

Mata-Lima (2008) proposed a framework of regional (local) perturbation. Which is basically defining an area of influence for each producer well, and thereby establishing a match criterion for each area of influence, based on the dynamic performance of each well. One way is to choose areas of influence based on polygons which can convey the spatial patterns determined by the variograms. After each iteration, best porosity and permeability cube are created and the perturbation on properties, are conditioned to these cubes, as a secondary variable (soft data), through a correlation coefficient that is calculated based on the dynamic data evaluation. Voronoi polygons can be used to address this issue.

Figure 3.3 shows the zonation resulting from the voronoi partition and shows the existence of a zone for every group of well (group 1 to 9). Each color represents the area assigned to each production well.

After simulating each realization, a patch of best porosity and permeability is made, along with

composing their respective local correlation coefficient into a cube, which are responsible for strength of the geostatistical assimilation of properties into next iteration, considering local match quality.

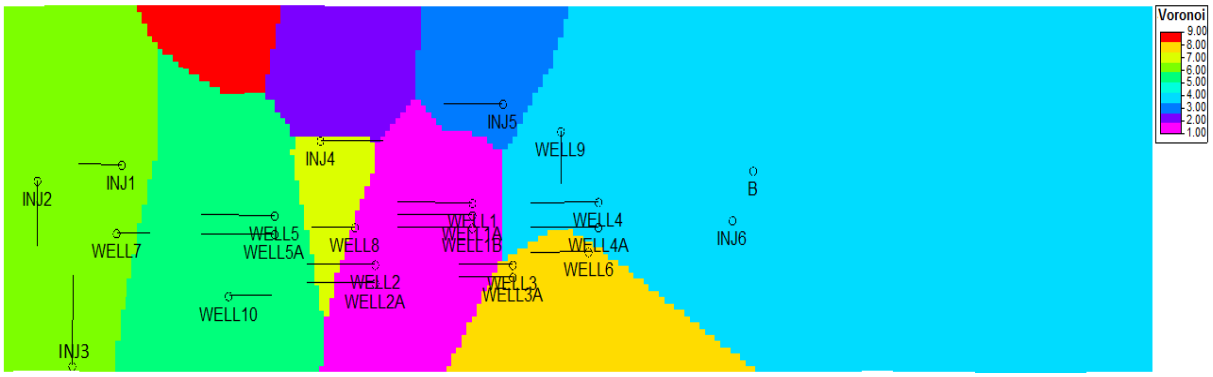

Figure 3.3: *Voronoi zonation pattern.*

4. CASE STUDY AND RESULTS

4.1 Data Set Description - Watt Field Reservoir

The Watt field reservoir was used as case study under the scope of this thesis. It is a semi-synthetic reservoir based on a mixture of real field and synthetic data to describe a realistic field example. It was developed by the Uncertainty Quantification Group of the Heriott – Watt University (Arnold *et al*., 2013).

The model spans across 12.5km by 2.5 km^2 surface area, in the East-West direction. It has a thickness of around 190m, much of which is below the oil water contact. The field is located around 1555m subsurface with an initial reservoir pressure of 2445psi as measured from repeat formation test and well test data. The OWC is identified from wireline and RFT data at a constant 1635m subsurface. The field development plan is also synthetic resulting in an artificial production response.

4.1.1 Petrophysical Properties

Permeability is one of the most influential factors for understanding fluid flow in porous media. The permeability is heterogeneous also with an average value of 526 mD in X and Y direction, while it is 52 mD in Z direction. Figure 4.1 shows the permeability distribution in the x direction of the Watt field reservoir model, Figure 4.2 shows the histogram and Table 2 shows basic statistics of permeability.

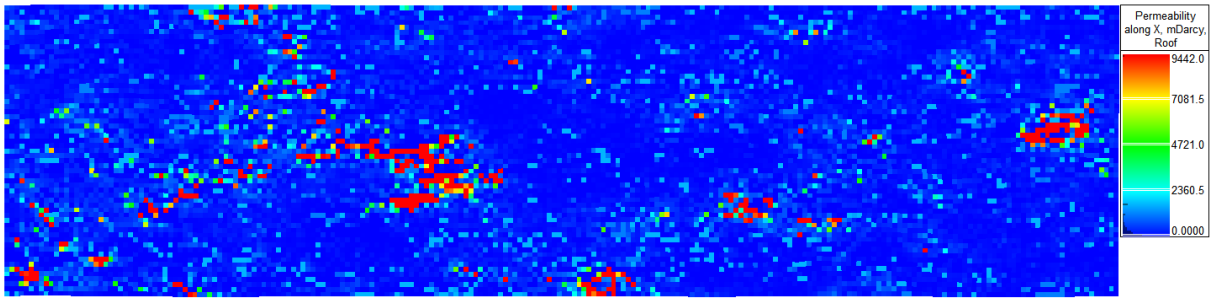

Figure 4.1: *2D view of permeability model*

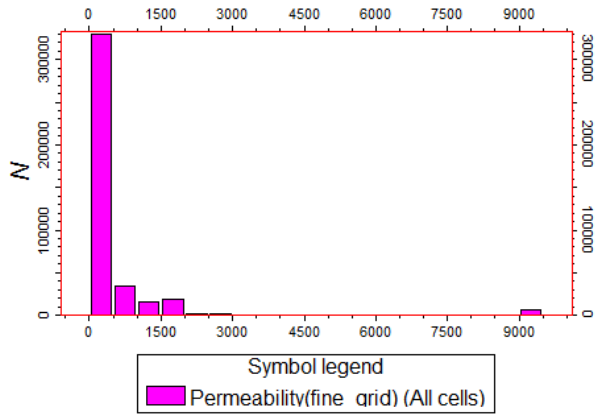

Figure 4.2: *Fine grid Permeability histogram*

Table 2: Permeability statistics of Watt Field

Property	Permeability
Mean	526.6
Standard deviation	1392.4
Minimum	0
Maximum	9442

The porosity distribution in the reservoir is heterogeneous with a mean value of 0.16. Figure 4.3 below shows the porosity distribution. Figure 4.4 shows the porosity histogram and Table 3 shows basic statistics of porosity.

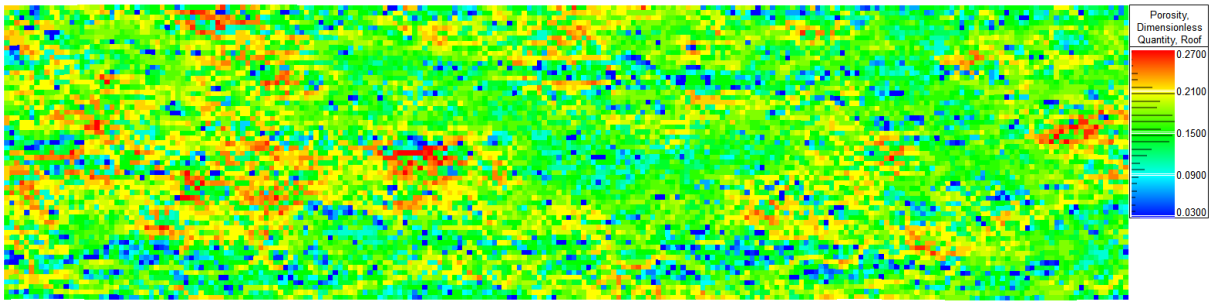

Figure 4.3: *2D view of porosity model. (High porosity regions are in orange-red)*

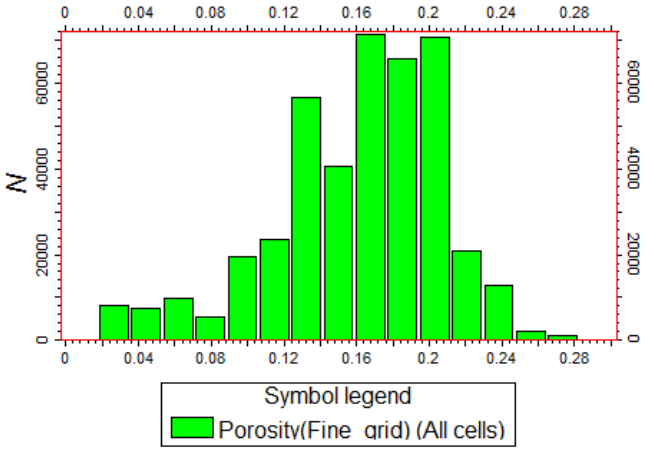

Figure 4.4: *Fine grid Porosity histogram*

Table 3**:** Porosity statistics of the Watt Field

Property	Porosity
Mean	0.1612
Standard Deviation	0.04621
Minimum	0.03
Maximum	0.27

4.1.2 Production Scheme

The available production history shows that the reservoir produced for an 8 year period (2903 days) approximately. The field was initially appraised through a set of 6 wells, Well A-F then further developed through a set of 16 producer wells which are horizontal and located across the central part of the reservoir. Also 7 injection wells, 5 horizontal and 2 vertical (one of which is a recompletion of Well B) were developed around the edges to help increase oil production by providing pressure. According to Arnold et al., (2013), these horizontal multi-lateral wells were selected to maximize the distance from the WOC due to the low relief of the field and increase oil production rates while reducing water production rates in the original development plan.

The production period started with drilling 7 wells (production) on the first day. 3 wells (production) were added after 6months. After 11months of production, 2 extra production wells were added. Another 2 wells (production) were added after 14 months. 1 more well (1production) was added 3months later. Finally, 1 last production well was added after 3 months and ran for further 73 months. This schedule sequence is shown in Table 4 below.

The tables below shows a list of the of all control data for all production wells as well as injection wells

Table 4: Control data for all production wells

Name of well	**Producer Type**	**Production start date**	**Control Mode**	**Flow Rate Target *(stb/day)***
WELL1	OIL and GAS	01/01/2011	Liq. Rate	8000
WELL1A	OIL and GAS	01/01/2011	Liq. Rate	8000
WELL1B	OIL and GAS	01/01/2011	Liq. Rate	8000
WELL2	OIL and GAS	07/11/2011	Liq. Rate	6500
WELL2A	OIL and GAS	07/11/2011	Liq. Rate	6500
WELL3	OIL and GAS	05/06/2011	Liq. Rate	8000
WELL3A	OIL and GAS	05/06/2011	Liq. Rate	8000
WELL4	OIL and GAS	01/01/2011	Liq. Rate	8000
WELL4A	OIL and GAS	01/01/2011	Liq. Rate	8000
WELL5	OIL and GAS	10/03/2012	Liq. Rate	8000
WELL5A	OIL and GAS	10/03/2012	Liq. Rate	8000
WELL6	OIL and GAS	01/01/2011	Liq. Rate	8000
WELL7	OIL and GAS	11/06/2012	Liq. Rate	8000
WELL8	OIL and GAS	05/06/2011	Liq. Rate	8000
WELL9	OIL and GAS	01/01/2011	Liq. Rate	6500
WELL10	OIL and GAS	12/09/2012	Liq. Rate	7000

Table 5: Control data for all injector wells

Name of well	Injector Type	Control Mode	Flow Rate *(stb/day)*	BHP *(psia)*
INJ1	WATER	Flow Rate	12500	3500
INJ2	WATER	Flow Rate	15000	3500
INJ3	WATER	Flow Rate	15000	3500
INJ4	WATER	Flow Rate	15000	3500
INJ5	WATER	Flow Rate	15000	3500
INJ6	WATER	Flow Rate	15000	3500
B	WATER	Flow Rate	10000	3500

4.1.3 Conditional data

Well-log data: porosity, permeability and acoustic impedance are used as hard data. They are gotten from the six vertical appraisal wells (WELL A-F) in this case study. The 6 appraisal wells have a significant influence on the GRV calculation (Arnold et al., 2013).

4.1.3.1 Porosity Permeability Relationship

The relationship between the porosity and permeability from well-log data is a positive logarithm. With correlation coefficient at 0.723. This means as one variable increases, the other variables increases as well. Permeability values are between 0.00 to 897md while porosity values are between 0.03 and 0.261. The Figure below shows the relationship between both variables.

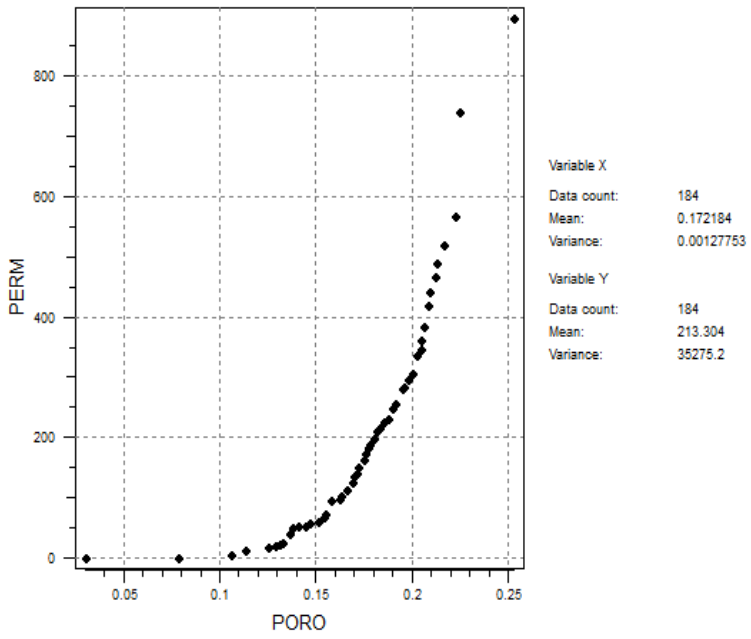

Figure 4.5: *bivariate analysis of Porosity (φ) and permeability (K). x-axis(Poro), y-axis (Perm).*

In Figures 4.6 and 4.7 below, the well-log data, permeability and porosity are presented as well as their histogram distribution. These histograms enable us read the frequencies of occurrences corresponding to each set. They also represent the variable distribution and enable the DSS and co-DSS validation when compared to simulated models.

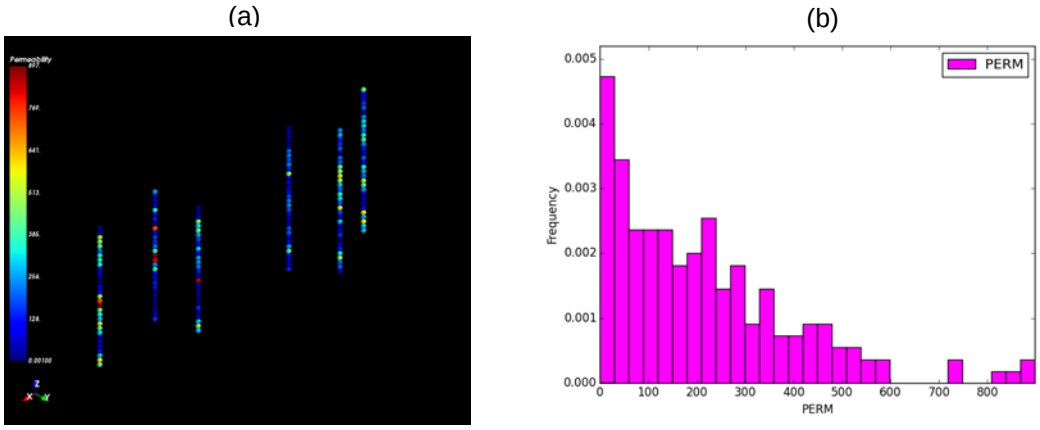

Figure 4.6: *Permeabilty Models: a) Hard data from wells, b)Histogram from Hard Data*

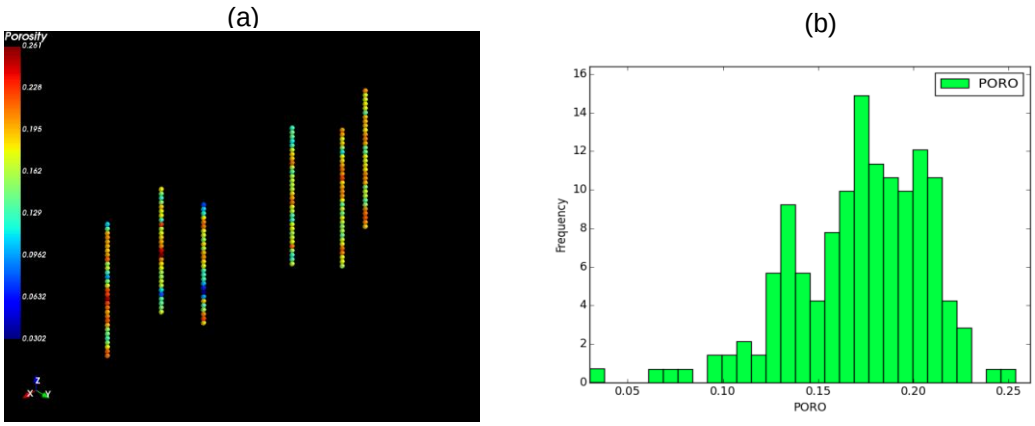

Figure 4.7**:** *Porosity Model: (a) Hard data from wells, (b)Histogram from Hard Data*

The well-log histograms from porosity and permeability are similar to the histogram from grid model. The experimental bi histogram is used in the sequential simulation with joint- distribution which allows the reproduction of the non-linear relationships between properties, in this case porosity and permeability.

4.1.4 Spatial Continuity

The variogram model is key to any geostatistical modelling procedure. The variogram model adjusted for each variable of the experimental variogram defines the spatial continuity. The semi-variogram model used to model the three directions (two horizontal and one vertical) in space for this work was spherical model and are shown in the Figures 4.8 and 4.9 below.

Porosity Variogram models

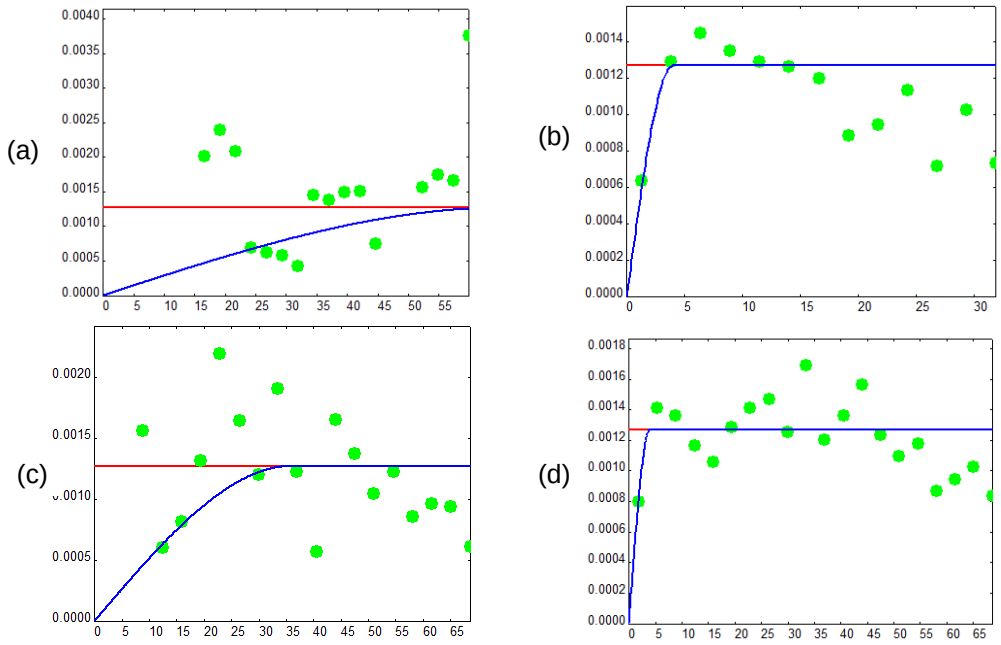

Figure 4.8**:** *experimental porosity variograms (blue line) (a) x,y direction fine scale (b) z direction fine scale. (c) x,y direction coarse scale (d) z direction coarse scale*

Permeability variogram models

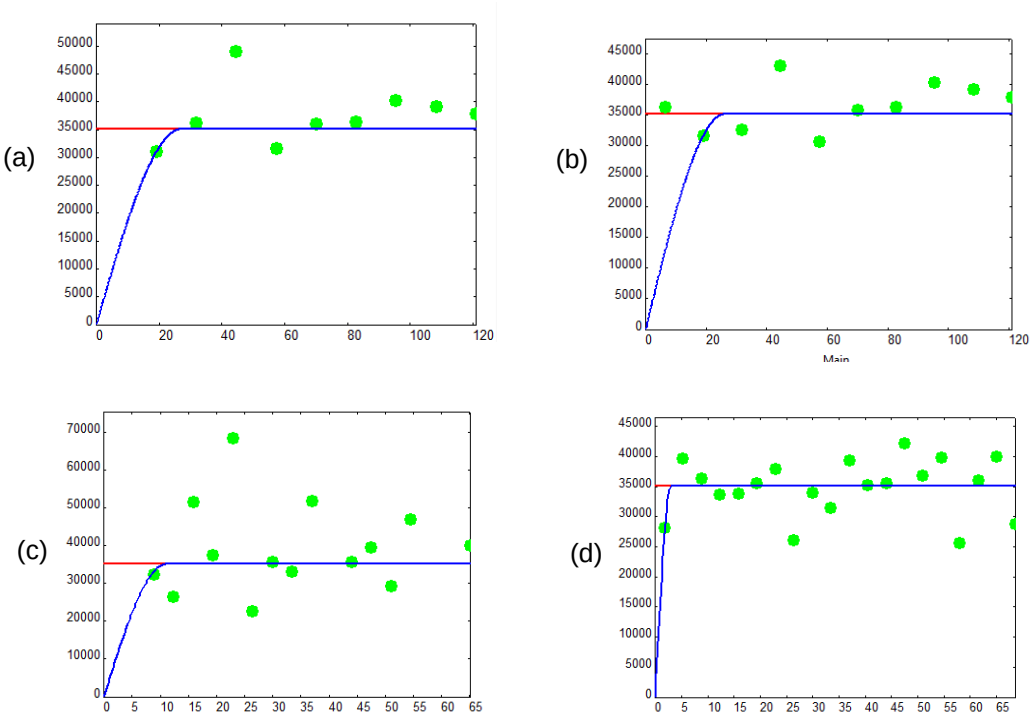

Figure 4.9**:** *experimental permeability variograms (blue line) (a) x,y direction fine scale (b) z direction fine scale. (c) x,y direction coarse scale (d) z direction coarse scale*

4.2 Results and Discussion

This section discusses the results obtained by applying the methodology described in Chapter 3, which was applied to the case study - Watt Field, based on two stages, Upscaling of Reservoir and Geostatistical History Matching.

4.2.1 Upscaling Results

The upscaling was done so as to have different scales to enable the comparison of the GHM and this is the result. The fine grid earlier described in Figures 4.1 and 4.3 is defined by 533,660 blocks discretized by [226x59x140] cells with 100mx100mx5m each and the upscaled coarse grid is defined by 135,600 blocks discretized by [113x30x140] with 200mx200mx5m each. The reduction scale factor for each direction x, y is 2. Figures 4.10 and 4.11 below show the permeability and porosity distribution of the coarse grid respectively. Table 6 and Table 7 show the permeability and Porosity statistics of the coarse grid respectively.

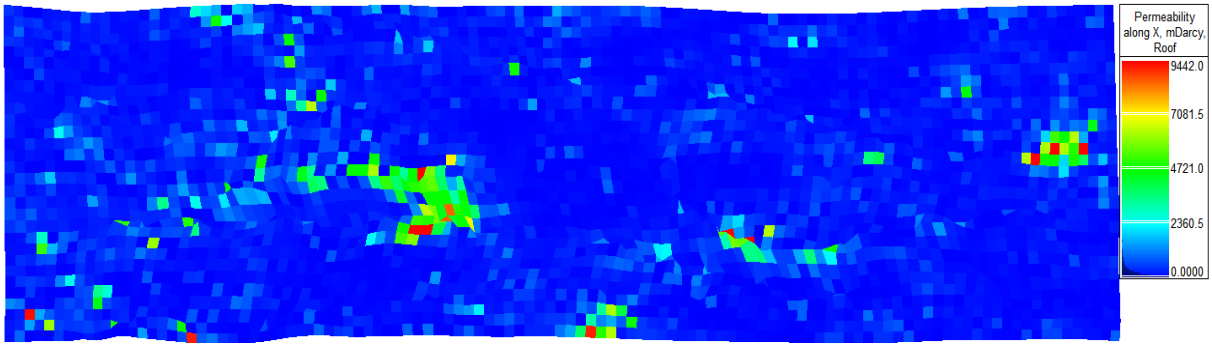

Figure 4.10: *2D view of permeability Image showing the upscaled cell size to 200x200x5m.*

Table 6**:** Permeability statistics of coarse grid

Property	**Permeability**
Mean	368.21 mDarcy
Standard Deviation	836.95 mDarcy
Min	0 mDarcy
Max	9442 mDarcy

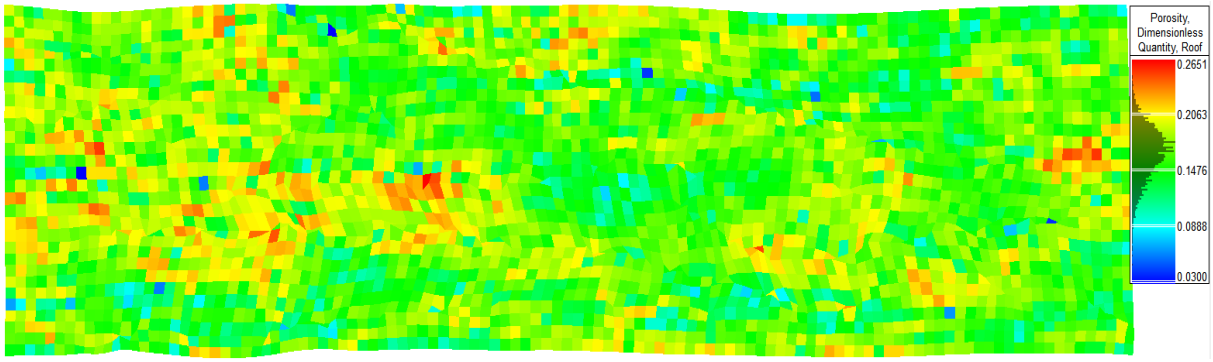

Figure 4.11: *2D view of porosity Image showing the upscaled cell size to 200x200x5m*

Table 7: Porosity statistics of coarse grid

property	Porosity
Mean	0.16862
Standard Deviation	0.029672
Min	0.03
Max	0.27

Figures 4.12 and 4.14 shows the 3D views of permeability and porosity of the Watt Field reservoir at both scales respectively. Figure 4.13 and 4.15 show permeability and porosity histograms comparing the fine scale and the coarse scale. Table 8 shows the comparison of basic statistics of both reservoir scales.

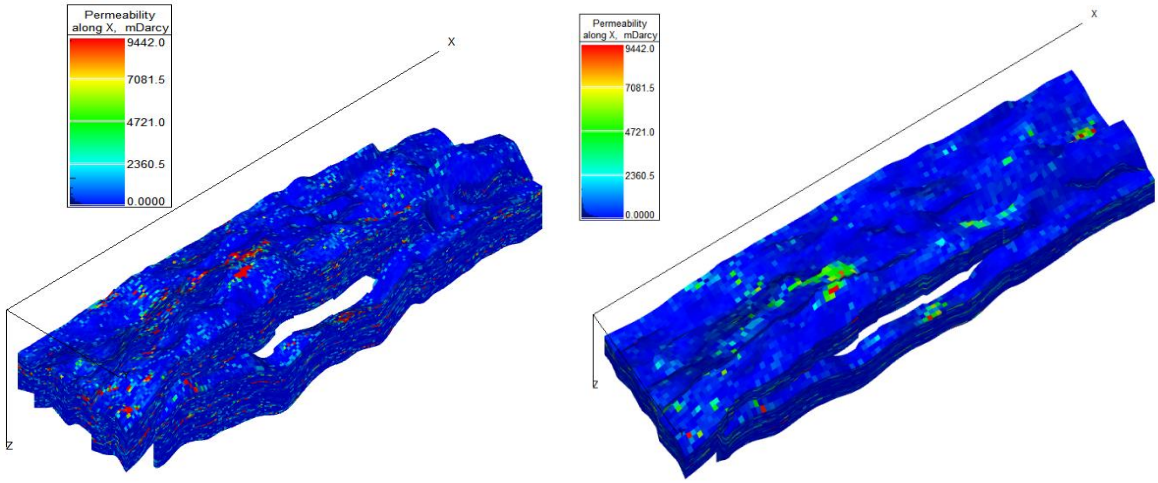

Figure 4.12: 3D view *comparison of Watt Field Reservoir permeability (left) fine scale (right) coarse scale.*

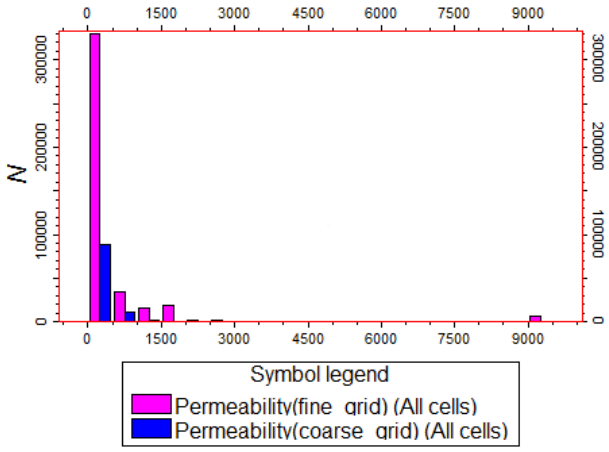

Figure 4.13**:** *Permeability histogram of Watt Field Reservoir (pink) fine scale (blue) coarse scale*

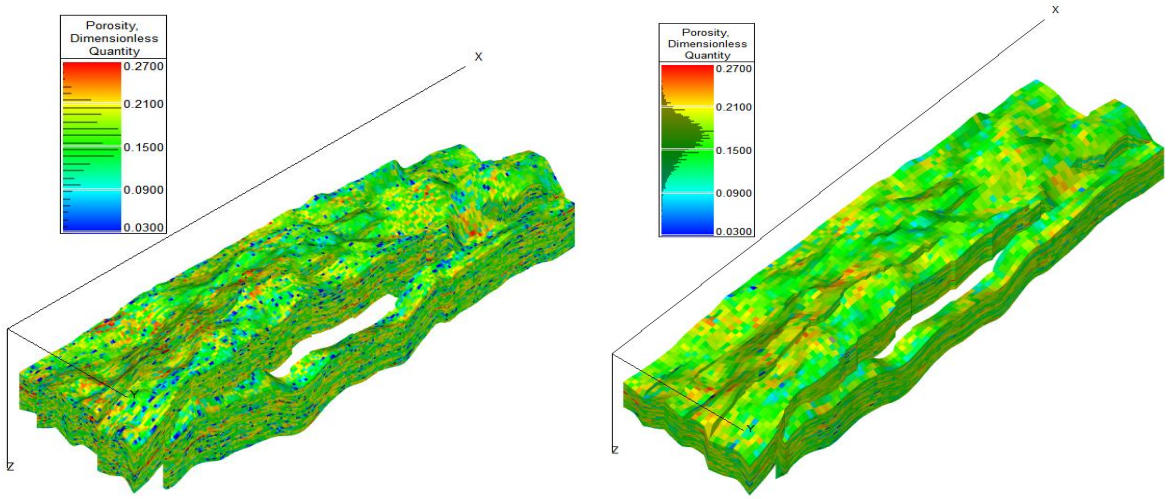

Figure 4.14: 3D view *comparison of Watt Field Reservoir porosity (left) fine scale (right) coarse scale.*

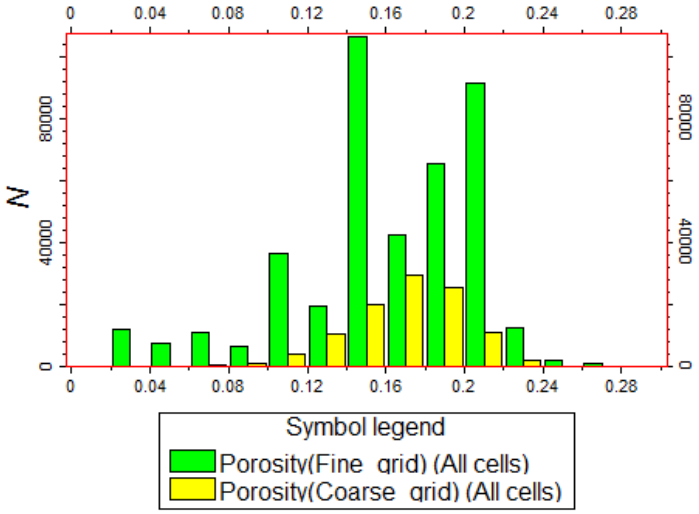

Figure 4.15: *Porosity histogram of Watt Field Reservoir (green) fine scale (yellow) coarse scale*

Table 8: Table showing differences in Reservoir scales.

	Fine Scale	***Coarse Scale***
Grid cell dimension	100mx100mx5m	200mx200mx5m
Grid cell count	226*59*40	113*30*40
Number of cells	533,360	135,600

4.2.2 Dynamic Simulation Results

After upscaling the Watt field reservoir, fluid flow simulation for both scales were carried out. Some differences were noticed and are discussed below.

Firstly, the fluid flow simulation time drastically reduced on both the Tnavigator® software as well as the eclipse software where the simulations were ran. For the fine grid reservoir, the CPU time was fifty-two (52) minutes and that of coarse grid was five (5) minutes. This infers that an upscaled grid (i.e. coarser model) has a less CPU time.

Secondly, slight differences in production data are noticed. The field oil production total (FOPT) of the coarse grid is slightly higher than that of the fine grid as can be interpreted in Figure 4.16(a). This also has an effect on the oil production rate (FOPR) as there is a higher production rate in the coarse grid Figure 4.16(b). The water production rate (FWPR) is higher in the fine grid than in the coarse grid which is expected since the reservoir is measured by the same liquid rate for both reservoir sizes. This is seen in Figure 4.17(a). The field average pressure (FPR) is more or less the same for both the fine and coarse grids Figure 4.17(b).

With these curves and statistics seen we can say the upscaling is validated as the upscaled model of 200m*200m*5m closely matches the initial model of 100m*100m*5m. The decline curve still shows that they are generally the same.

(a) (b)

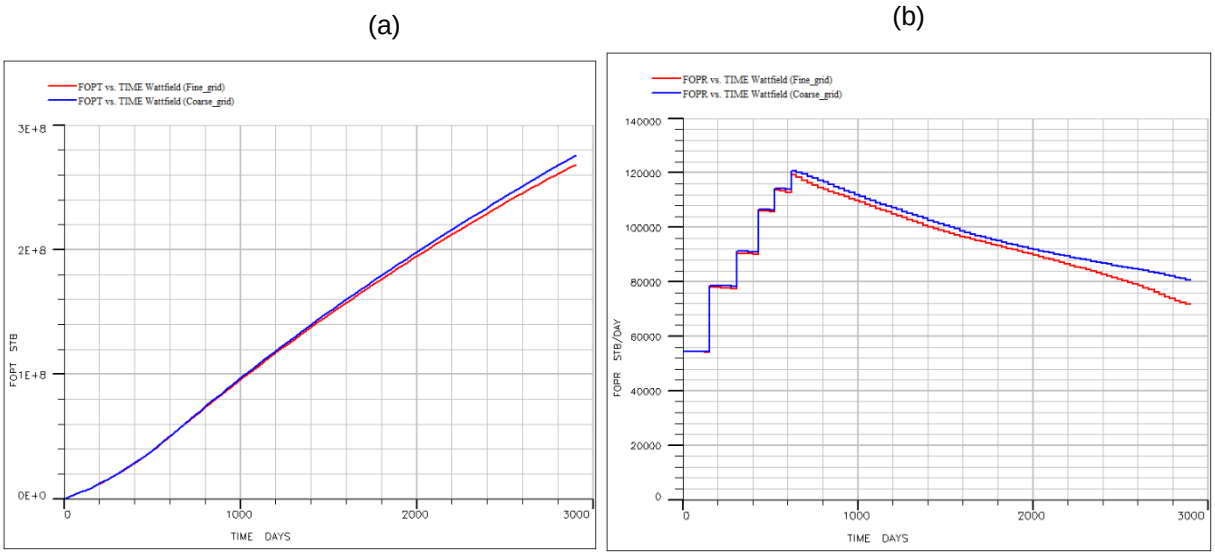

Figure 4.16**:** *Field Oil Production Total and Field Oil Production Rate for both reservoir scales. The*

coarse grid (blue) had increased oil production total as against the fine grid (red) (left) and also an increased oil production rate (FOPR) as against the fine grid (right)

(a) (b)

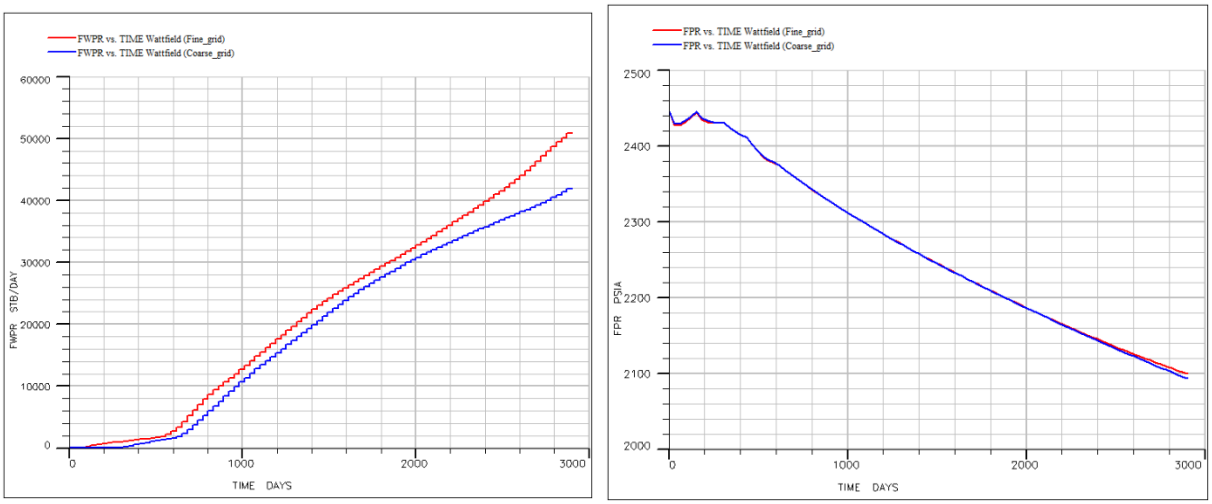

Figure 4.17: *Field Water Production Total and Field average pressure for both reservoir scales.*

As discussed earlier describing our case study, there are 16 producer wells, for the sake of the work we have selected 2 wells (Well 1 and Well 5) to have better understanding of the reservoir and to evaluate the bottom hole pressure (WBHP), oil production rate (WOPR) and water production rate (WWPR) for each well. Figure 4.18(a) and (b) show the WBHP and WOPR of Well 1 with both reservoir grid sizes. The coarse grid (blue) has a higher values than fine grid (red). Figure 4.19 shows the WWPR of well 1. The fine grid (red) has a higher water production rate than, the coarse grid (blue).

(a) (b)

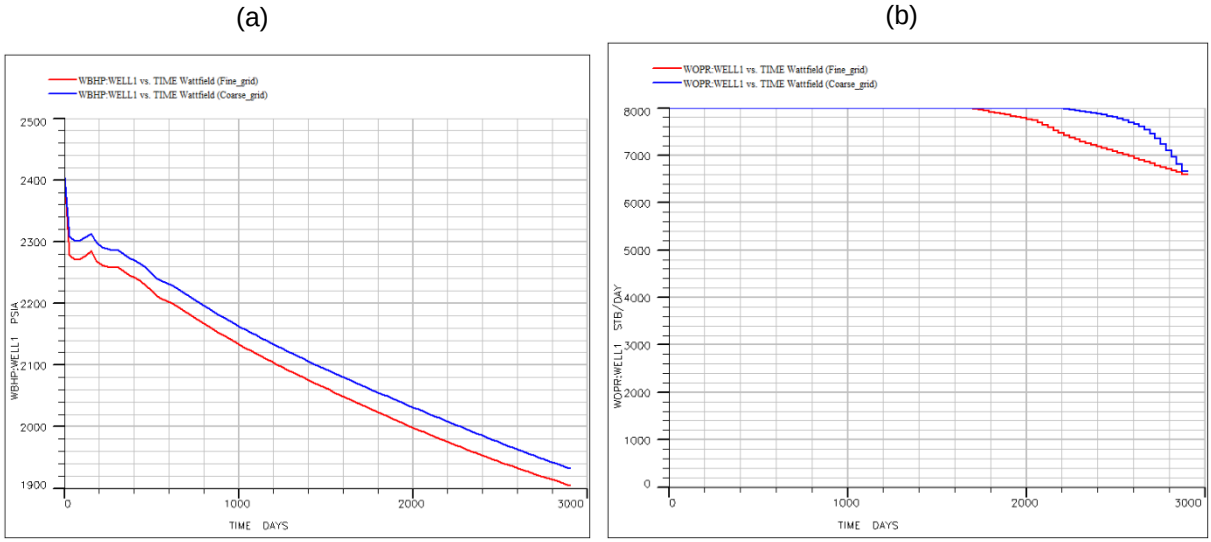

Figure 4.18: Well 1 (a) Bottom Hole Pressure (WBHP) and (b) Oil Production Rate (WOPR).

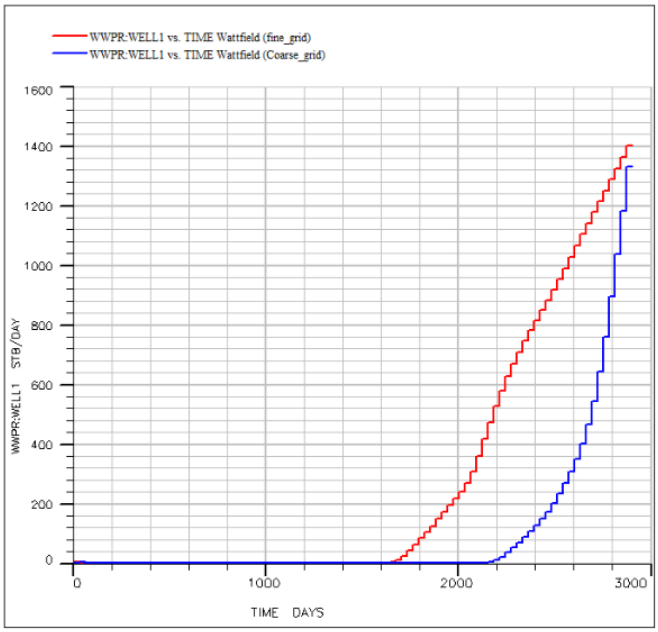

Figure 4.19: *Well 1 Water Production Rate (WWPR).*

In the case of Well 5, Figure 4.20(a) both reservoir grid sizes have almost the same (WBHP). The fine scale had a higher oil production rate (WOPR) than the coarse scale as seen in 4.20(b). In Figure 4.21, *the coarse grid (blue) has a higher water production rate (WWPR) than the fine grid (red) for well 5.*

(a) (b)

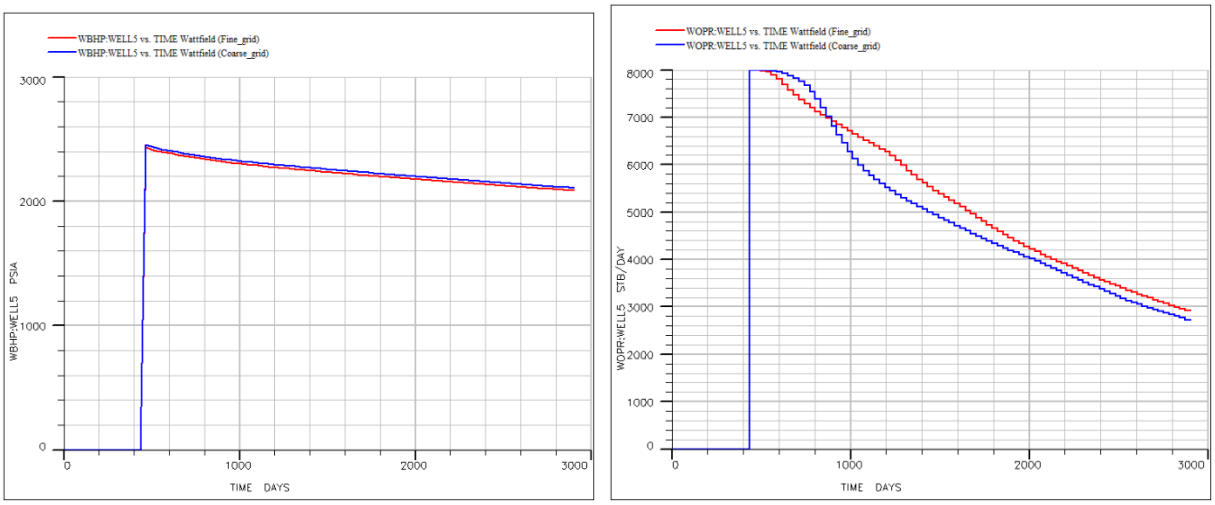

Figure 4.20: *Well* 5 *(a) Bottom Hole Pressure (WBHP) and (b) Oil Production Rate (WOPR).*

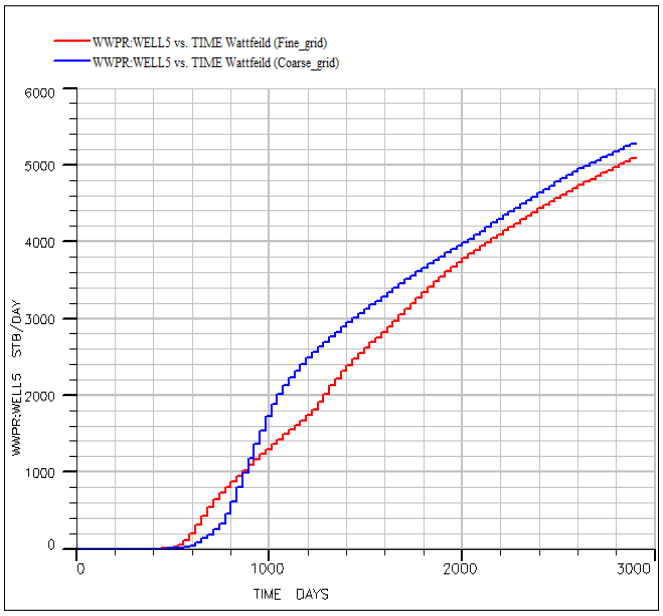

Figure 4.21: *Well 5 Water Production Rate (WWPR).*

The rest of the production curves results for all wells is added at appendix A at the end of the thesis.

The production data that will be used for history matching are Oil Production Rate, Water Production Rate and also Bottom Hole Pressure for each well from the historical data. The misfit depends on these variables.

4.2.3 History Matching Results

For this stage, a total of 6 iterations with 18 simulations each (a total of 108 stochastic realizations) was carried out. The permeability and porosity generated from the first and last iterations and the best fit model are shown here.

The geostatistical history matching in the fine grid ran for a total of 39h11m. The first simulation (iteration 1 simulation 1) does not represent the spatial distribution of the reservoir effectively and the misfit has high values, however with the increase of the number of iterations the spatial reproduction improves. Figure 4.22 and Figure 4.24 show the permeability and porosity variation in simulated models. The histogram of each model Figure 4.23 show that the higher value in the reference model are not observed in the simulated models and this in turn affects the results obtained. Figure 4.25 shows the porosity histogram of the reference model and the simulated models obtained after the GHM.

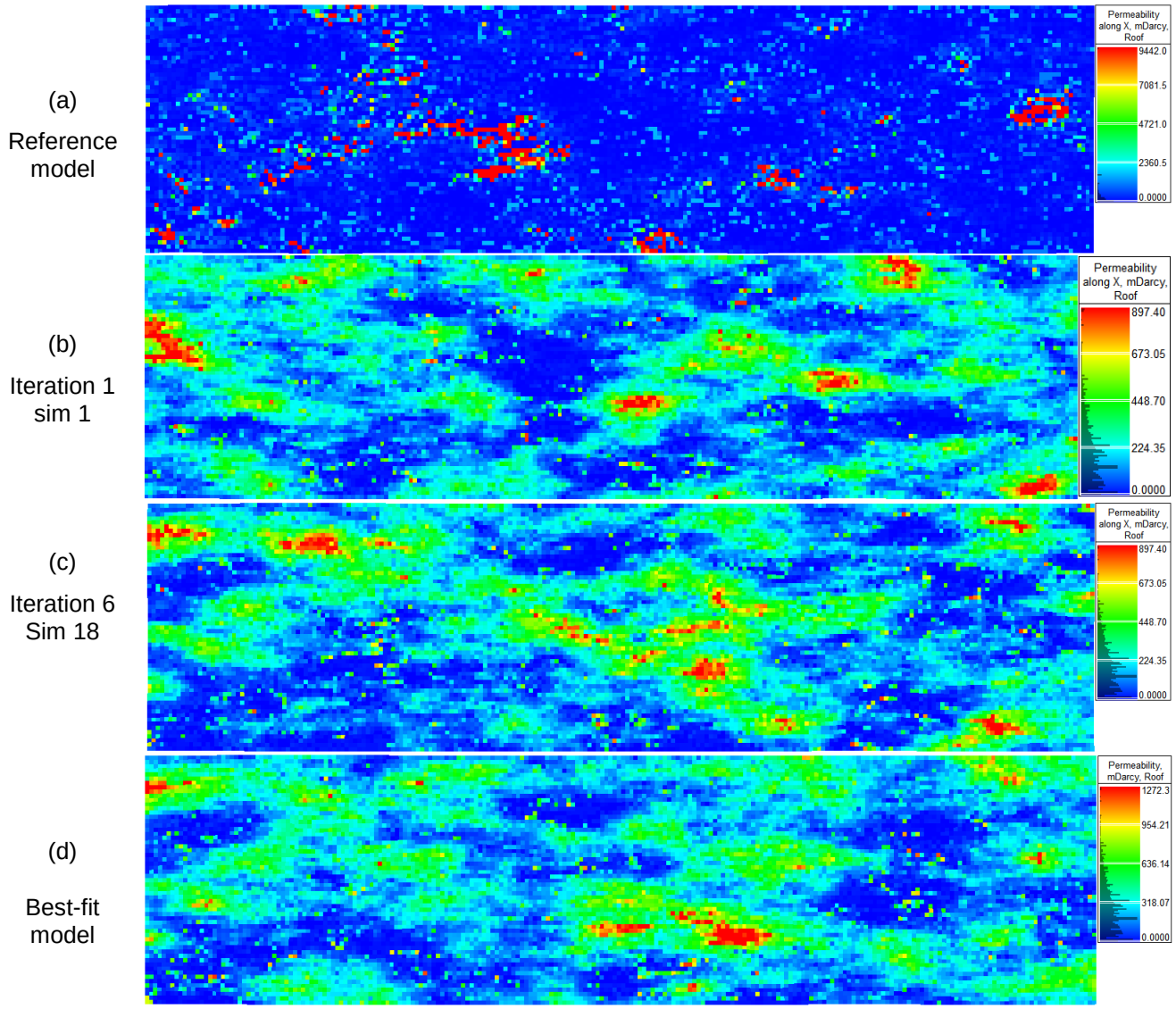

Figure 4.22: *Permeability of Watt Field (a) reference model, (b) Iteration 1 simulation 1 (c) Iteration 6 simulation 18 (d) Best-fit model obtained after GHM.*

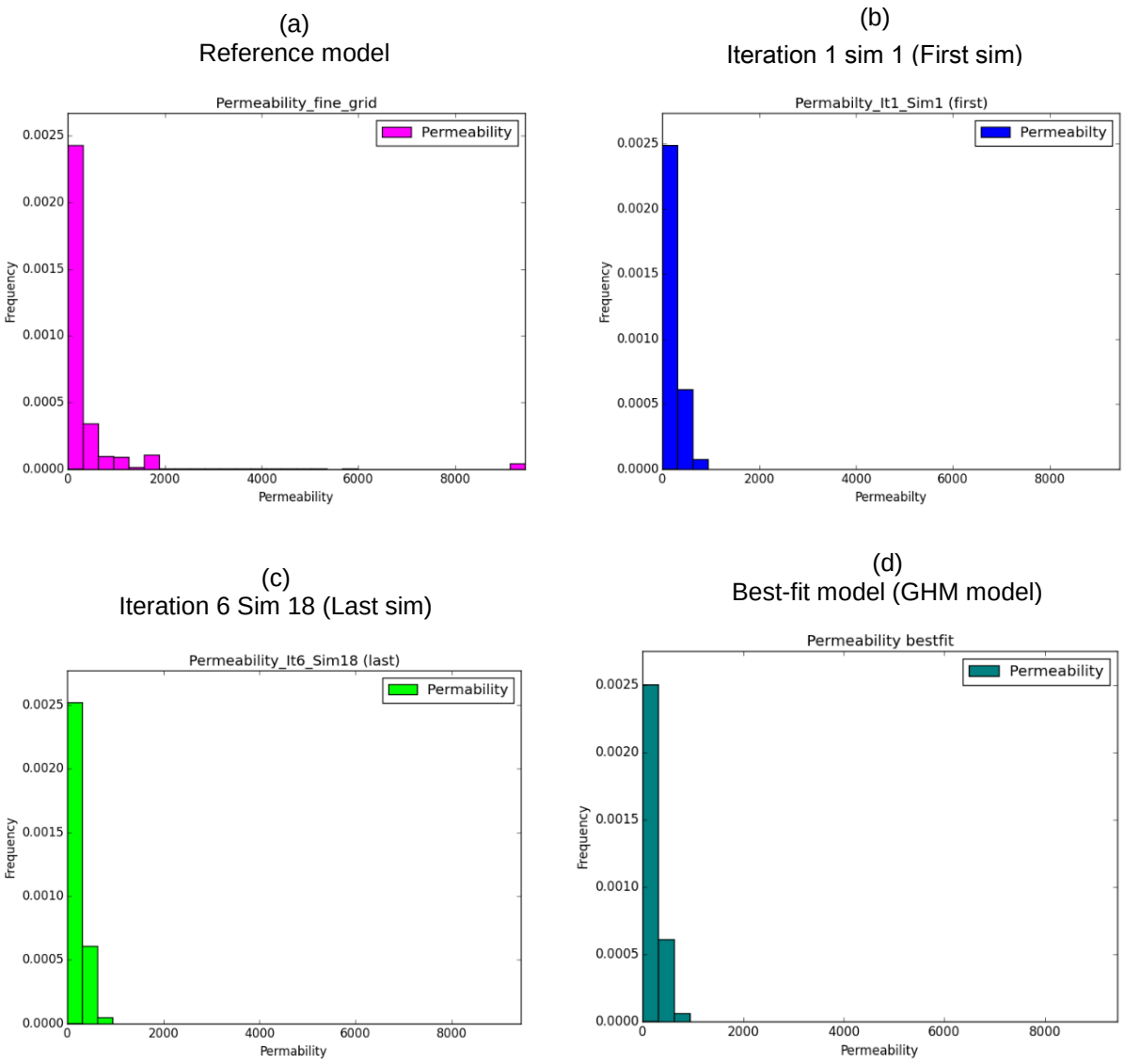

Figure 4.23: *Permeability histogram comparison; (a) reference model (b) First simulation (c) bottom left last simulation (108) (d) best fit model.*

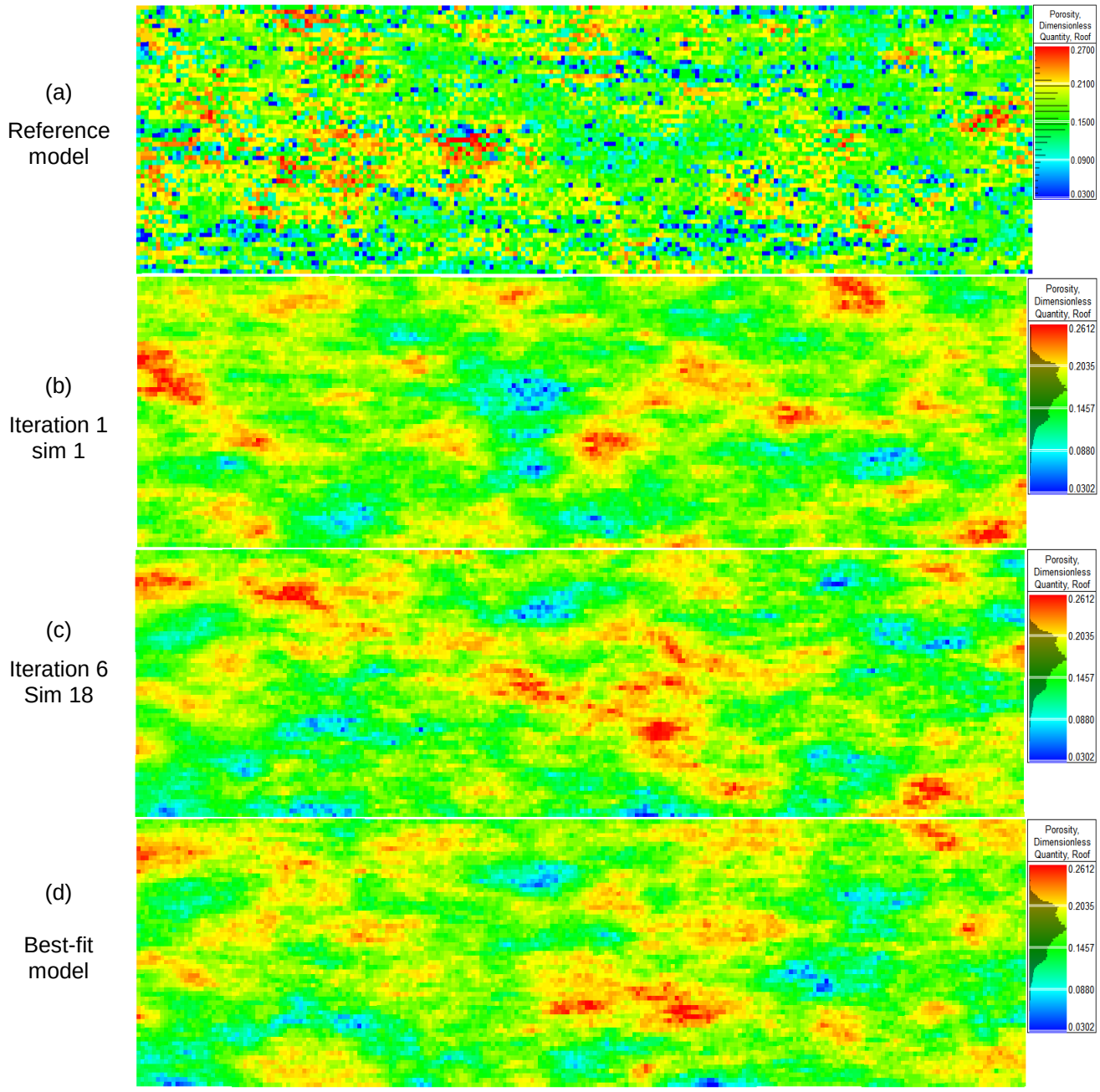

Figure 4.24: *Porosity of Watt Field (a) reference model (b) Iteration 1 simulation 1 (c) Iteration 6 simulation 18 (d) Best-fit model obtained after GHM.*

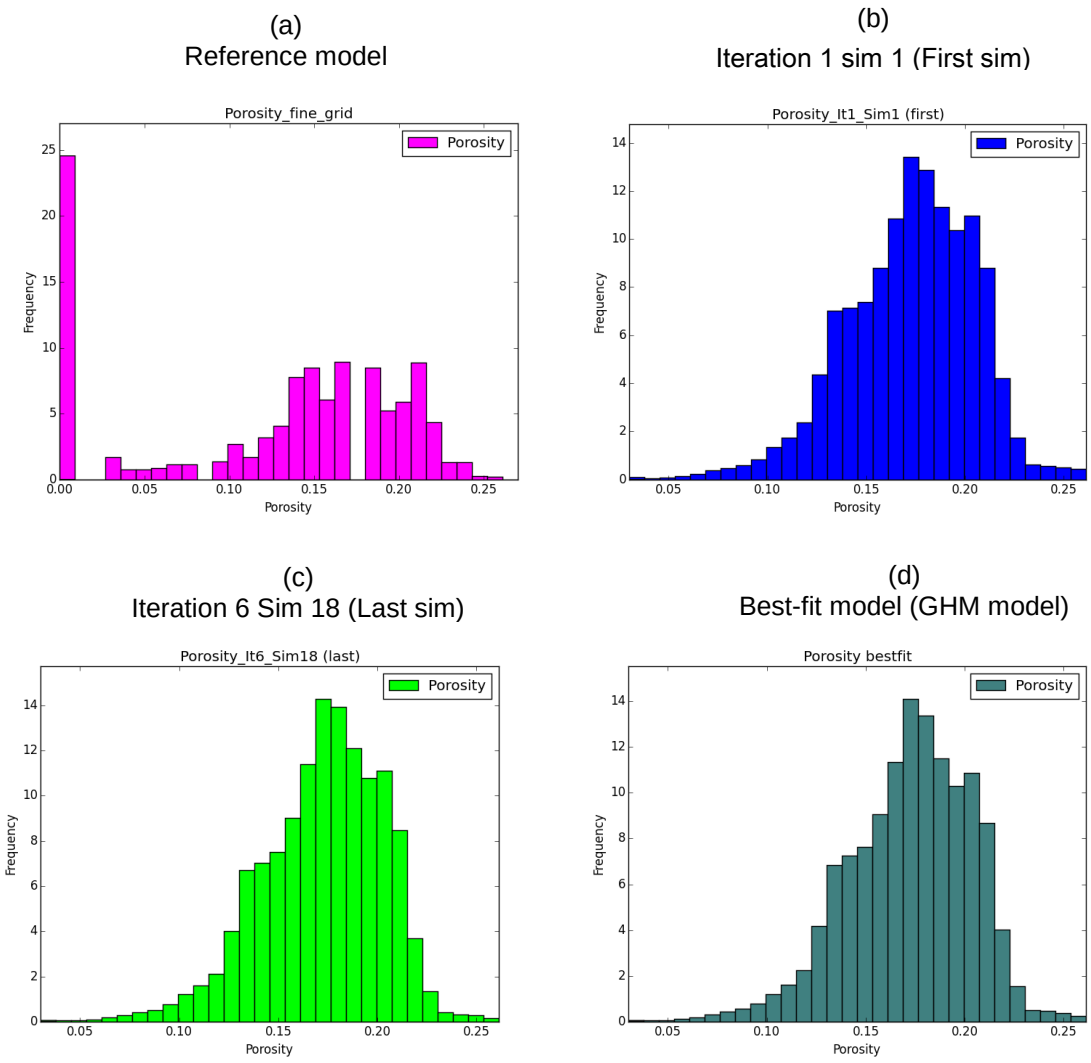

Figure 4.25: *Porosity histogram comparison; (a) reference model (b) Iteration 1 sim 1 (First sim) (c) Iteration 6 Sim 18 (Last sim) (d) best fit model*

For the coarse grid, we run the model with 6 iterations and 18 simulations. The computational time reduced to 09h17m which is an improvement mathematically. The minimum misfit is observed in iteration 6, simulation 11. The permeability and porosity generated from the first, last and the best fit model are also shown below in Figures. 4.26 and 4.28 respectively while Figures 4.27 and Figure 4.29 show the histogram of permeability and porosity of the coarse grid after the GHM respectively.

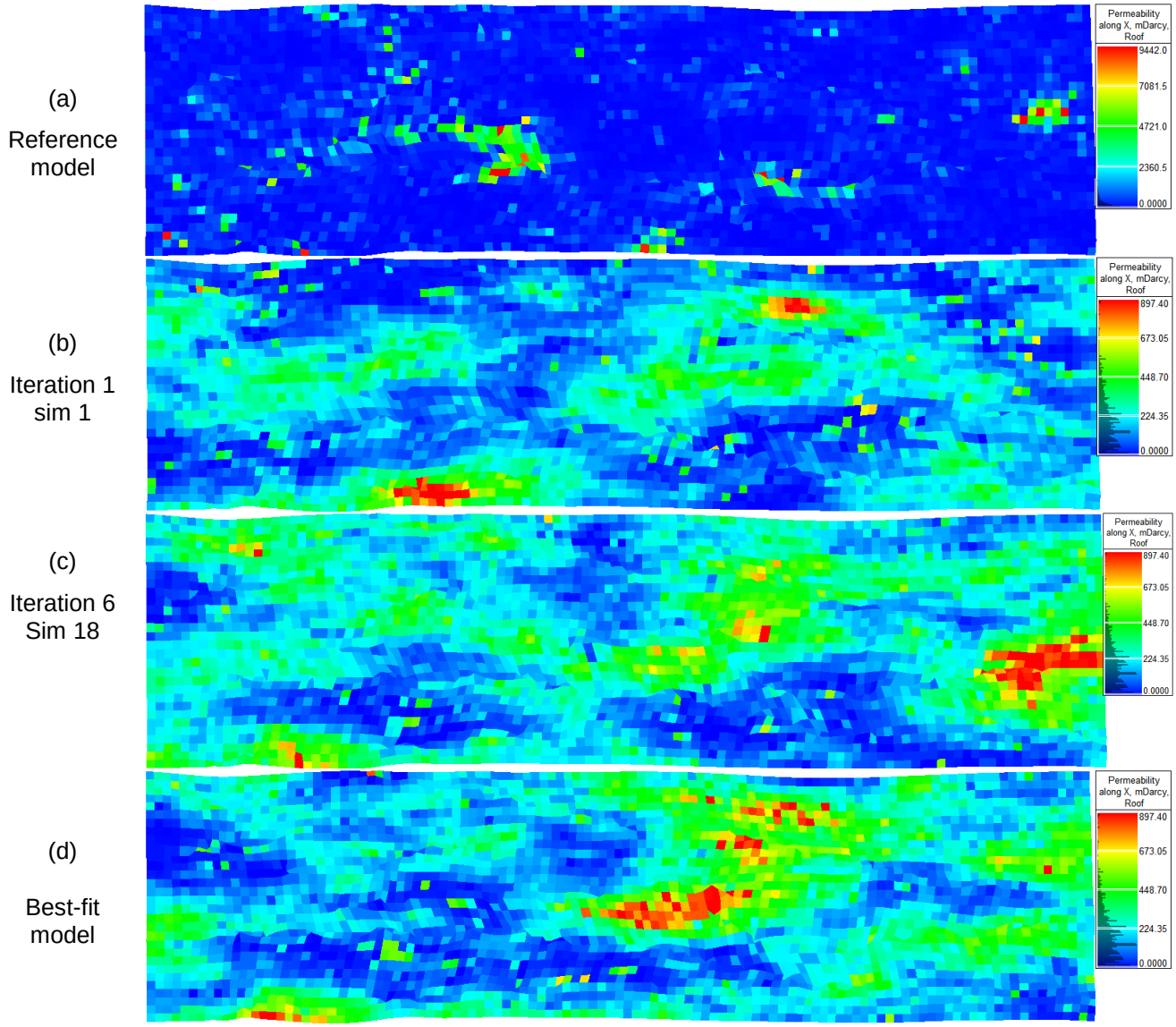

Figure 4.26: *Permeability of Coarse scale Watt Field (a) reference model, (b) Iteration 1 simulation 1(1) (c) Iteration 6 simulation 18 (108) (d) Best-fit model obtained after GHM*

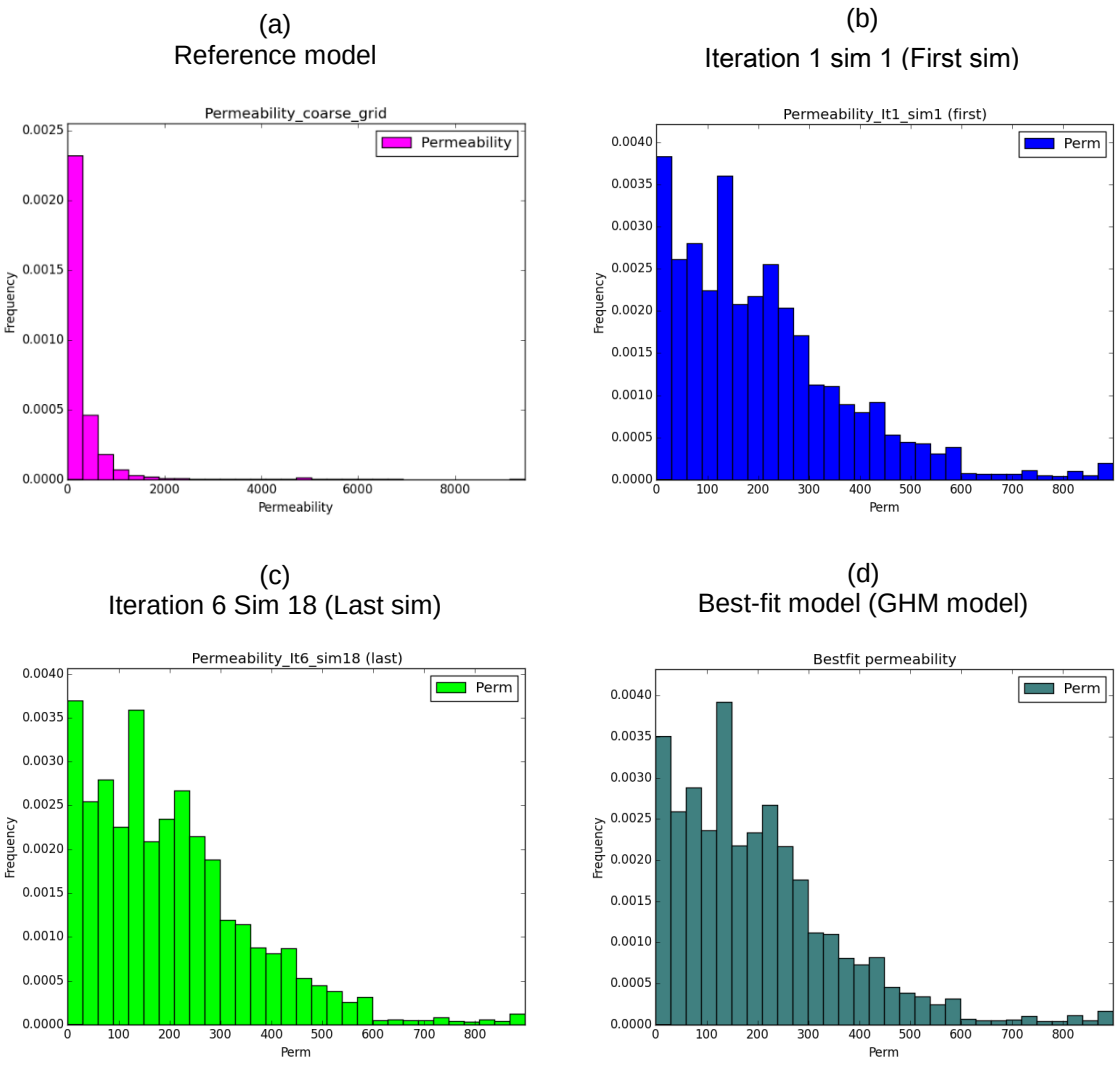

Figure 4.27: *Coarse grid permeability histogram comparison; (a) reference model (b) First simulation (1) (c) last simulation (108) (d) best fit model*.

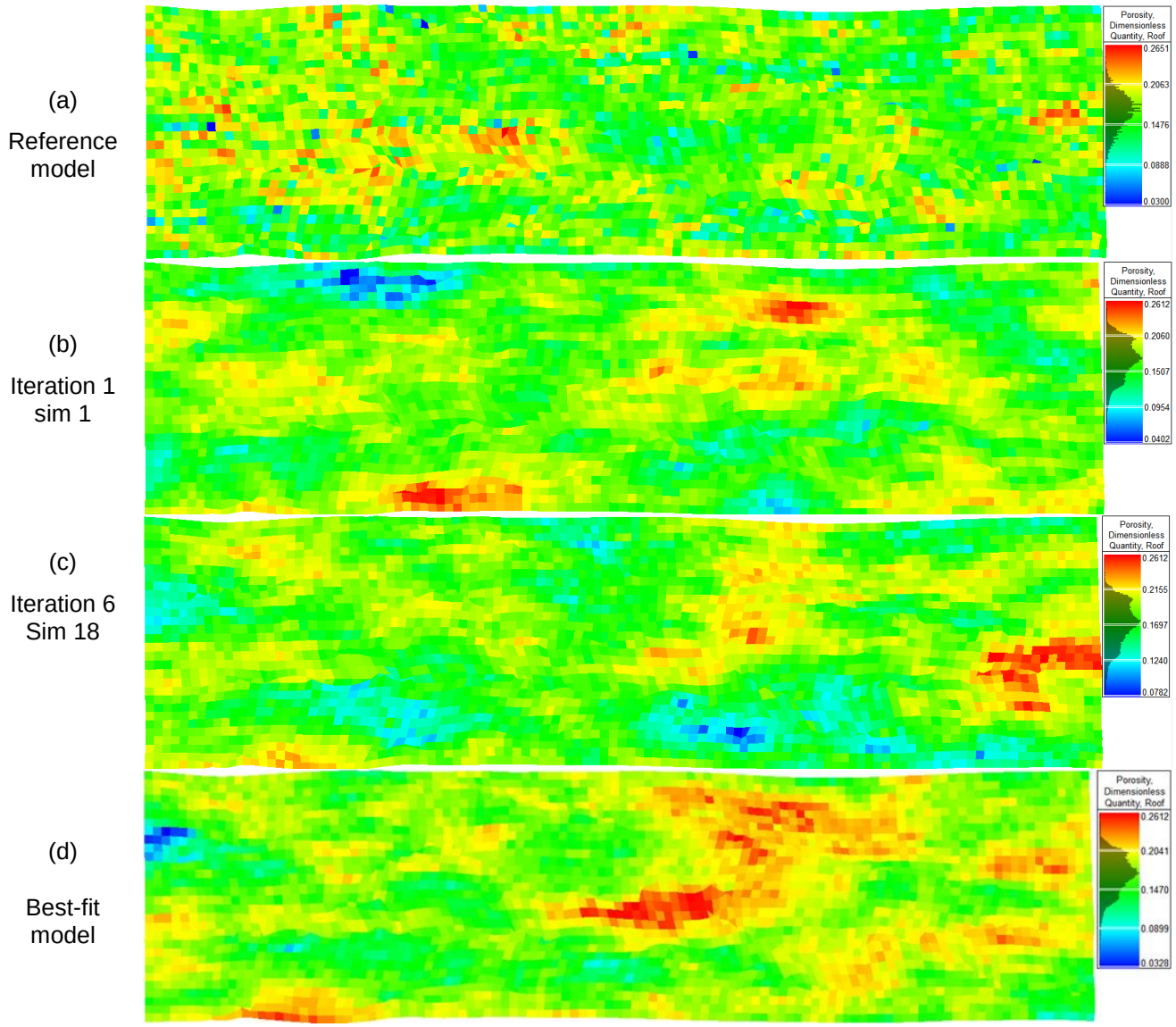

Figure 4.28: *Porosity of Coarse scale Watt Field (a) reference model, (b) Iteration 1 simulation 1 (c) Iteration 6 simulation 18 (d) Best-fit model obtained after GHM*

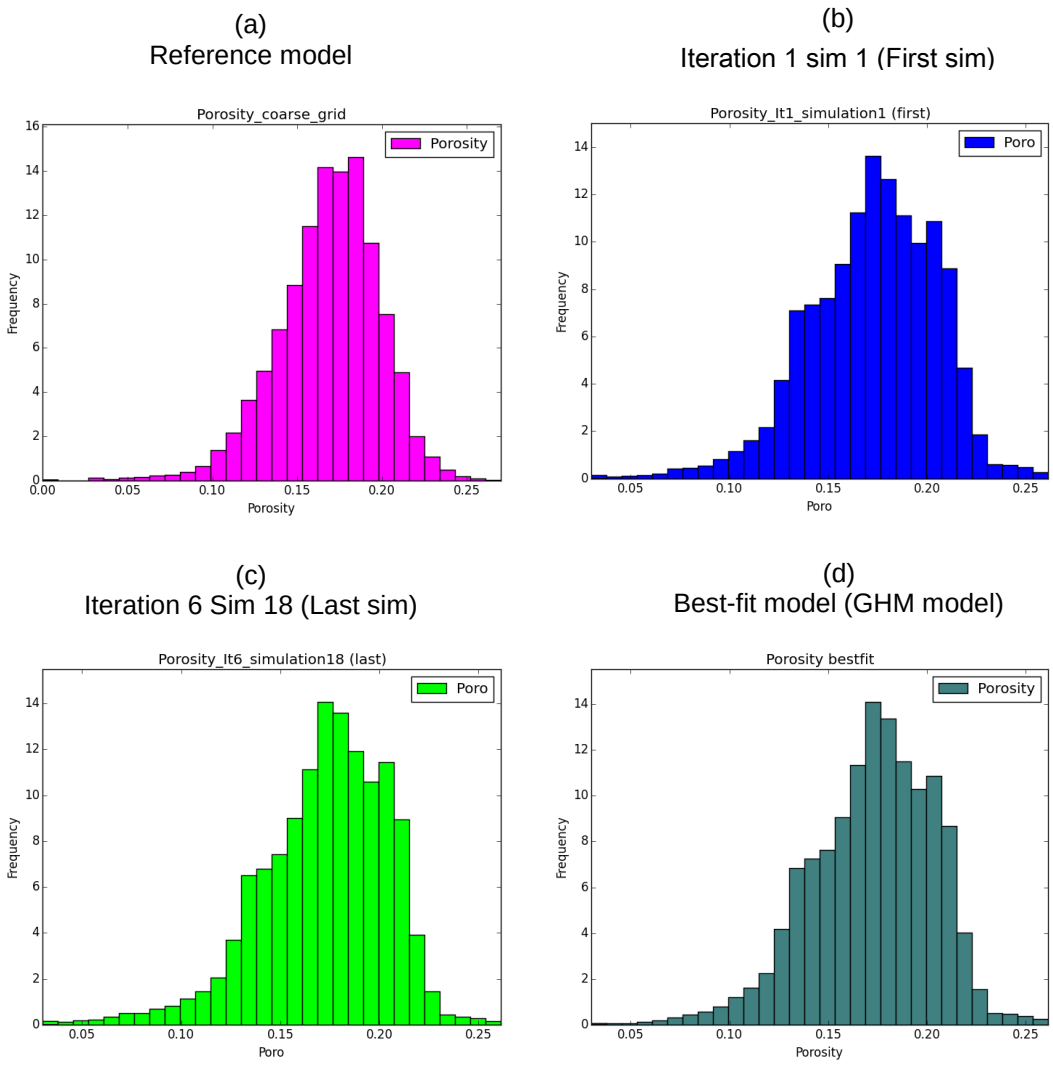

Figure 4.29: *Coarse grid porosity histogram comparison; (top left) well l), reference model (top right) First simulation (1) bottom left last simulation (108) (bottom right) best fit model*

4.2.4 Production Match Analysis

Plots of production curves as well as plots of misfit are shown here to explain match quality and convergence obtained.

The production data from the simulated reservoir models match considerably well the production data from the historical model. We can see the first simulation (1) in blue compared to the last simulation (108) in yellow (Figure 4.30 and 4.31) below. This explains the convergence being reached.

(a)

WBHP

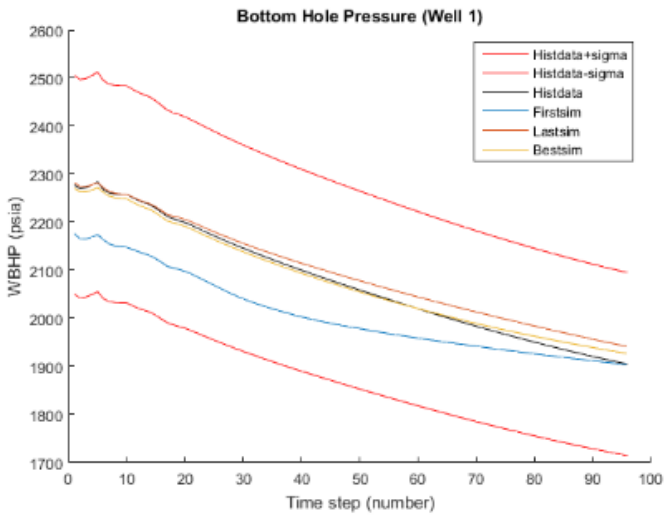

(b)

WOPR

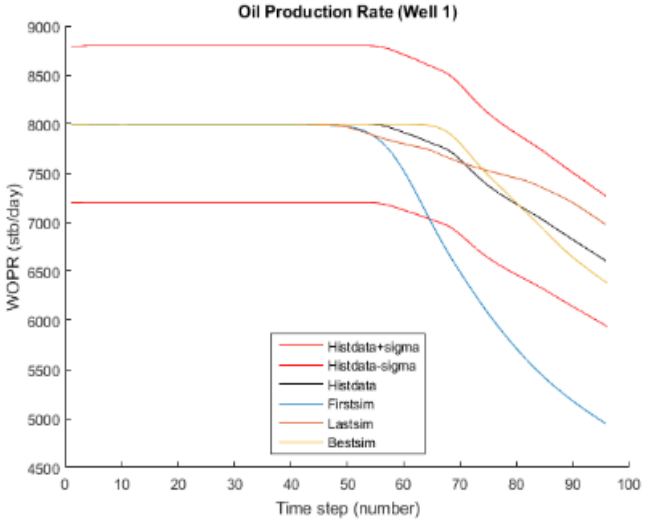

(d)

WWPR

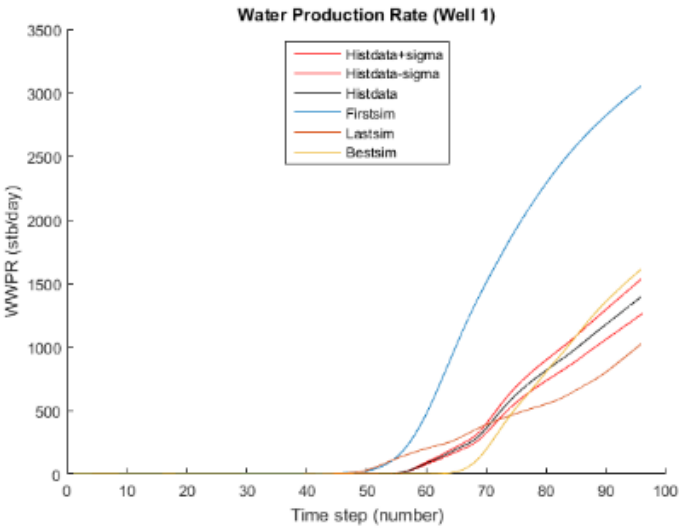

Figure 4.30: *History matching variables Well 1. Reference model (black), First simulation (blue) last simulation (brown), best fit model (yellow). (a) WBHP (b) WOPR (c) WWPR*

(a)

WBHP

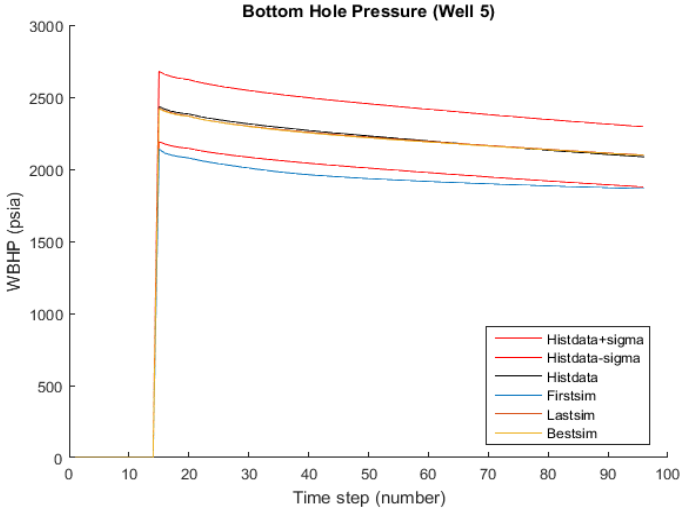

(b)

WOPR

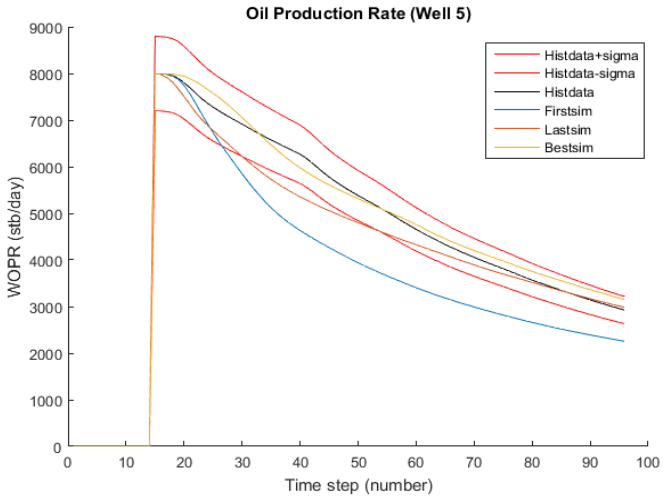

(d)

WWPR

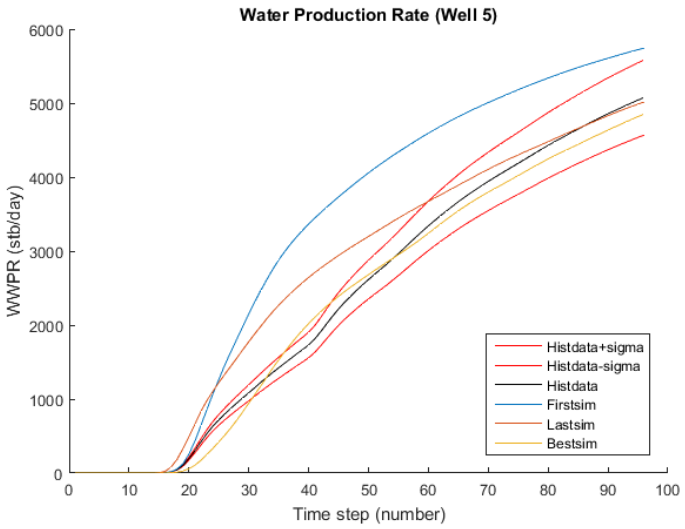

Figure 4.31: *History matching variables Well 5. Reference model (black), First simulation (blue) last simulation (brown), best fit model (yellow). (Top) WBHP (middle) WOPR (bottom) WWPR*

To have a better understanding about the convergence during the geostatistical history matching, it is necessary to plot all models from the first and the last iteration. By plotting the iteration 1 against iteration 6 it becomes easy to see that the stochastic process is converging towards the real model (Figure 4.32 and 4.33).

From Figure 4.32 and 4.33and in Appendix B, it is possible to interpret that the production wells show a very good convergence in terms of bottom hole pressure (WBHP) when we consider the 10 percent margin of error (sigma) from the history data. In terms of oil production rate (WOPR) and water production rate (WWPR) the convergence is not homogeneous in the production wells since well 1 (Figure 4.32) does not show a good convergence, well 5 (Figure 4.33) shows a better convergence. The porous connectivity or production strategy used could be the reason for this. Appendix B at the end of the thesis show the fine scale evolution curves for all wells.

The pattern for the run (Figure 4.34) shows a huge drop in the results from iteration 1 to iteration 2. After this drop a slow and steady decrease of the values is observed until iteration 5 and a sharp drop to the last iteration. Convergence of the run is obtained at iteration 6 with a minimum misfit of 214.0977 for the run. There is a reduction in the misfit showing that the production data from the simulated models tends to approach to the values of the of watt field model. The results show that this GHM with voronoi zonation is capable of replicating the reservoir petrophysical properties as well as the flow patterns.

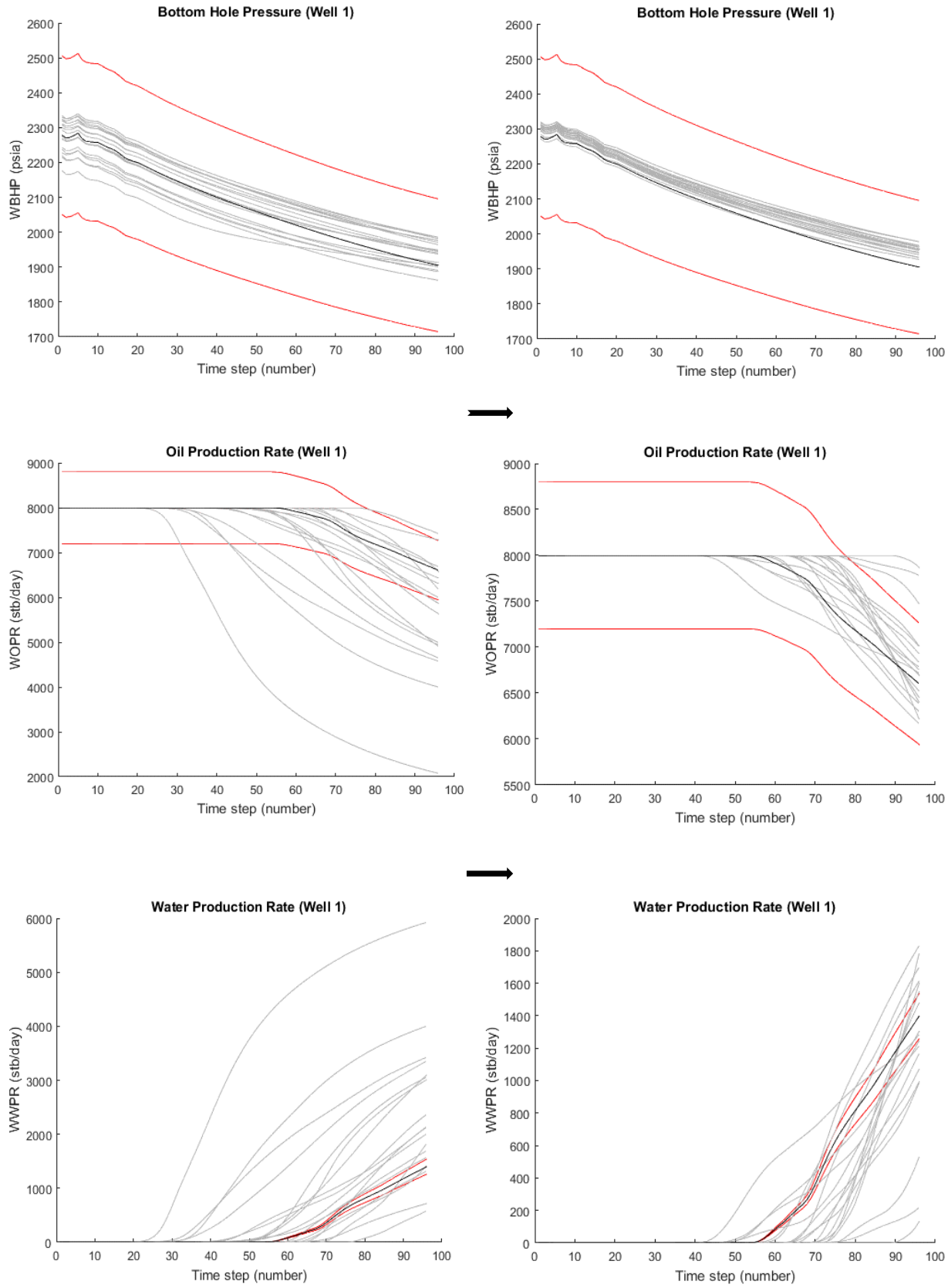

Figure 4.32: *Fine scale production curves evolution of Well 1, (Top) WBHP, (middle) WOPR (bottom) WWPR. Iteration 1 is on the left. Iteration 6 on the right. We can see that at iteration 6 the production curves have moved closer to the history data*.

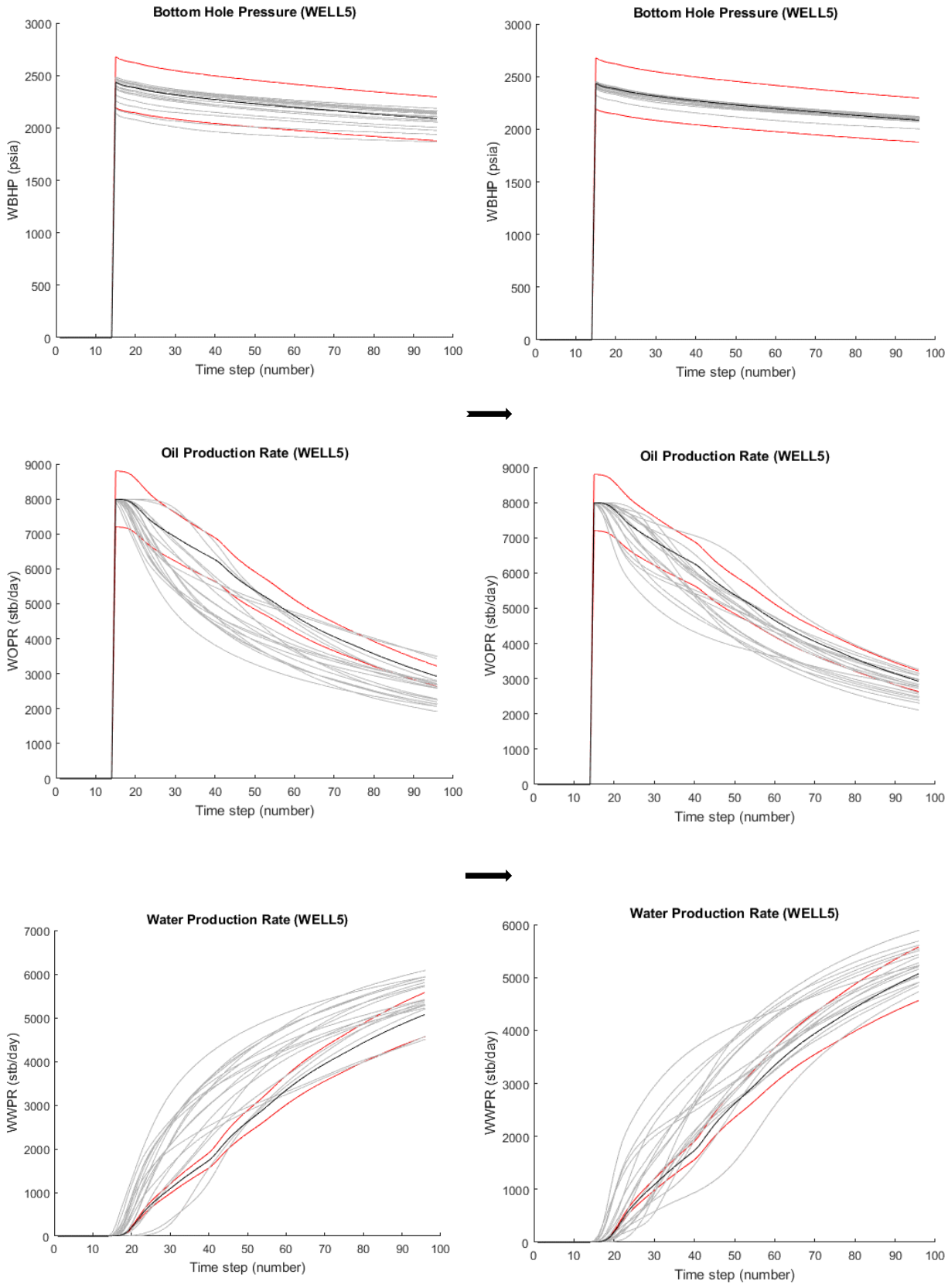

Figure 4.33: *Fine scale production curves evolution of Well 5, (Top) WBHP, (middle) WOPR (bottom) WWPR. Iteration 1 is on the left. Iteration 6 on the right. We can see that at iteration 6 the production curves have moved closer to the history data*.

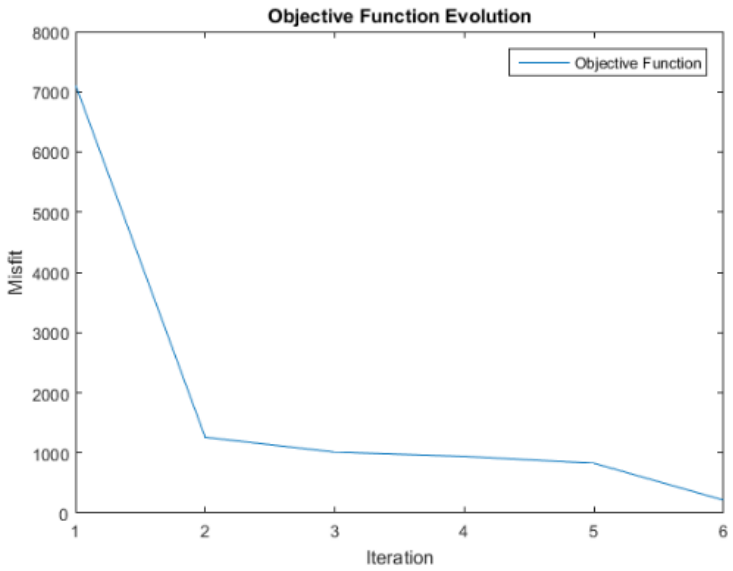

Figure 4.34: *Objective function evolution at the end of the GHM (fine scale).*

For the coarse grid, the GHM did not produce a good match. For all the wells we observed a better match in the fine grid compared to the coarse grid. However, there is a convergence from iteration to iteration and the simulated curves at the last iteration are in general within the sigma (10 percent margin of error) range.

Results in terms of production rates for well 1 and well 5 are shown in the following Figures 4.35 and 4.36.

From Figure 4.37 and 4.38 below, it can be inferred that the simulated responses for well 1 and well 5 do not closely match the observed production data. The production curves of the best fit models in the fine scale and that of the coarse scale in wells 1 and 5 shown are compared in the Figures 4.39 and 4.40 below.

The result in this coarse scale history matching generally shows a poor match compared to the fine scale (Figure 4.41). Although, we can see a convergence, and the minimum misfit value is higher when compared to the fine scale. These high misfit value means that the deviation between history and simulated data is outside admissible error. However, the coarse grid is able to converge at much smaller computational costs and can be used in further steps of the geo-modelling workflow as an initial model.

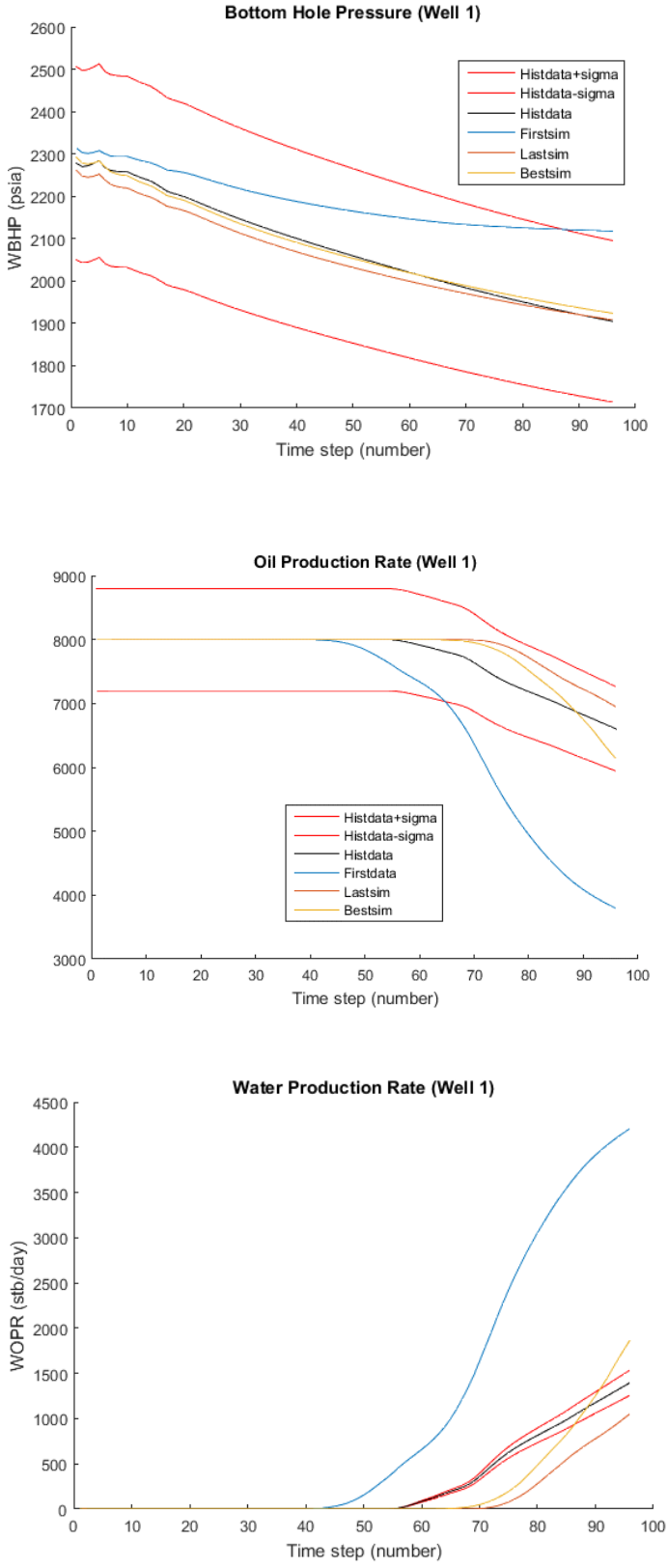

Figure 4.35: *coarse scale history matching variables Well 1. Reference model (black), First simulation (blue) last simulation (brown), best fit model (yellow). (Top) WBHP (middle) WOPR (bottom) WWPR*

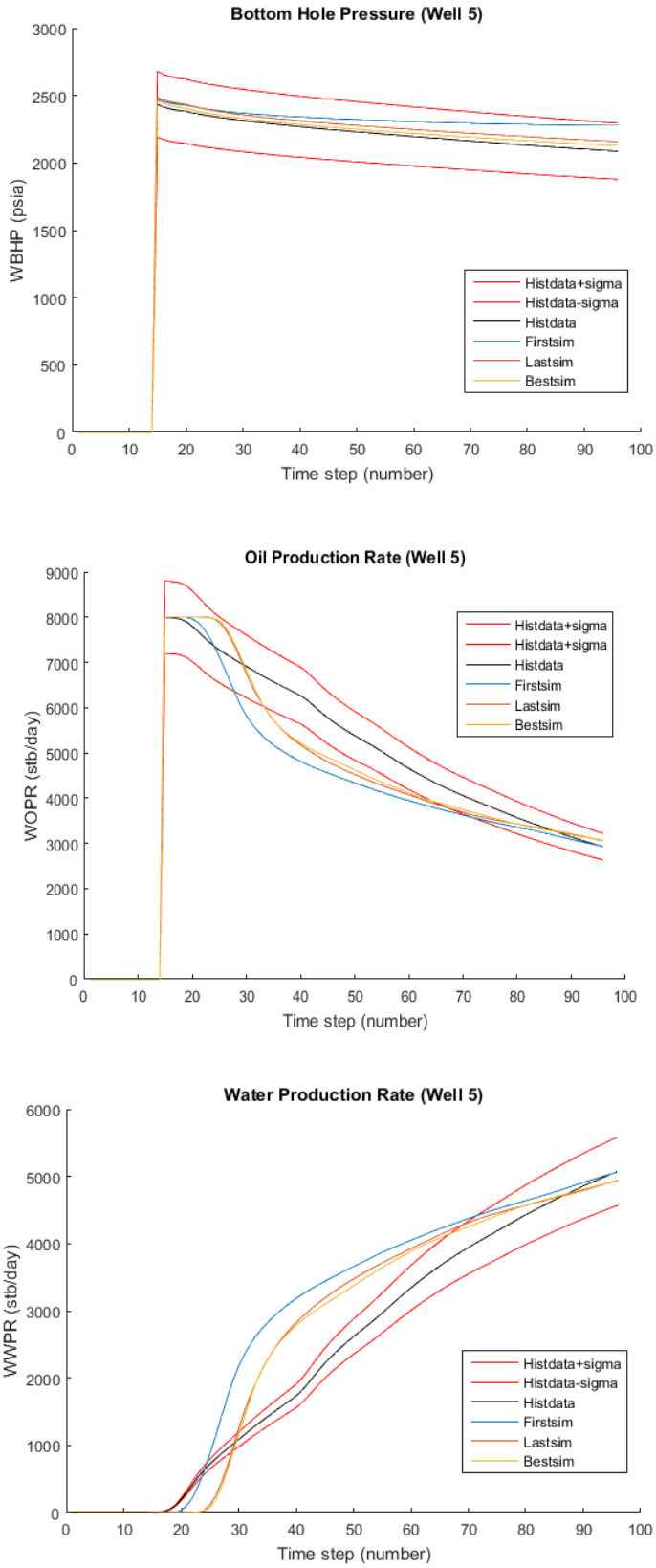

Figure 4.36: *coarse scale history matching variables Well 5. Reference model (black), First simulation (blue) last simulation (brown), best fit model (yellow). (Top) WBHP (middle) WOPR (bottom) WWPR*

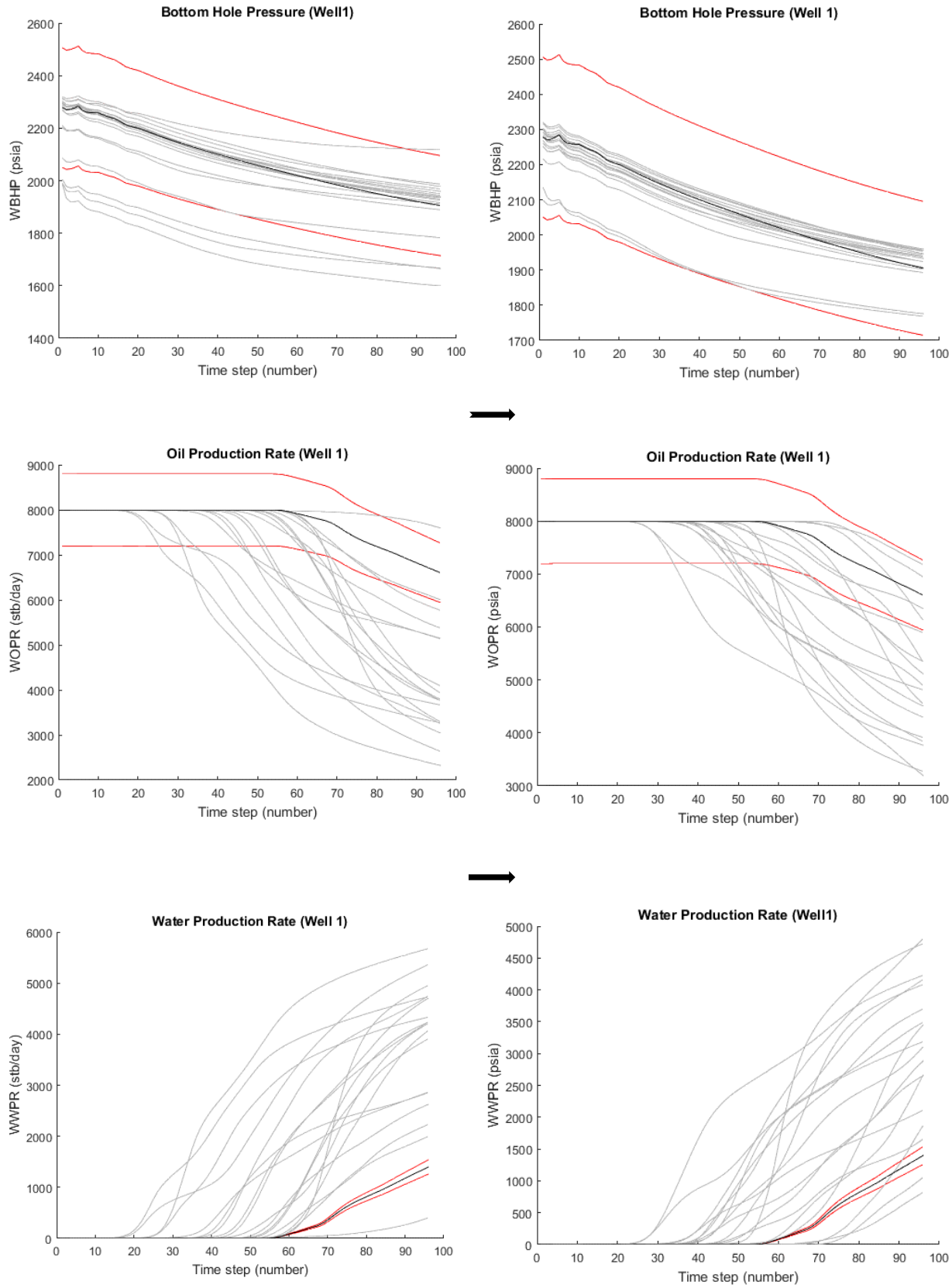

Figure 4.37: *Coarse scale production curves evolution of Well 5, (Top) WBHP, (middle) WOPR (bottom) WWPR. Iteration 1 is on the left. Iteration 6 on the right. We can see that at iteration 6 the production curves are still far apart from the history data*.

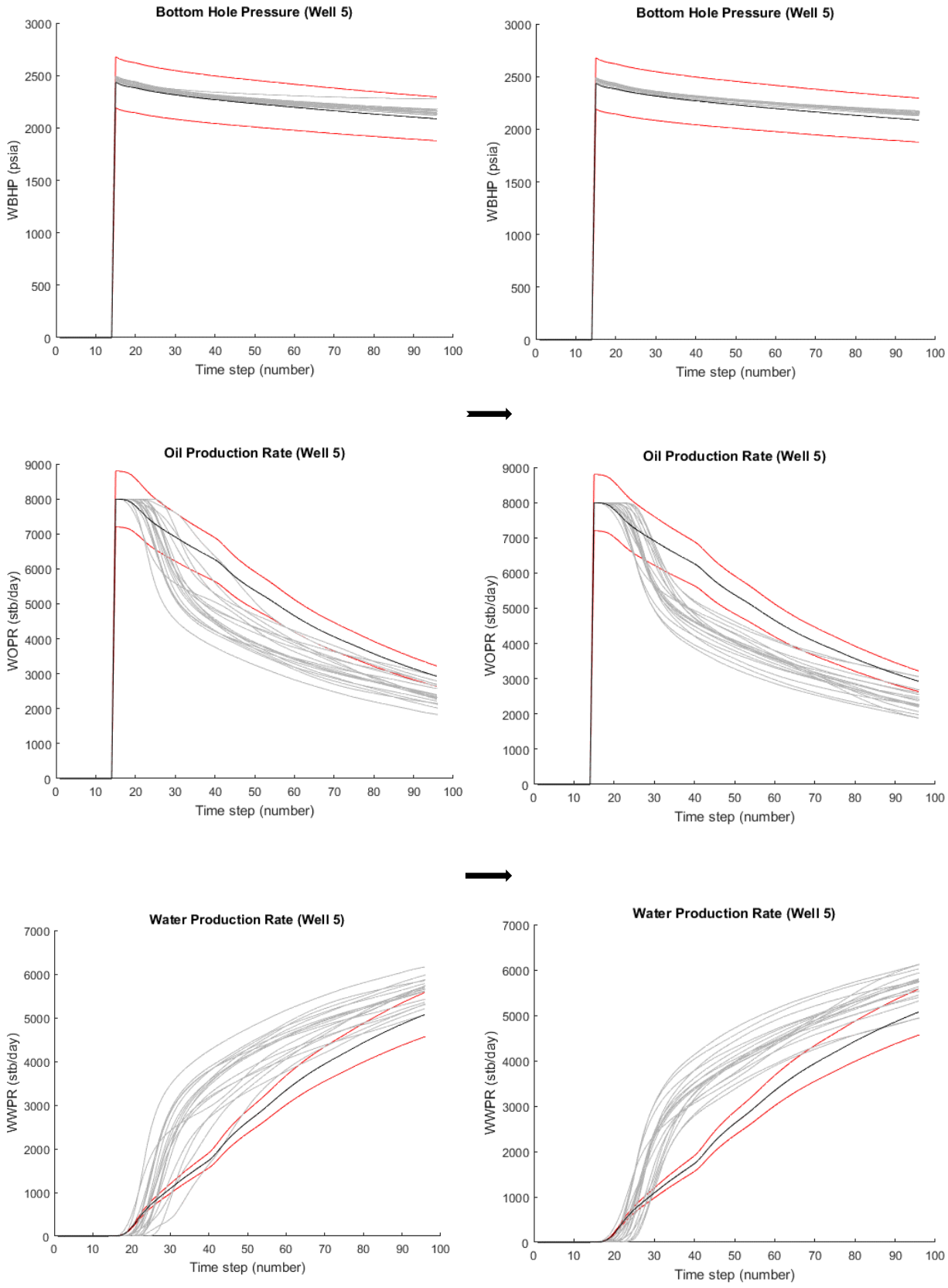

Figure 4.38: *Coarse scale production curves evolution of Well 5, (Top) WBHP, (middle) WOPR (bottom) WWPR. Iteration 1 is on the left. Iteration 6 on the right. We can see that at iteration 6 (below) the production curves are still far apart from the history data*.

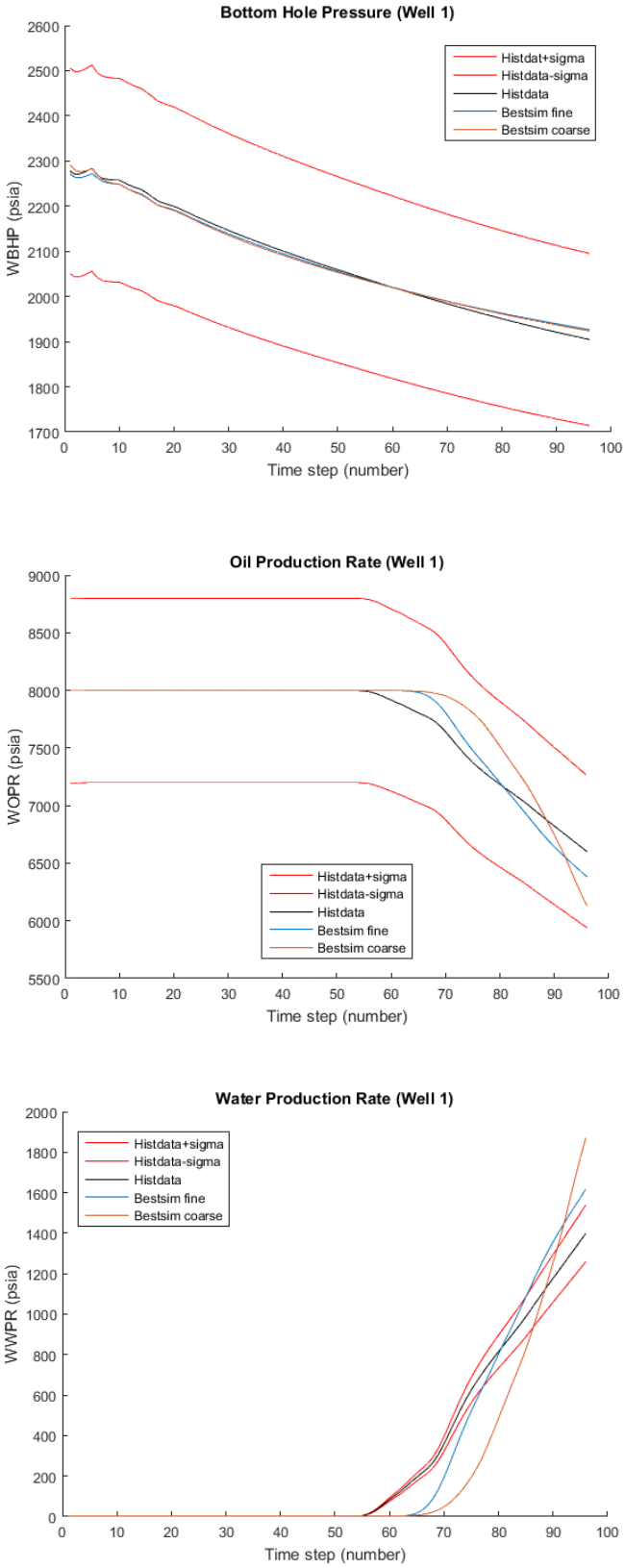

Figure 4.39: *Comparison of best fit history matching variables Well 1. Reference model (black), fine scale (blue) coarse scale (brown). (Top) WBHP (middle) WOPR (bottom) WWPR.*

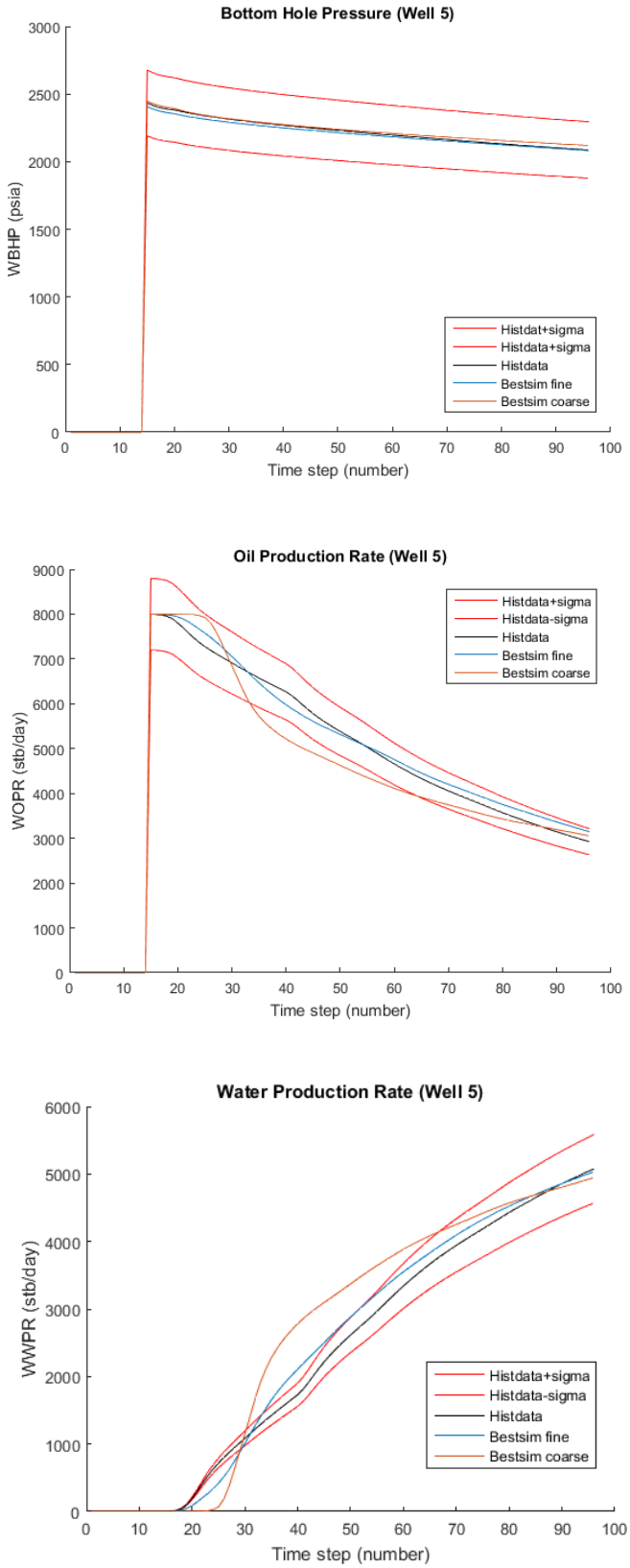

Figure 4.40: *Comparison of best fit history matching variables Well 5. Reference model (black), fine scale (blue) coarse scale (brown). (Left) WBHP (middle) WOPR (right) WWPR.*

Again we can further see this in the Objective function evolution in of both scales Figure 4.41 below.

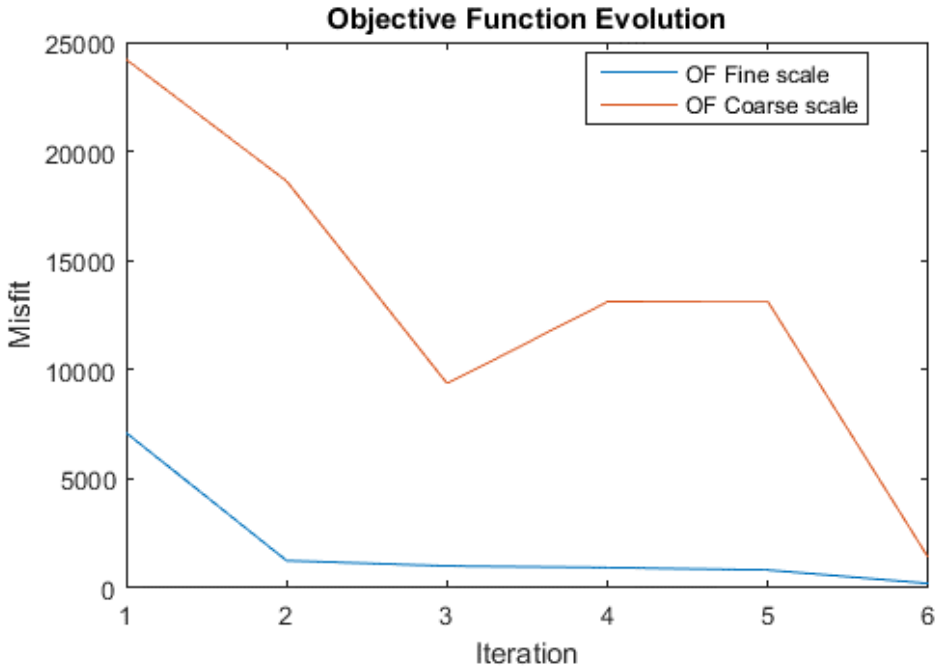

Figure 4.41**:** *comparison between the two OFs, fine scale (blue), coarse scale (red).*

5. CONCLUSION AND RECOMMENDATIONS

This thesis intended to analyse the overall performance of a geostatistical history matching on different scales, to know the CPU time as well as convergence point and the consistency in models. The main goal of the thesis was to upscale a reservoir model ensuring that it remains geologically consistent with reference model, then perform a geostatistical history matching at the different scales using co-DSS of porosity and permeability data from well log and compare results.

With stage 1 implementation of the methodology, the upscaling produced really good results as the coarse grid was geologically consistent with fine grid (reference model). The production curves after fluid flow simulation showed a high accuracy rate both in field and well variables.

On the GHM, The fine scale had a better match than the coarse scale but takes longer time to achieve a good match. The main advantage of the coarse scale over the fine scale is the processing time: It was noticed that CPU time of fine scale was cut down by over 80% in the coarse scale. This is a great improvement especially in a real life situations where senior management of companies depend on history matching results to forecast production and proceed with field development. Table 8 below shows Processing time for both scales.

Table 9: History Matching Processing Time

Scale Model	Simulation number	CPU time
Fine Scale	108	09h17m
Coarse Scale	108	39h11m

Further studies on this area could be focused towards prediction of reservoir behaviour with other types of parameter perturbation or towards its integration with seismic inversion. The methodology can also be tried on other case studies.

For Watt Field reservoir, it is concluded that not all wells have direct impact on the field performance. By studying the results further, not all the wells seen converged entirely. A recommendation would be addition of appraisal wells to aid experimental data as the reservoir is large and six (6) wells are a bit difficult to model with. This will reduce uncertainty and will help achieve better reservoir behaviour prediction. Also water production match could and should be studied further to improve match quality by other perturbation parameters or by change of production implementation strategy.

In general, the implementation of the geostatistical history matching with co-simulation is very promising since the results from areas of influence are consistent with the simulated models. In the coarse models, the major patterns are replicated even though it is without great detail. The iterative optimization assures simultaneously the match between simulated and historic production data. The well influence areas may be defined by the evaluation of the connectivity of the channels since the reservoir is dynamic the fluids

have preferential fluid paths and in non-stationary geological features such as the thickness, width and shape of deltaic reservoirs a small change can have huge impact on production forecast and match.

REFERENCES

Aanonsen, S.I (2005) Efficient History Matching Using a Multiscale Technique. 2005 SPE Reservoir Simulation Symposium, Texas, USA (31 January 2005 – 02 February 2005) https://doi.org/10.2118/92758-MS

Aanosen, S.I, and Eydinov, D. (2006). A multiscale method for distributed parameter estimation with application to reservoir history matching. Journal of Computational Physics, Vol. 10, 97-117.

Arnold, D., et al., (2013). Hierarchical benchmark case study for history matching, uncertainty quantification and reservoir characterization. Computers and Geosciences, 50, 4–15. http://doi.org/10.1016/j.cageo.2012.09.011

Al-Shamma, Basil & Gosselin, Olivier & King, Peter. (2018). History Matching Using Hybrid Parameterization and Optimization Methods. 10.2118/190776-MS.

Azevedo, L., (2013) "Geostatistical methods for integrating seismic reflection data into subsurface Earth models", PhD Thesis, Instituto Superior Técnico, Portugal.

Baker et al, (2006), History Matching Standards; Quality Control and Risk analysis for Simulation. Paper 2006-129 (Canadian International Petroleum Conference).

Barrela, E., (2016). Multiscale Geostatistical History Matching coupled with Adaptive Stochastic sampling. MSc Thesis, Instituto Superior Tecnico, Lisbon, Portugal.

Bertolini, A. & Schiozer, D. (July 2011) Influence of the objective function in the history matching process, Journal of Petroleum Science and Engineering.

Caeiro, M. H., (2014) "Optimized history matching using non-stationary geostatistical modelling", PhD Thesis, Instituto Superior Técnico, Portugal

Caers, J. (2002), History matching under geological control with the probability perturbation method, Department of Petroleum Engineering Stanford University.

Caers, J., (2011) "Modelling Uncertainty in the Earth Sciences" UK: Wiley-Blackwell

Christie, M., Demyanov, V. and Ebras, D. (2006) "Uncertainty quantification for porous media flows. Journal of computational physics, Vol. 21, No. 7 pp. 143-158.

Ertekin, T. & Abou-Kassem, J. H. and King, G. R. (2001), Basic Applied Reservoir Simulation, Society of Petroleum Engineering.

Gardet, Caroline & Le Ravalec, Mickaele & Gloaguen, Erwan. (2013). Multiscale Parameterization of Petrophysical Properties for Efficient History-Matching. Mathematical Geosciences. 46. 315-336. 10.1007/s11004-013-9480-3.

Heimhuber, R., Efficient History Matching for Reduced reservoir Models with PCE based Bootstrap Filters, in Institue for modelling hydraulic and environmental systems 2012, University Of Stuttgart: Sonthofen.

Hoffman, B. T., & Caers, J. (2003). Geostatistical History Matching Using a Regional Probability Perturbation Method. Society of Petroleum Engineers. doi:10.2118/84409-MS

Horta, A, and Soares, A., (2010) "Direct Sequential Co-Simulation with Joint Probability Distributions." Mathematical Geosciences 42: 269-292. Doi:10.1007/s11004-010-9265-x.

Ibrahim, F.A. (2012). History Matching with Reduced Parameterization and Fast Streamline-based Sensitivities. MSc Thesis, University of Bergen, Norway. http://hdl.handle.net/1956/6577

Mata-Lima, H. (2008), Reservoir characterization with iterative direct sequential co-simulation: Integrating fluid dynamic data into stochastic model, Journal of Petroleum Science and Engineering.

Maschio C., Davolio A., Correia M. G., & Schiozer, D. J., (2015) A new framework for geostatistics-based history matching using genetic algorithm with adaptive bounds. https://doi.org/10.1016/j.petrol.2015.01.033

Marques, C., (2015). Multiscale Geostatistical History Matching Using Block Direct Sequential Simulation and uncertainty quantification. MSc Thesis, Instituto Superior Tecnico, Lisbon, Portugal.

Nunes, R., Soares, A., Azevedo, L., & Pereira, P. (2016). Geostatistical Seismic Inversion with Direct Sequential Simulation and Co-simulation with Multi-local Distribution Functions. Mathematical Geosciences, 1-19.

Li, Dachang (1995). Scaling and upscaling of fluid flow through permeable media. Ph.D. dissertation 288 Austin, Texas: The University of Texas at Austin. https://trove.nla.gov.au/work/8754379

Oliveira, J., (2016). Geostatistical History Matching with seismic data integration. MSc Thesis, Instituto Superior Tecnico, Lisbon, Portugal.

Panfili, P., Cominelli, A., Calabrese, M., & Albertini, C., Savitsky, A., and Leoni, G. (2012). Advanced Upscaling for Kashagan Reservoir Modeling. SPE Reservoir Evaluation and Engineering - Spe Reserv Eval Eng. 15. 150-164. DOI: 10.2118/146508-PA.

Pereira Carneiro, J. D. T. (2010), Multi-Objective Stochastic Optimization by Co-Direct Sequential Simulation for History Matching of Oil Reservoirs, Dep. Mines, IST, Lisbon, Portugal.

Pettersen, Ø. (2006) Basics of Reservoir Simulation with the Eclipse Reservoir Simulator, Dept. of Mathematics, University of Bergen.

Qi, D., and Hesketh, T. (2005) An Analysis of Upscaling Techniques for Reservoir Simulation. Petroleum Science and Technology Vol. 23, Iss. 7-8. https://doi.org/10.1081/LFT-200033132.

Rodionov, Sergey & N. Sokolyuk, L & V. Rychkov, I. (2012). Upgridding methods in reservoir modeling. Mathematical Models and Computer Simulations. 5. 10.1134/S2070048213010092.

Rwechungura, R., Dadashpour, M., Kleppe, J. (2011) “Advanced History Matching Techniques Reviewed” SPE – 142497

Soares, Amílcar (2001) “Direct Sequential Simulation and Co-simulation” Mathematical Geology, Vol. 33, No. 8.

Streamsim (2016), Retrieved from http:///www.streamsim.com

Upscaling of grid properties in reservoir simulation (2013), Retreived from https://petrowiki.org

Appendix A **–** FLUID FLOW SIMULATION CURVES (WBHP, WOPR AND WWPR) FOR ALL WELLS

WELL 1

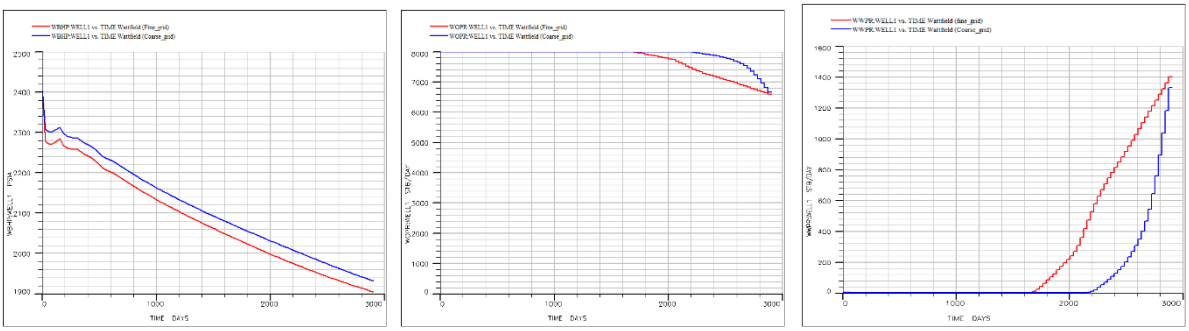

WELL 1A

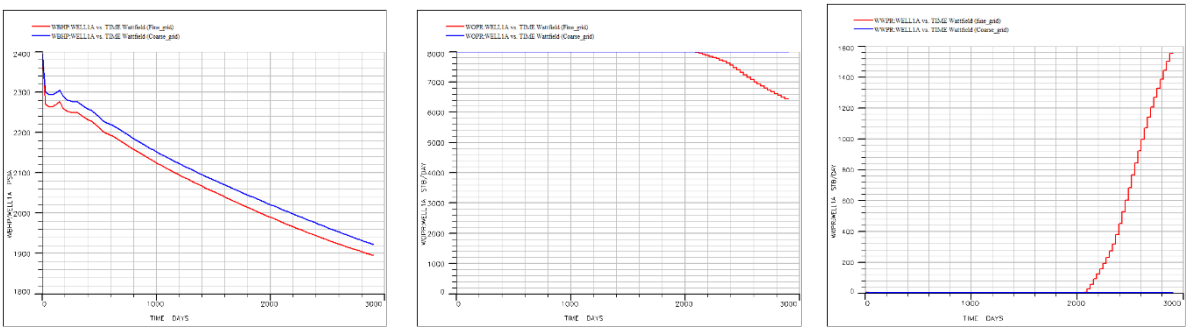

WELL 1B

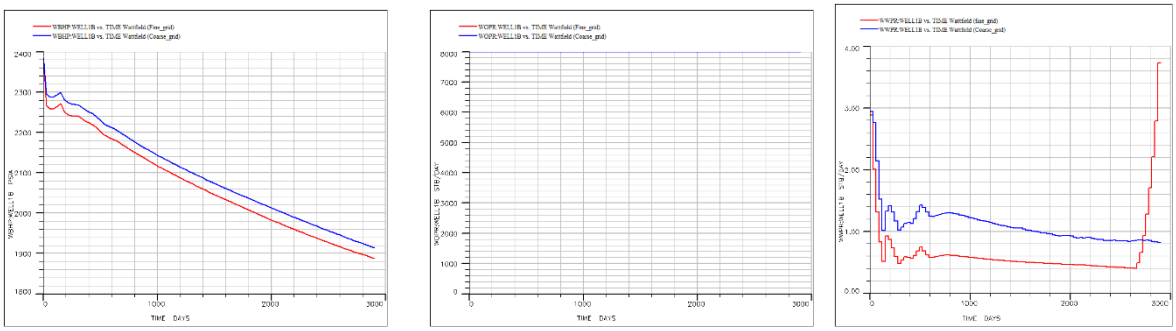

WELL 2

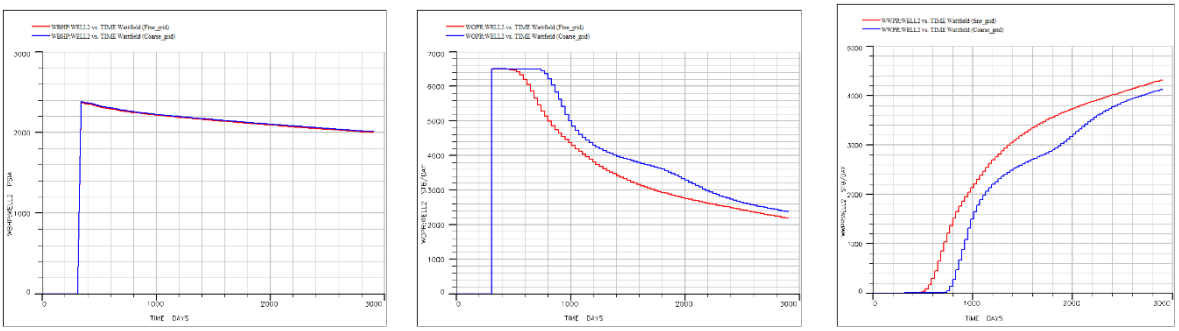

WELL 2A

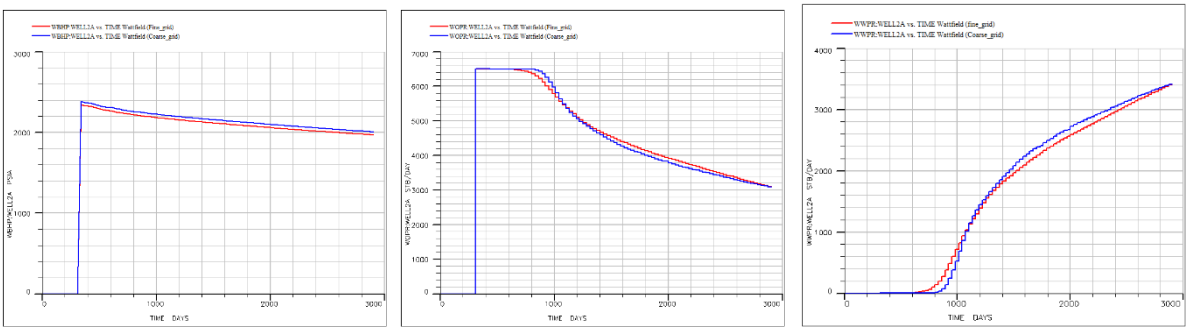

WELL 3

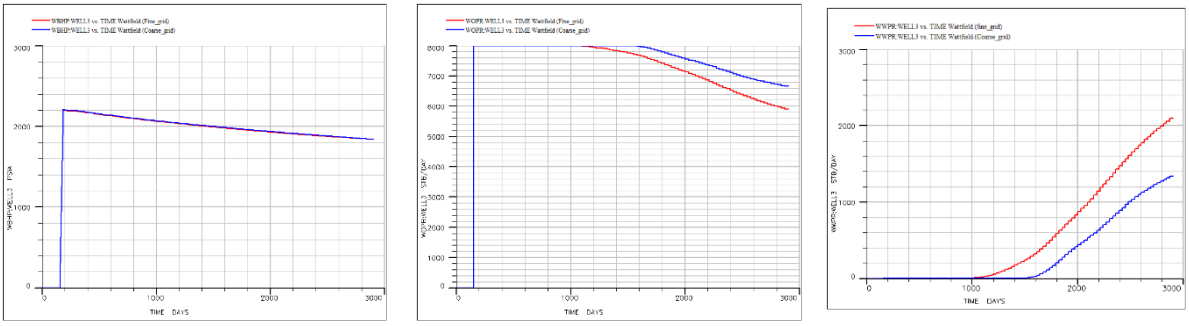

WELL 3A

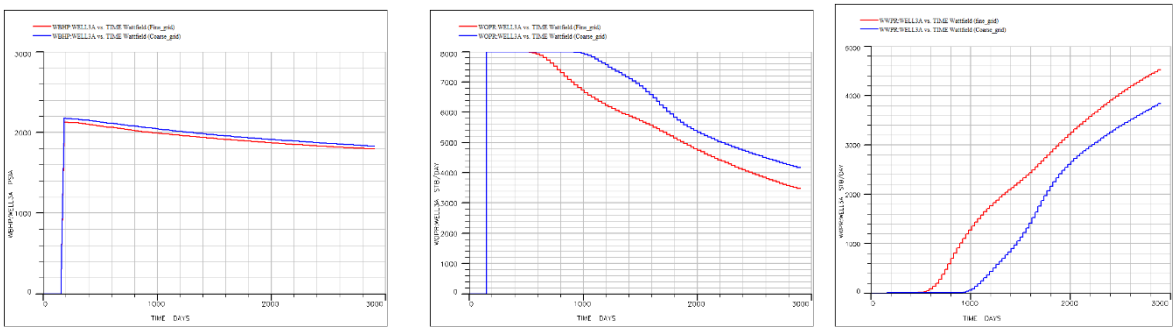

WELL 4

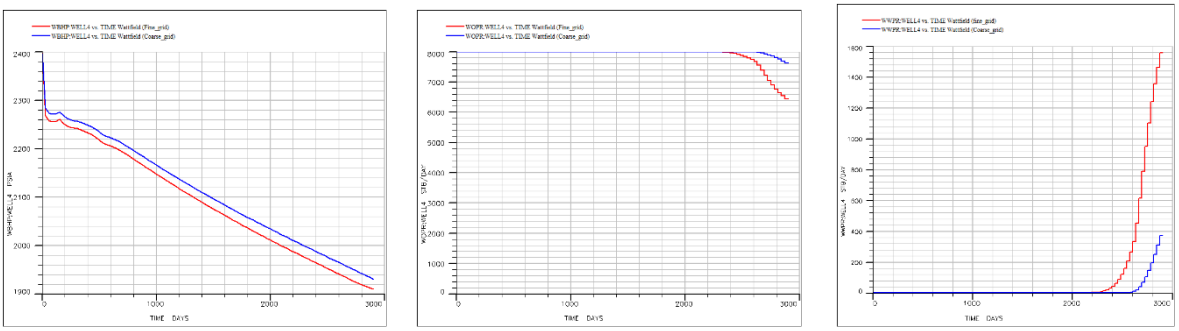

WELL 4A

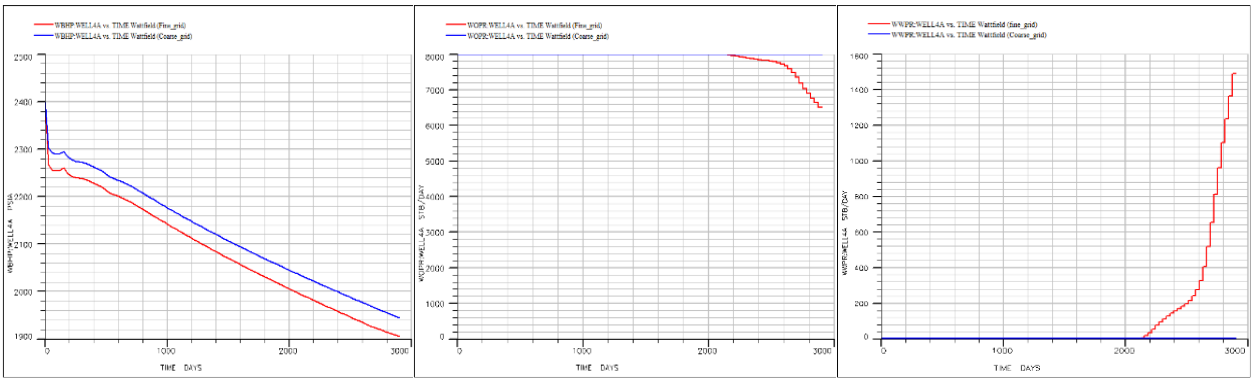

WELL 5

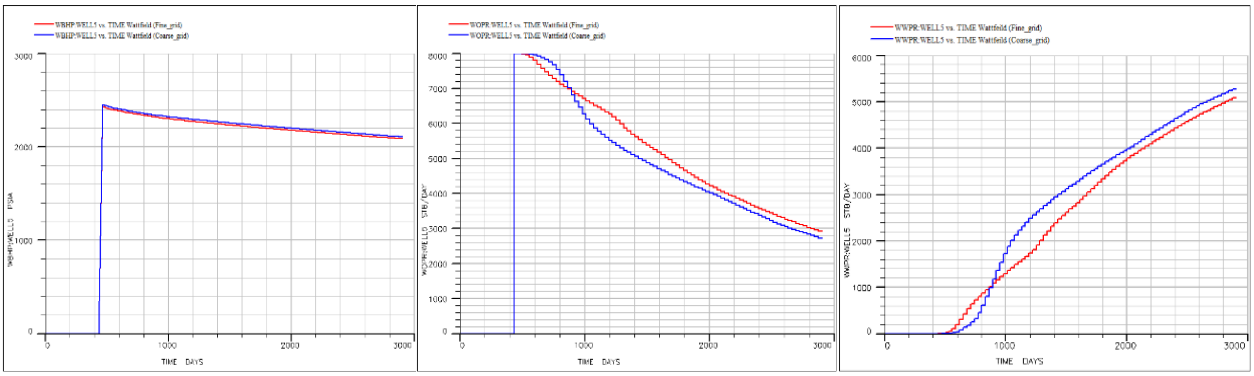

WELL 5A

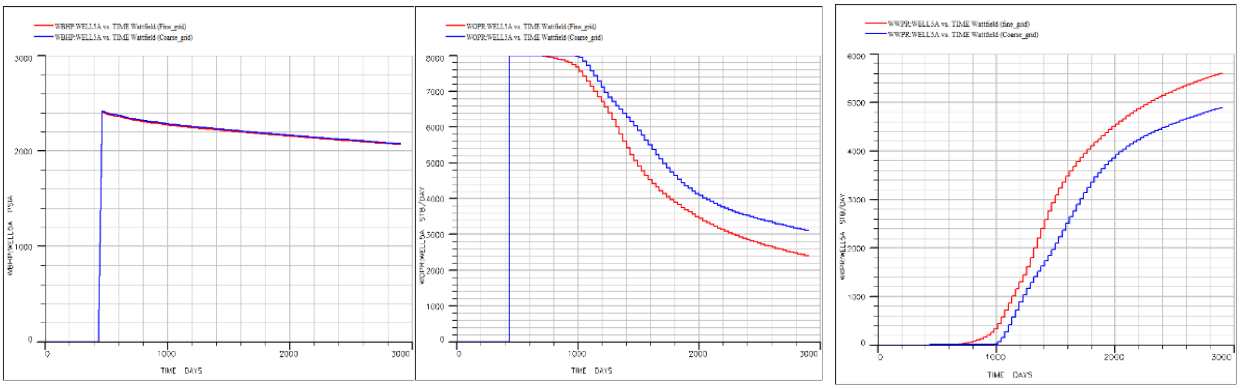

WELL 6

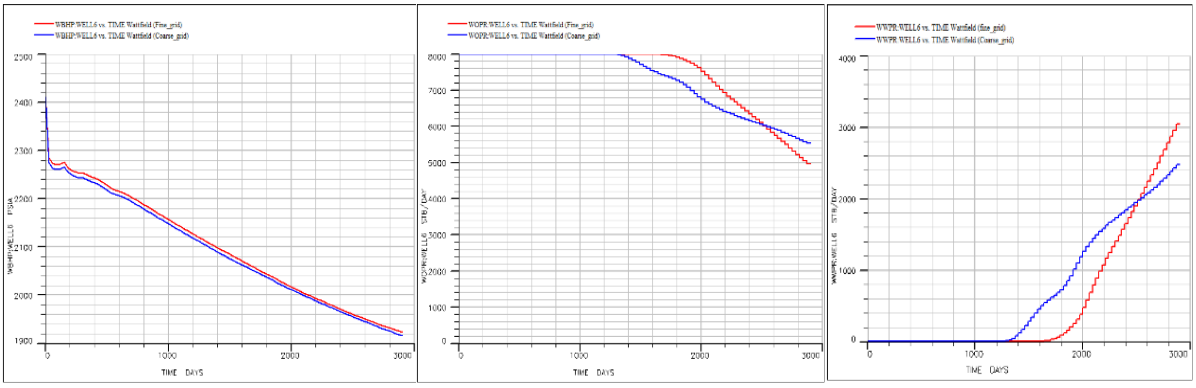

WELL7

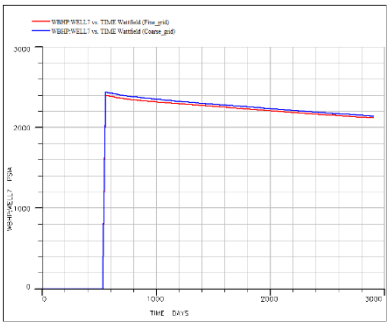
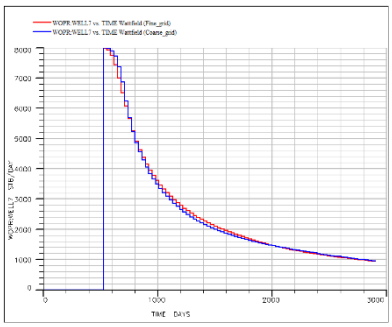
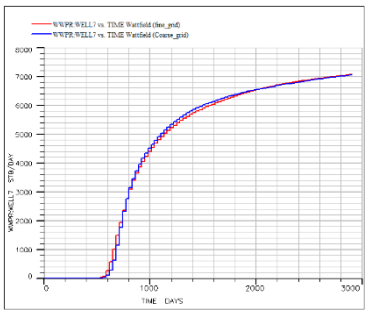

WELL 8

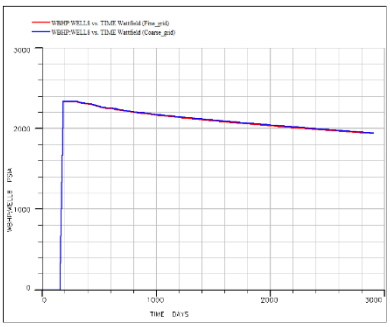
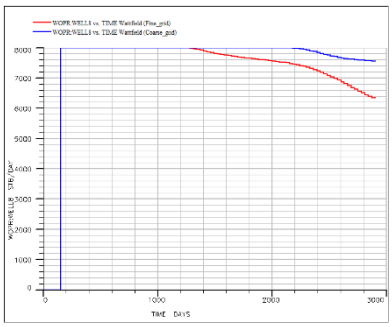
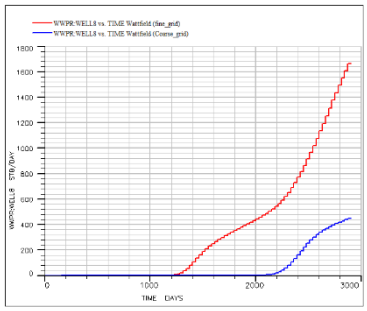

WELL 9

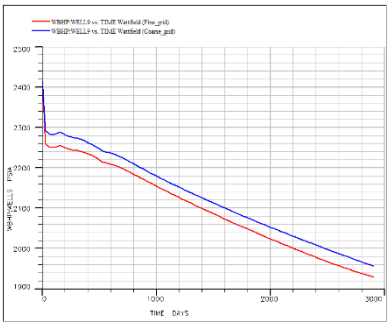
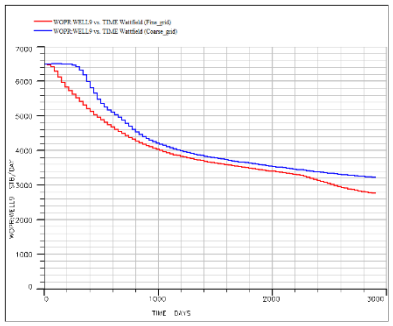
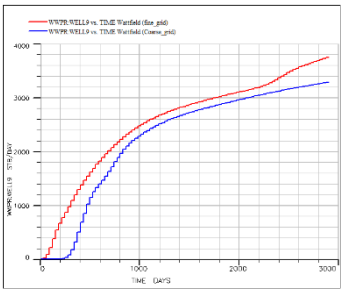

WELL 10

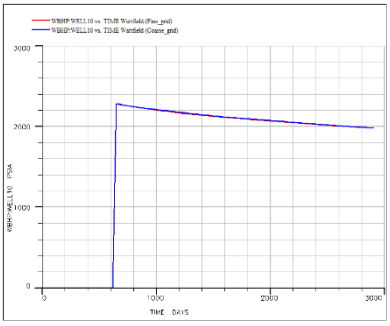
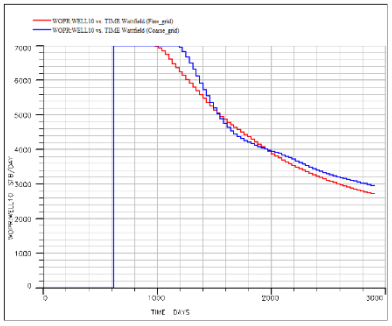
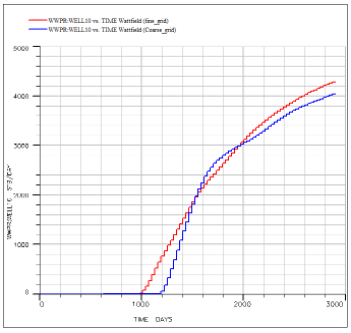

Appendix B – FINE SCALE PRODUCTION CURVES EVOLUTION (WBHP, WOPR AND WWPR) FOR ALL WELLS. ITERATION 1 LEFT ITERATION 6 RIGHT

WELL 1

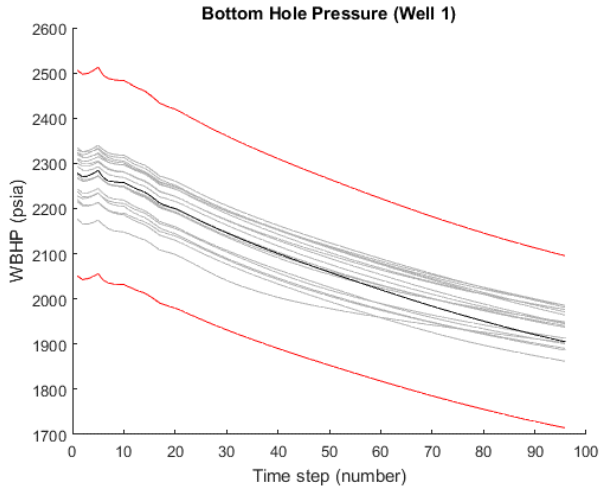

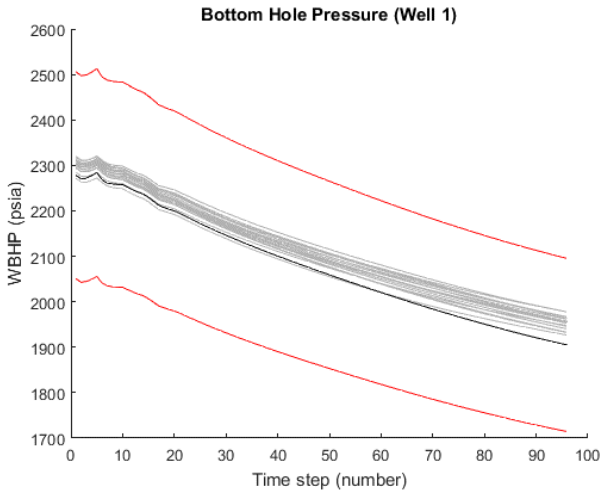

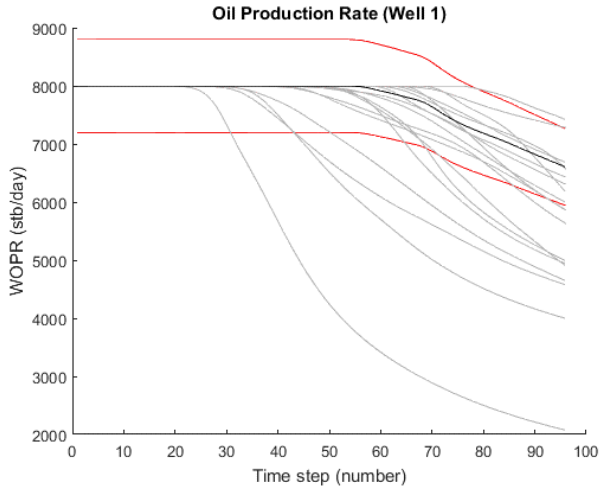

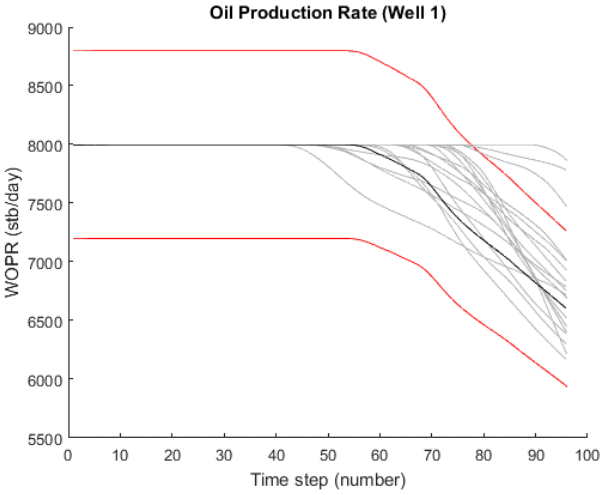

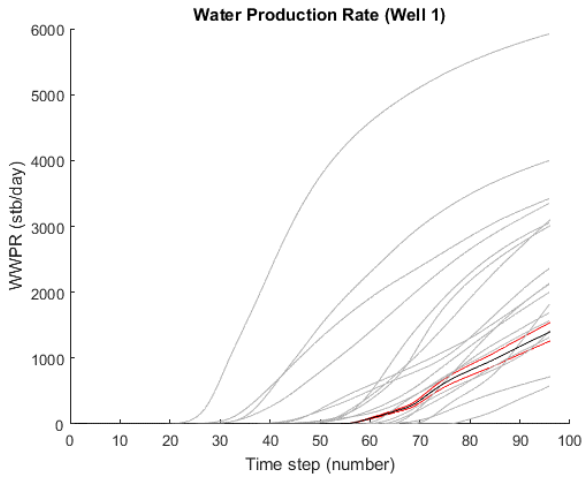

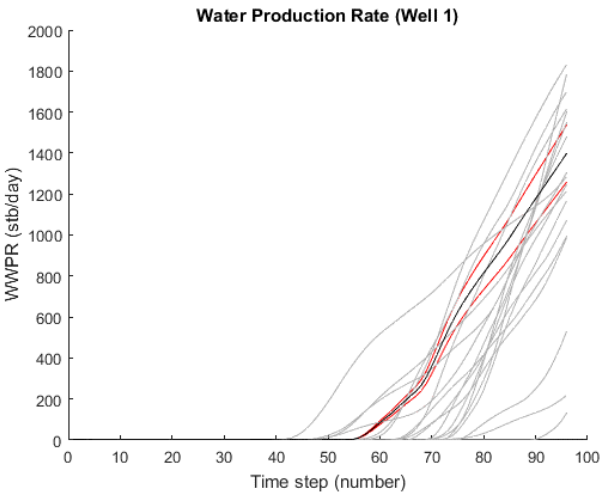

WELL 1A

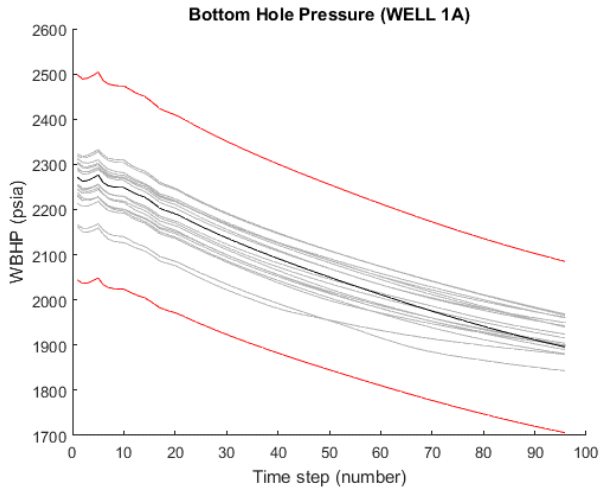
Bottom Hole Pressure (WELL 1A)
WBHP (psia)
Time step (number)

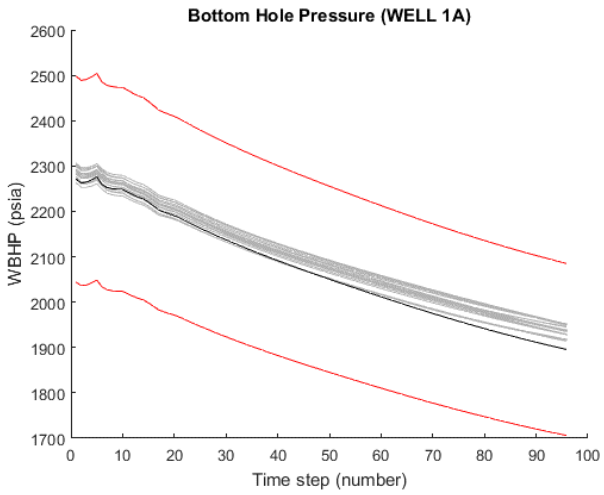
Bottom Hole Pressure (WELL 1A)
WBHP (psia)
Time step (number)

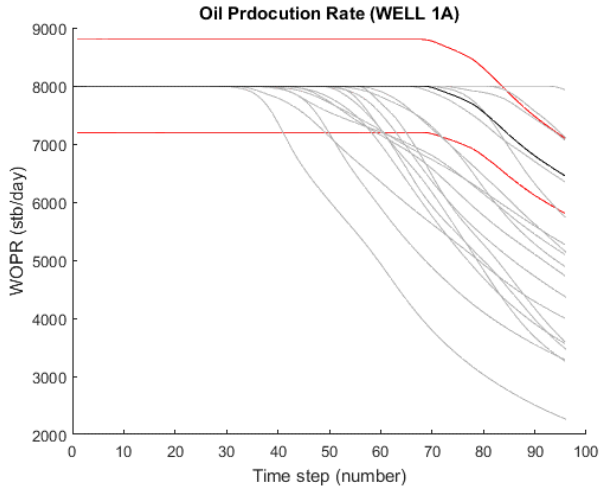
Oil Prdocution Rate (WELL 1A)
WOPR (stb/day)
Time step (number)

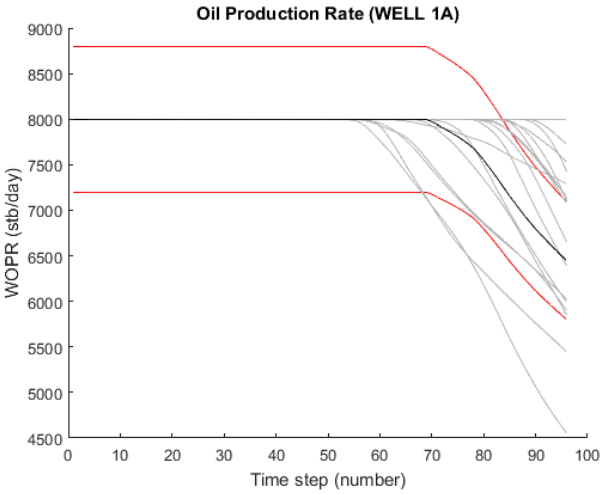
Oil Production Rate (WELL 1A)
WOPR (stb/day)
Time step (number)

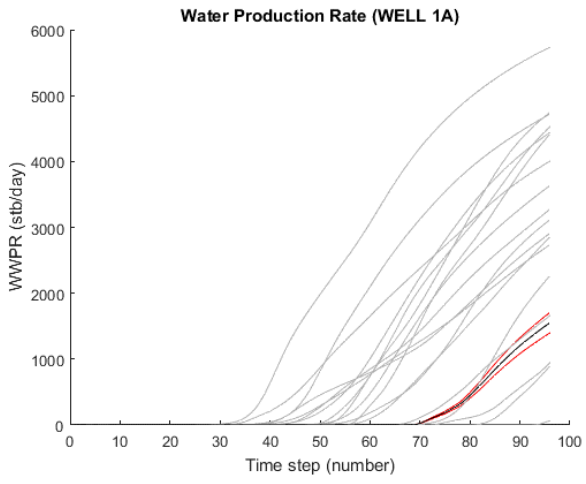
Water Production Rate (WELL 1A)
WWPR (stb/day)
Time step (number)

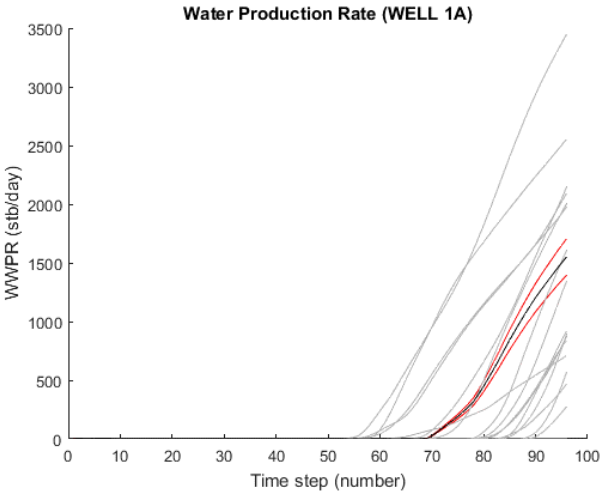
Water Production Rate (WELL 1A)
WWPR (stb/day)
Time step (number)

WELL 1B

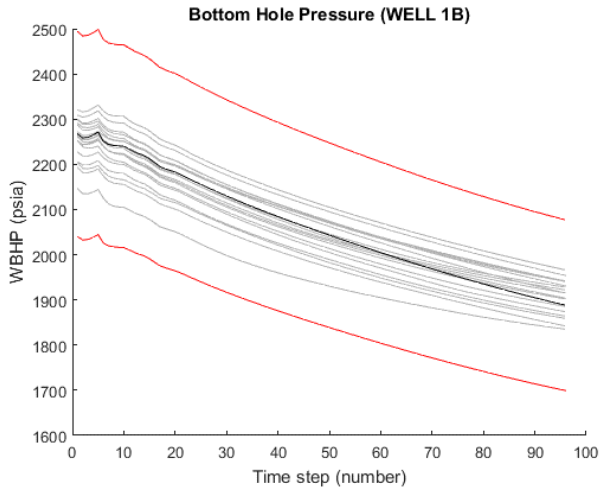
Bottom Hole Pressure (WELL 1B)
WBHP (psia)
Time step (number)

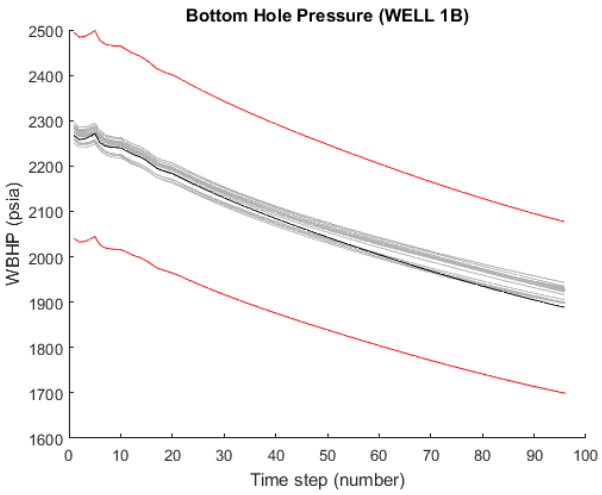
Bottom Hole Pressure (WELL 1B)
WBHP (psia)
Time step (number)

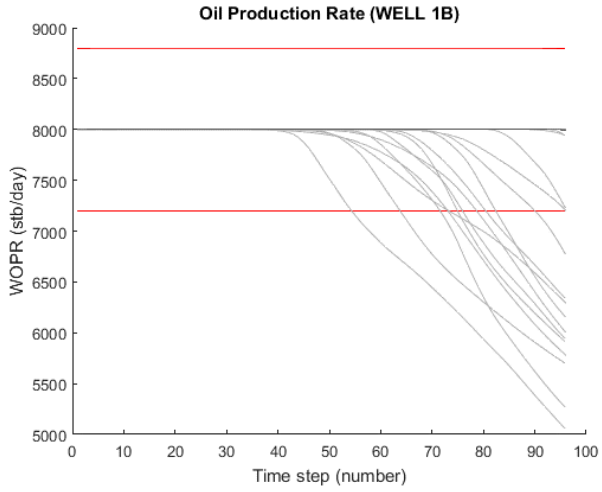
Oil Production Rate (WELL 1B)
WOPR (stb/day)
Time step (number)

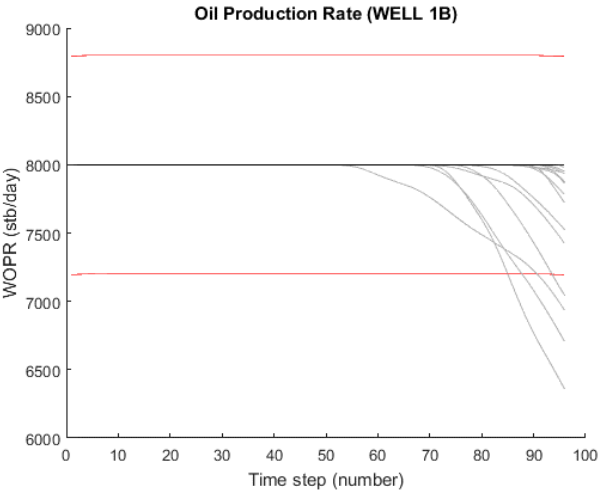
Oil Production Rate (WELL 1B)
WOPR (stb/day)
Time step (number)

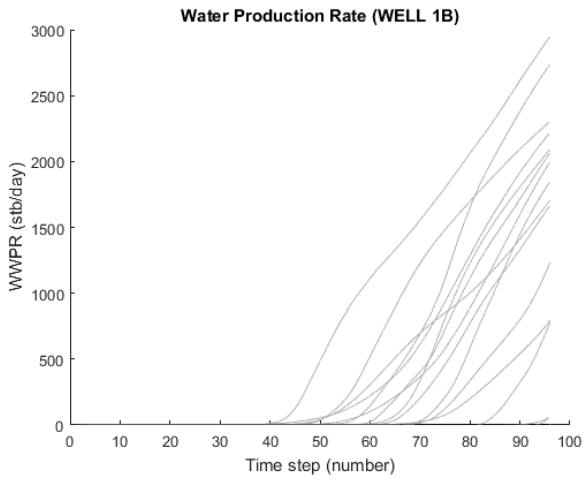
Water Production Rate (WELL 1B)
WWPR (stb/day)
Time step (number)

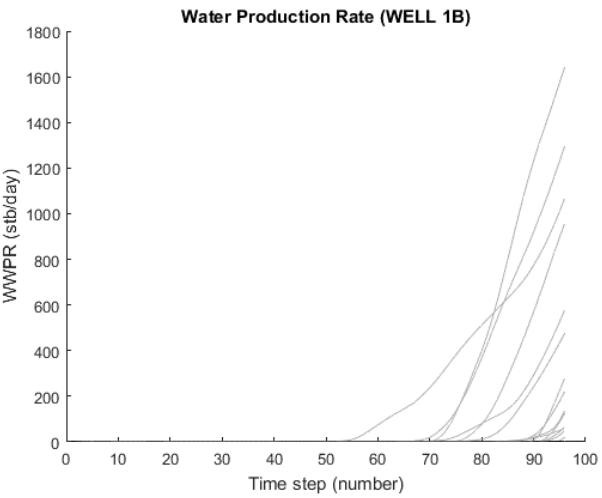
Water Production Rate (WELL 1B)
WWPR (stb/day)
Time step (number)

WELL 2

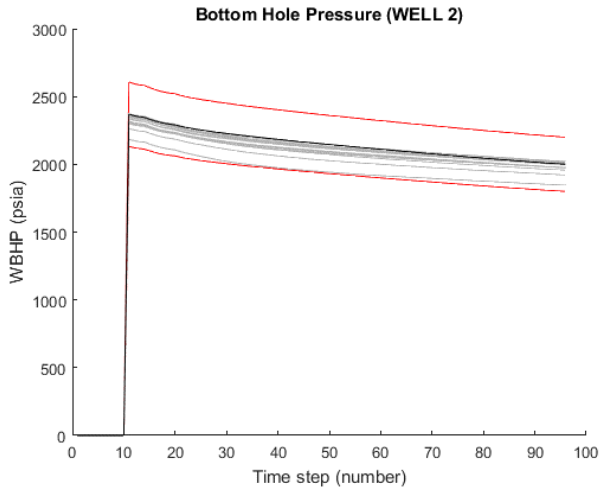
Bottom Hole Pressure (WELL 2)
WBHP (psia)
Time step (number)

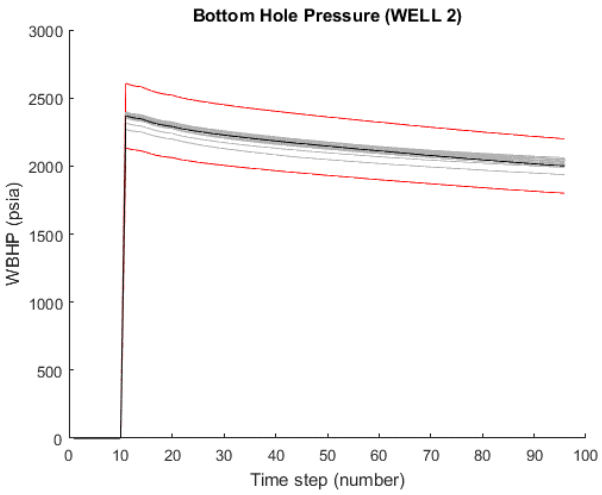
Bottom Hole Pressure (WELL 2)
WBHP (psia)
Time step (number)

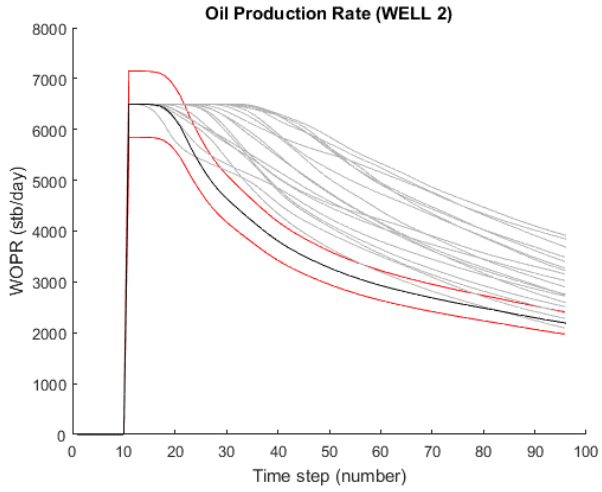
Oil Production Rate (WELL 2)
WOPR (stb/day)
Time step (number)

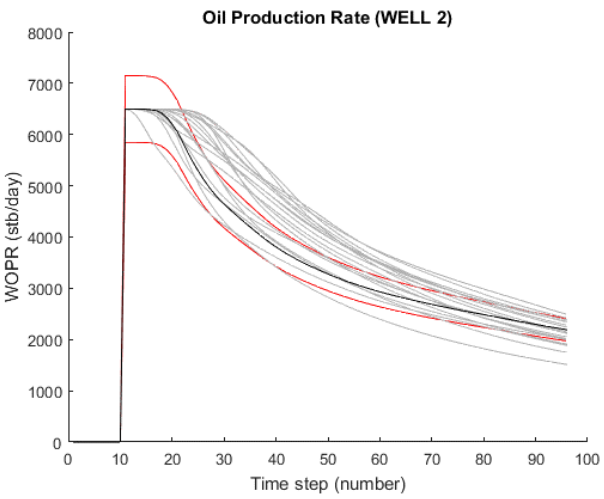
Oil Production Rate (WELL 2)
WOPR (stb/day)
Time step (number)

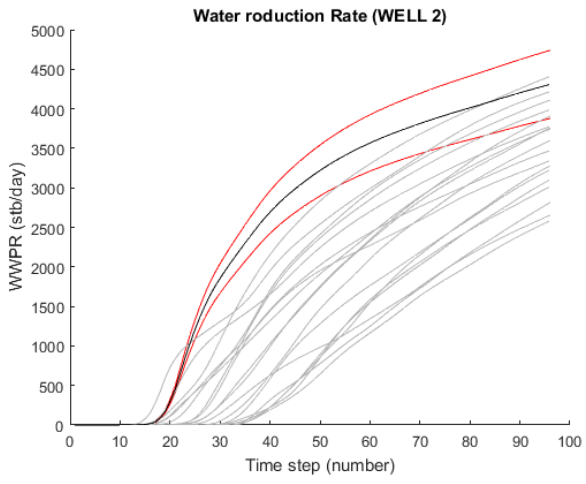
Water roduction Rate (WELL 2)
WWPR (stb/day)
Time step (number)

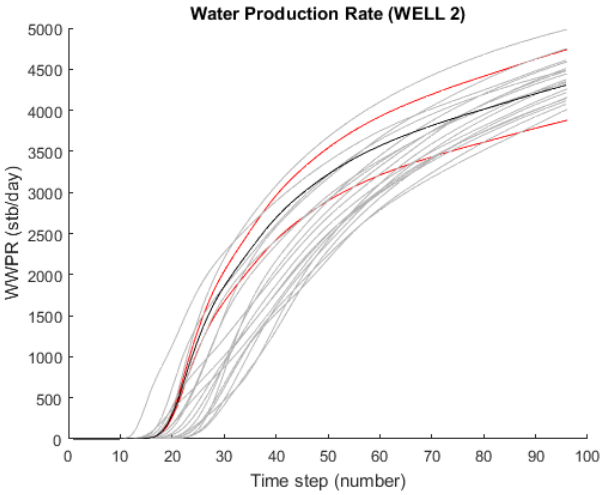
Water Production Rate (WELL 2)
WWPR (stb/day)
Time step (number)

WELL 2A

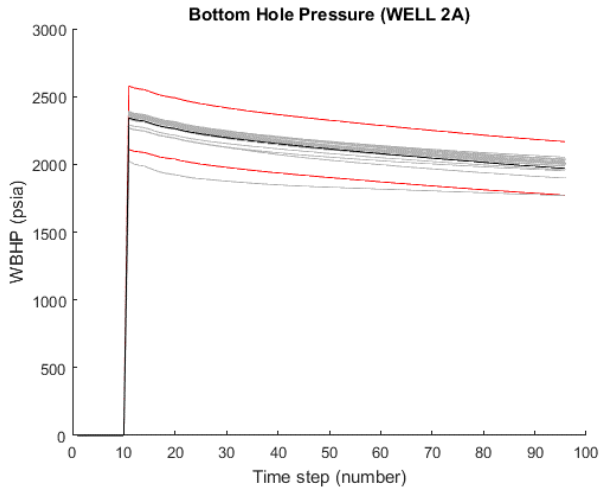
Bottom Hole Pressure (WELL 2A)
WBHP (psia)
Time step (number)

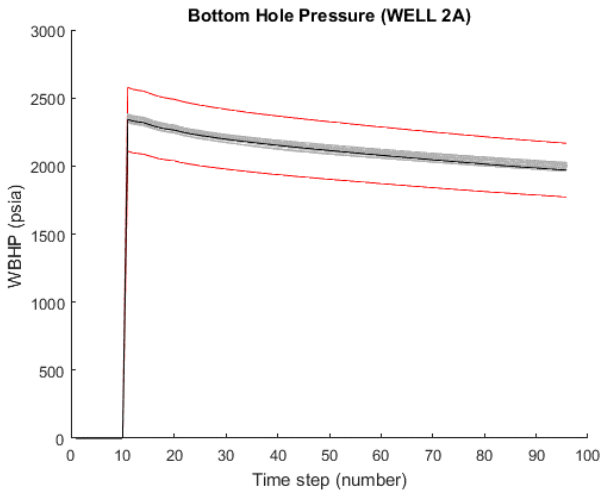
Bottom Hole Pressure (WELL 2A)
WBHP (psia)
Time step (number)

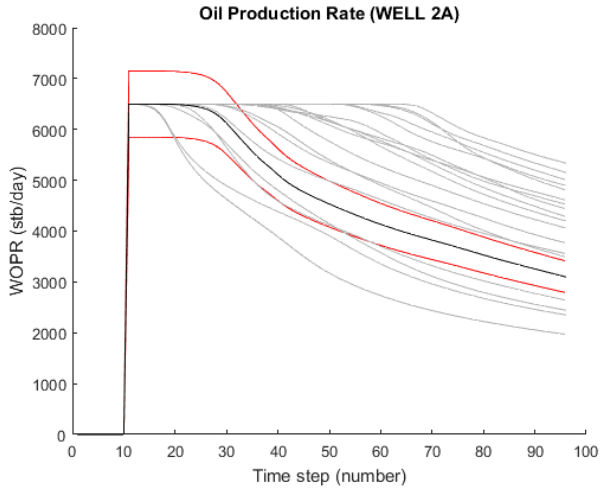
Oil Production Rate (WELL 2A)
WOPR (stb/day)
Time step (number)

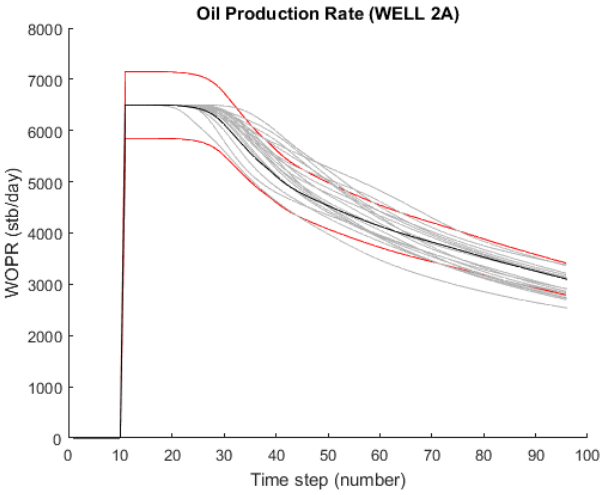
Oil Production Rate (WELL 2A)
WOPR (stb/day)
Time step (number)

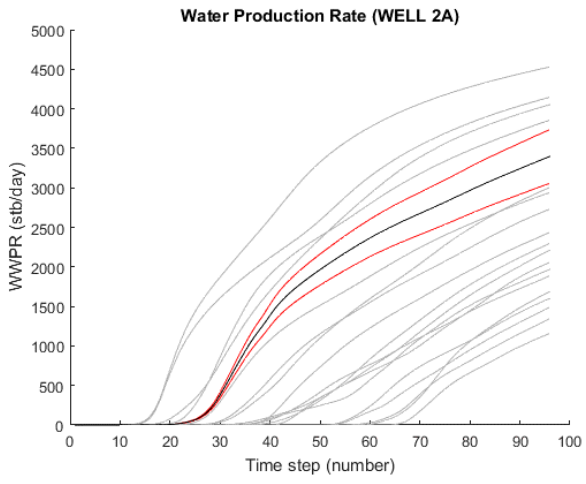
Water Production Rate (WELL 2A)
WWPR (stb/day)
Time step (number)

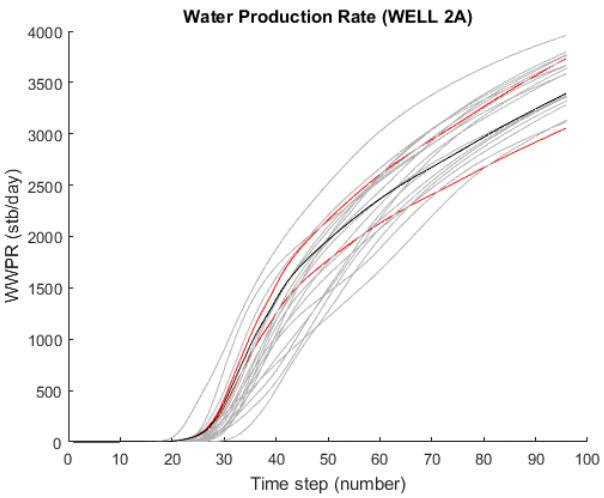
Water Production Rate (WELL 2A)
WWPR (stb/day)
Time step (number)

WELL 3

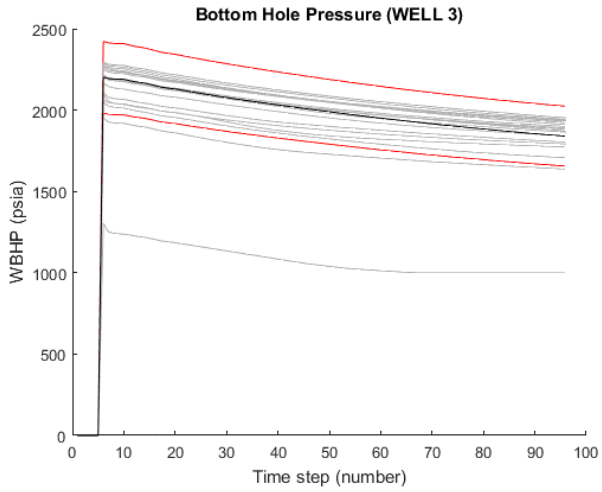
Bottom Hole Pressure (WELL 3)
WBHP (psia)
Time step (number)

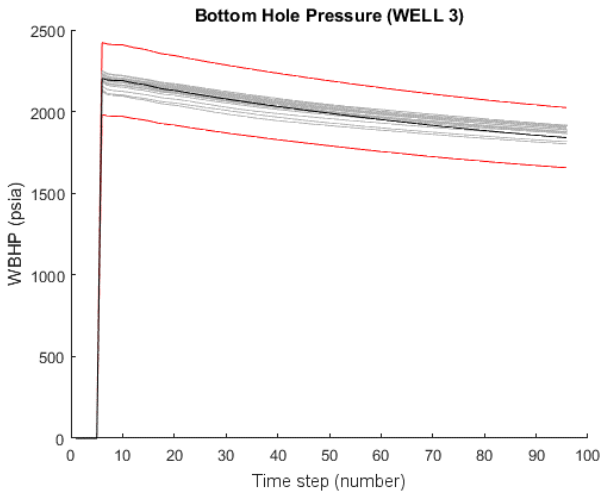
Bottom Hole Pressure (WELL 3)
WBHP (psia)
Time step (number)

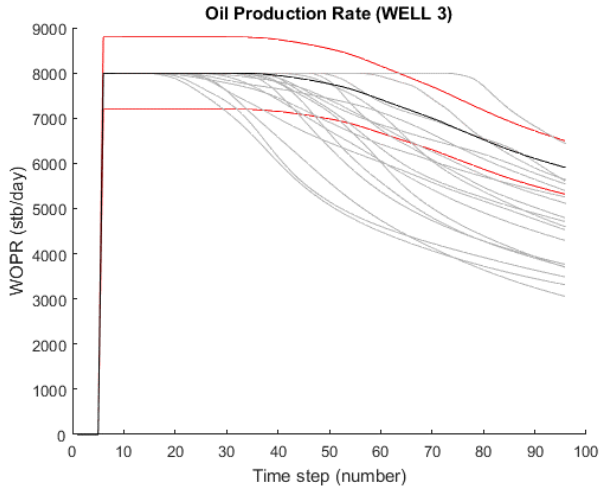
Oil Production Rate (WELL 3)
WOPR (stb/day)
Time step (number)

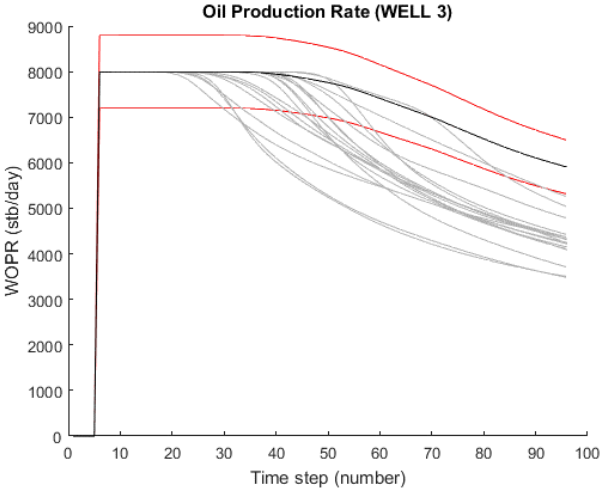
Oil Production Rate (WELL 3)
WOPR (stb/day)
Time step (number)

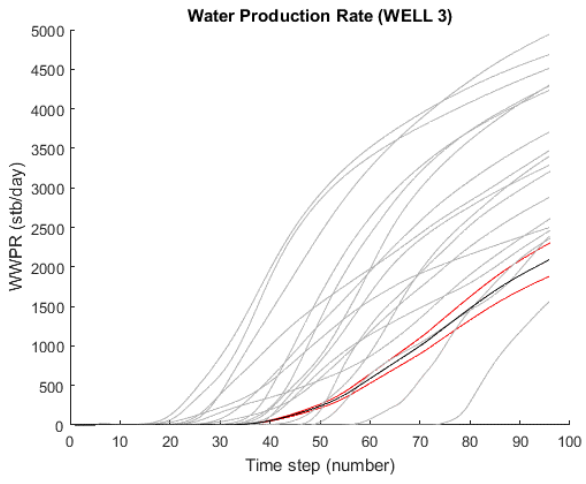
Water Production Rate (WELL 3)
WWPR (stb/day)
Time step (number)

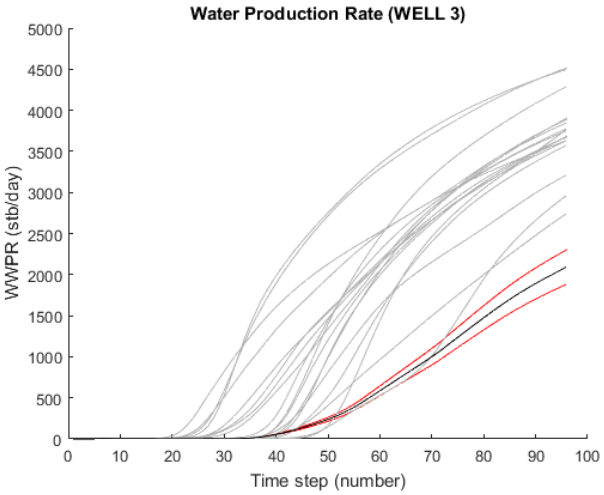
Water Production Rate (WELL 3)
WWPR (stb/day)
Time step (number)

WELL 3A

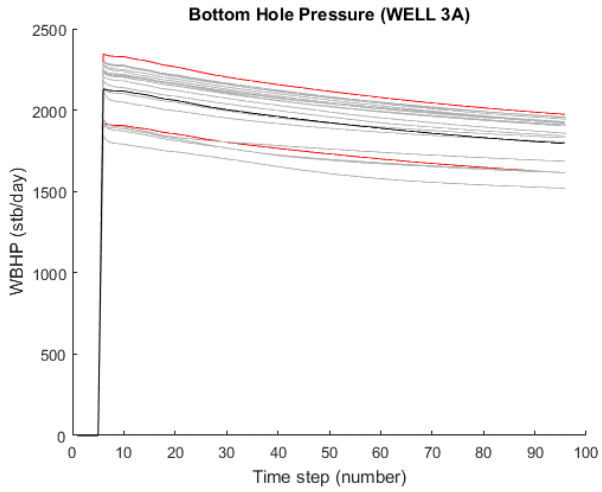
Bottom Hole Pressure (WELL 3A)
WBHP (stb/day)
Time step (number)

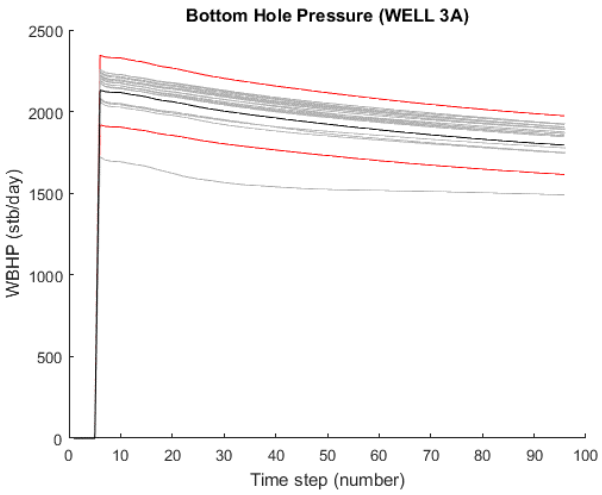
Bottom Hole Pressure (WELL 3A)
WBHP (stb/day)
Time step (number)

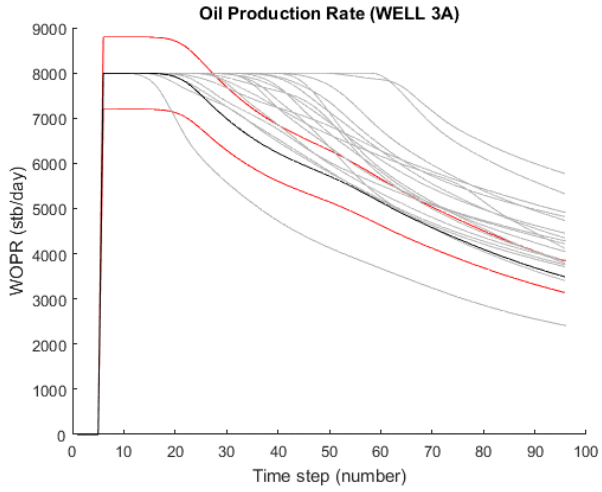
Oil Production Rate (WELL 3A)
WOPR (stb/day)
Time step (number)

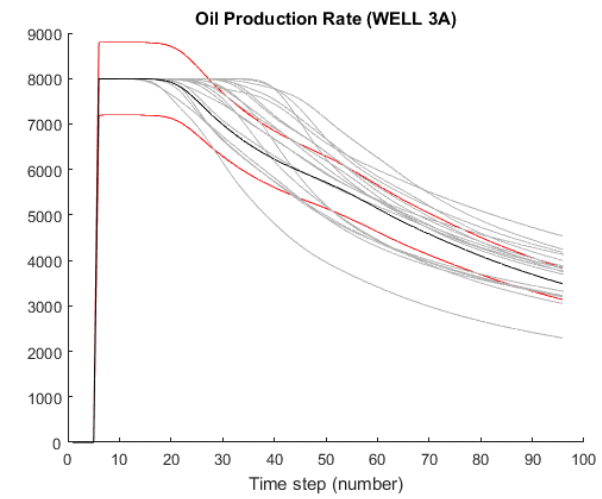
Oil Production Rate (WELL 3A)
Time step (number)

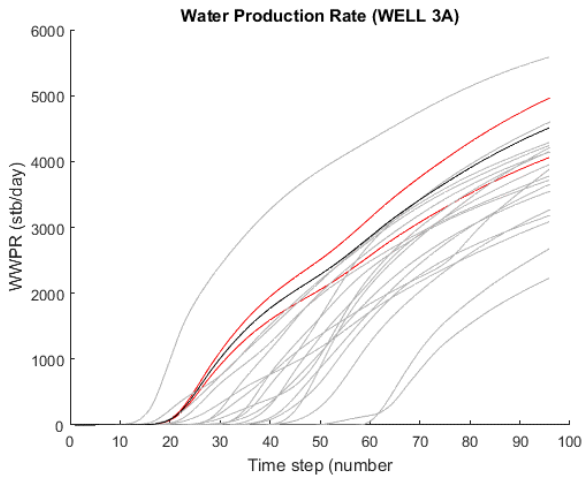
Water Production Rate (WELL 3A)
WWPR (stb/day)
Time step (number

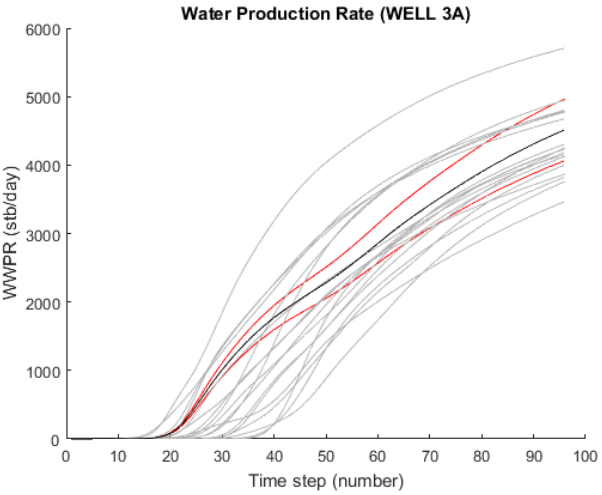
Water Production Rate (WELL 3A)
WWPR (stb/day)
Time step (number)

WELL 4

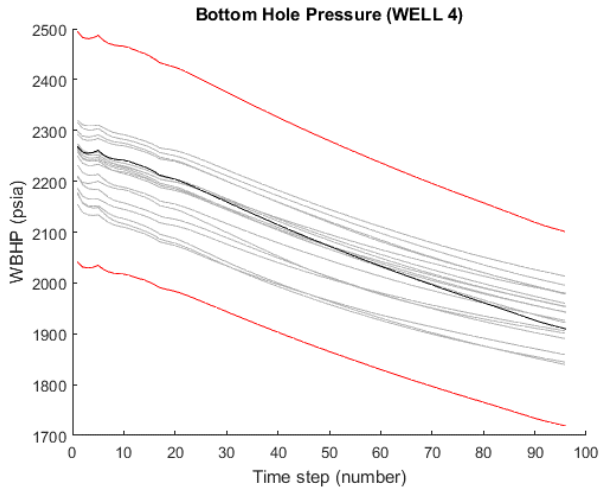
Bottom Hole Pressure (WELL 4)
WBHP (psia)
Time step (number)

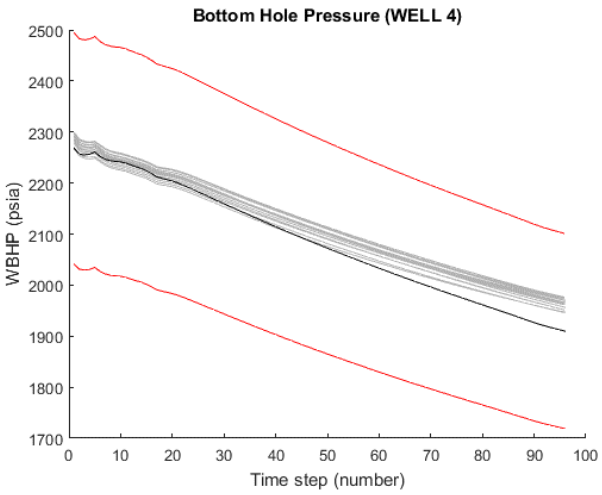
Bottom Hole Pressure (WELL 4)
WBHP (psia)
Time step (number)

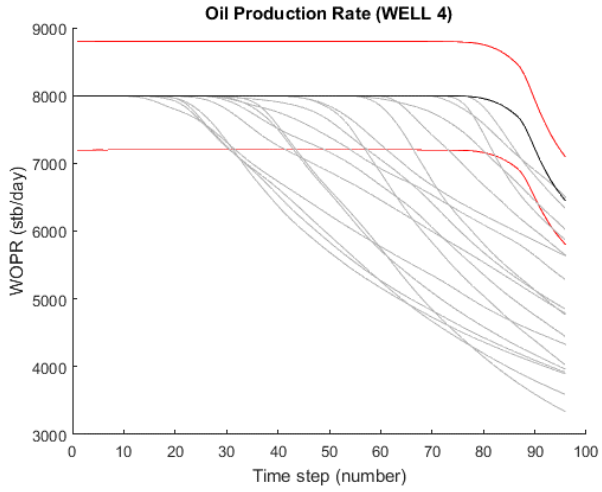
Oil Production Rate (WELL 4)
WOPR (stb/day)
Time step (number)

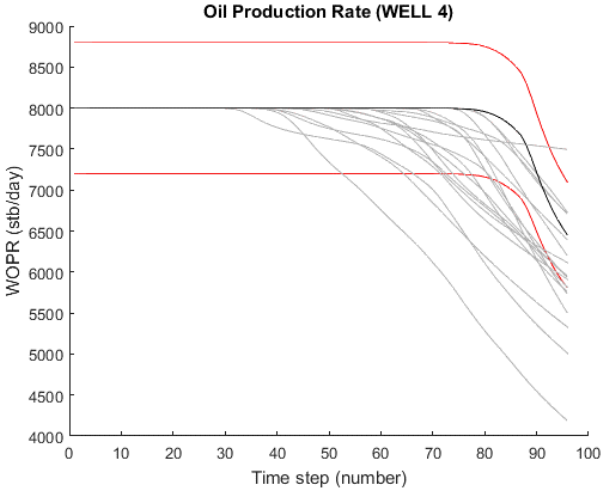
Oil Production Rate (WELL 4)
WOPR (stb/day)
Time step (number)

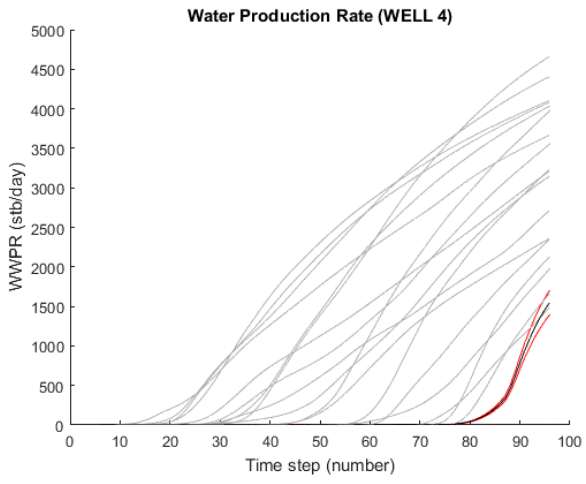
Water Production Rate (WELL 4)
WWPR (stb/day)
Time step (number)

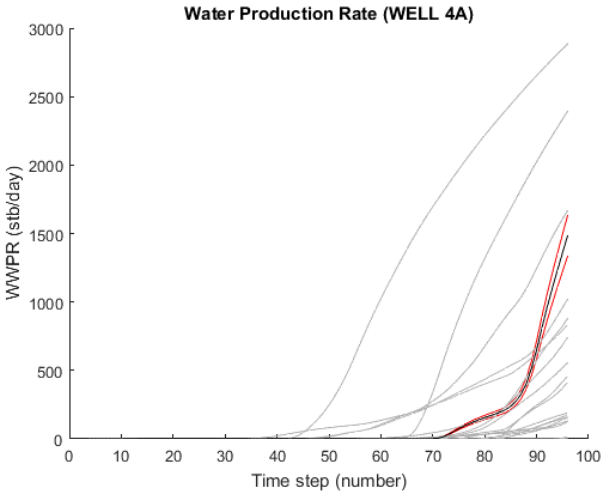
Water Production Rate (WELL 4A)
WWPR (stb/day)
Time step (number)

WELL 4A

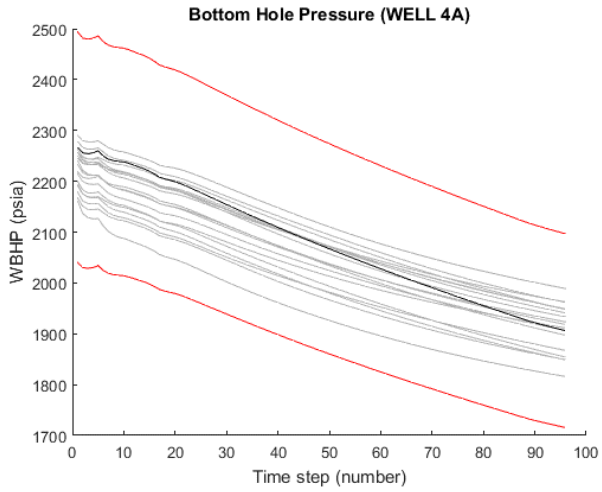
Bottom Hole Pressure (WELL 4A)
WBHP (psia)
Time step (number)

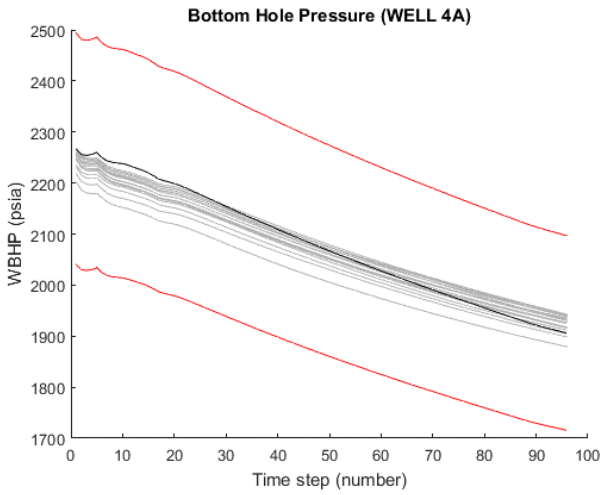
Bottom Hole Pressure (WELL 4A)
WBHP (psia)
Time step (number)

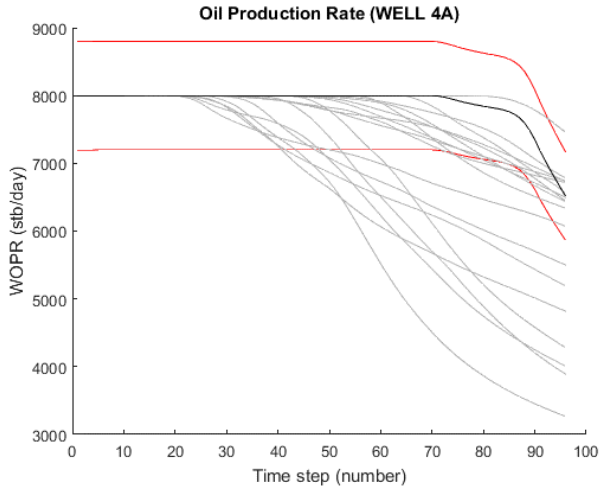
Oil Production Rate (WELL 4A)
WOPR (stb/day)
Time step (number)

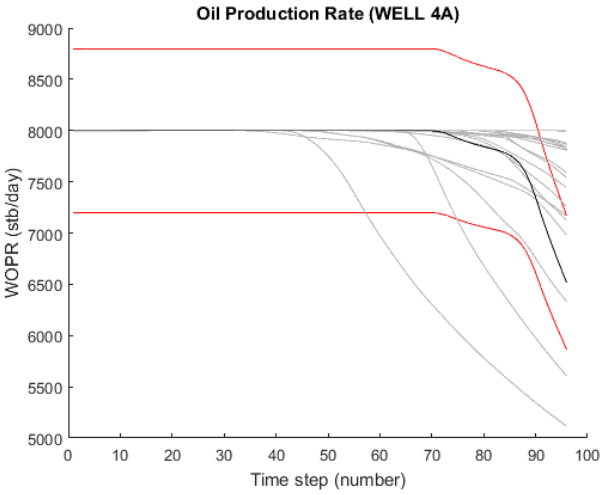
Oil Production Rate (WELL 4A)
WOPR (stb/day)
Time step (number)

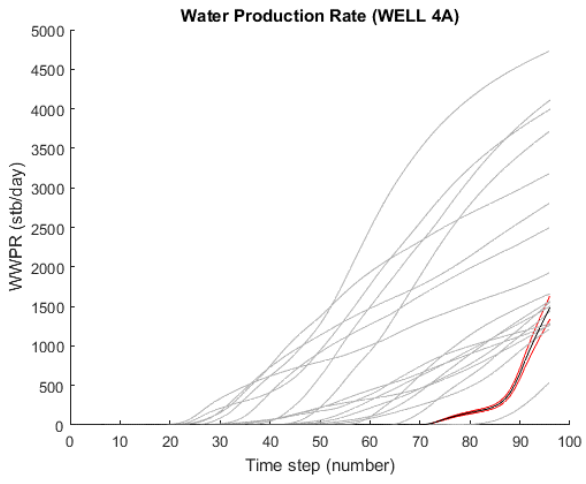
Water Production Rate (WELL 4A)
WWPR (stb/day)
Time step (number)

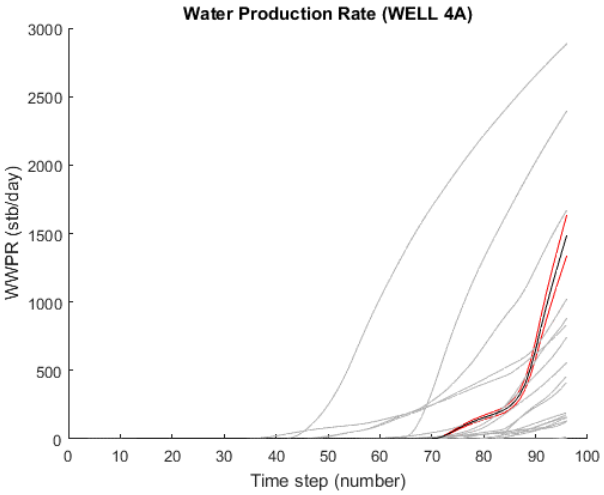
Water Production Rate (WELL 4A)
WWPR (stb/day)
Time step (number)

WELL 5

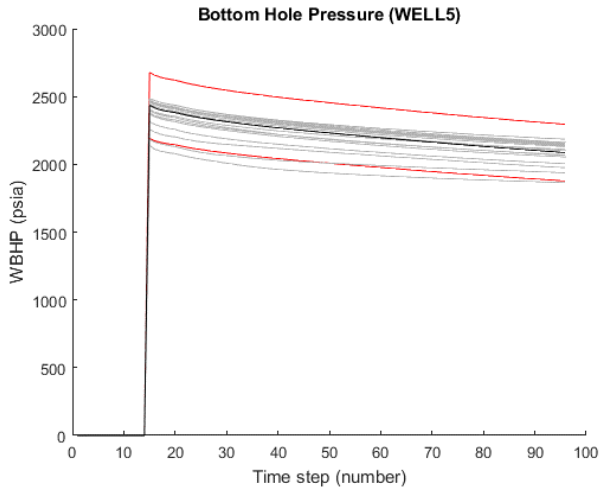
Bottom Hole Pressure (WELL5)
WBHP (psia)
Time step (number)

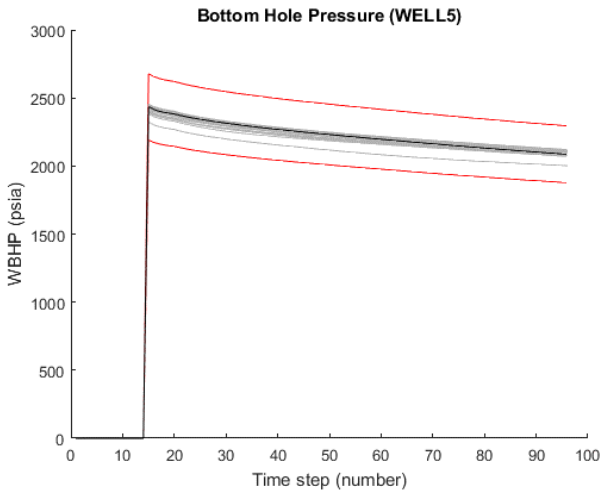
Bottom Hole Pressure (WELL5)
WBHP (psia)
Time step (number)

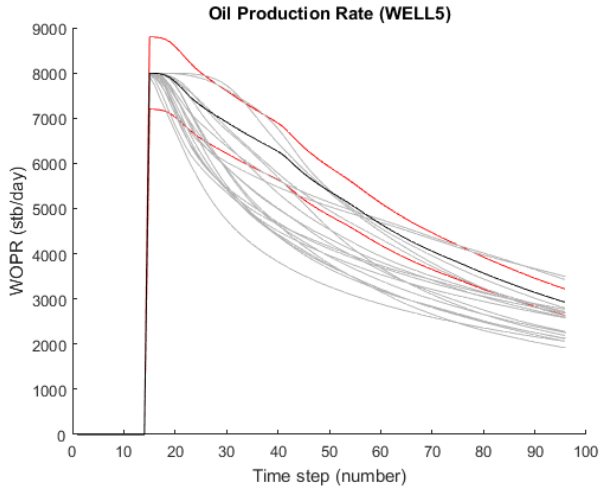
Oil Production Rate (WELL5)
WOPR (stb/day)
Time step (number)

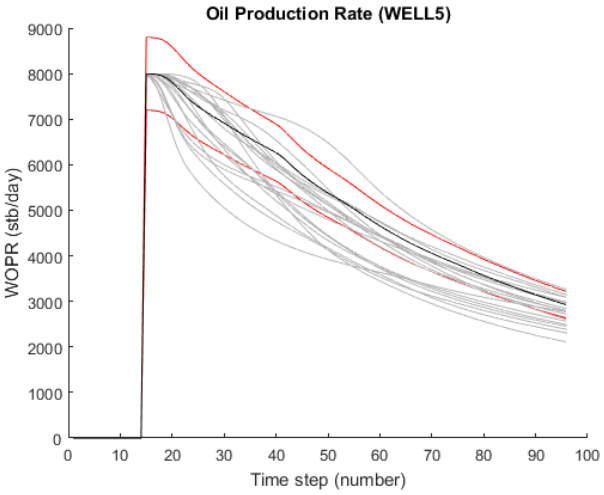
Oil Production Rate (WELL5)
WOPR (stb/day)
Time step (number)

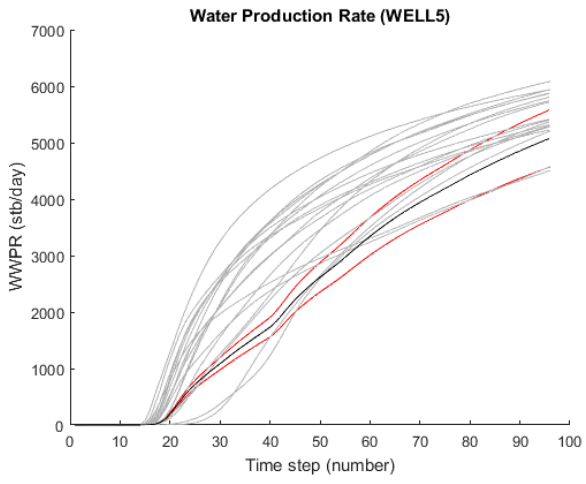
Water Production Rate (WELL5)
WWPR (stb/day)
Time step (number)

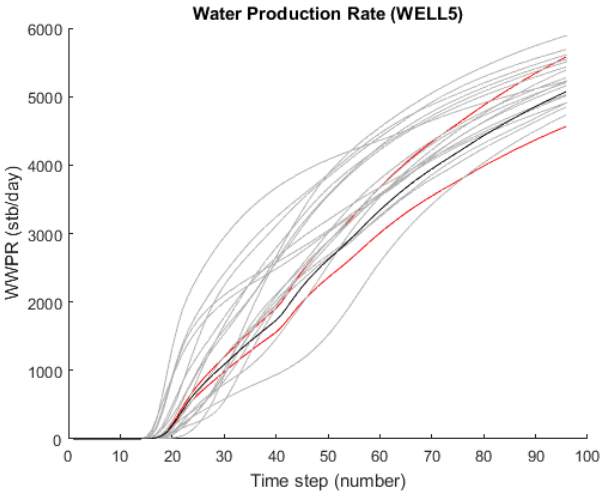
Water Production Rate (WELL5)
WWPR (stb/day)
Time step (number)

WELL 5A

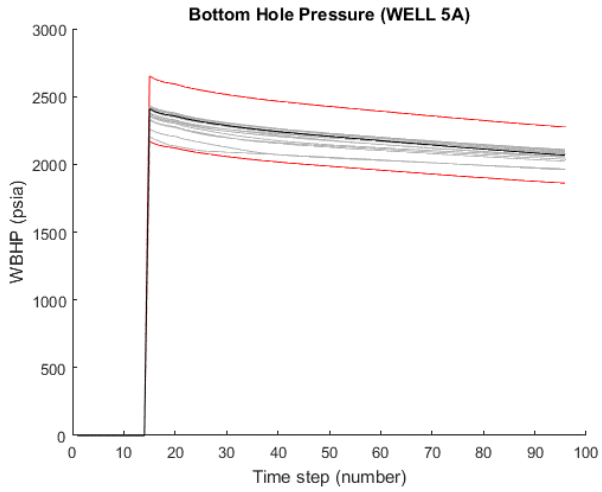
Bottom Hole Pressure (WELL 5A)
WBHP (psia)
Time step (number)

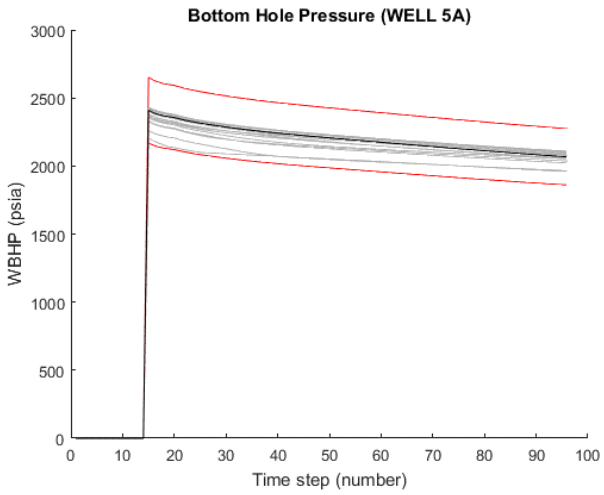
Bottom Hole Pressure (WELL 5A)
WBHP (psia)
Time step (number)

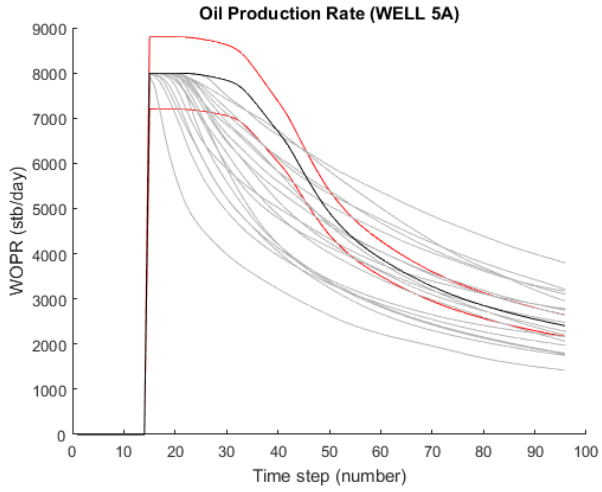
Oil Production Rate (WELL 5A)
WOPR (stb/day)
Time step (number)

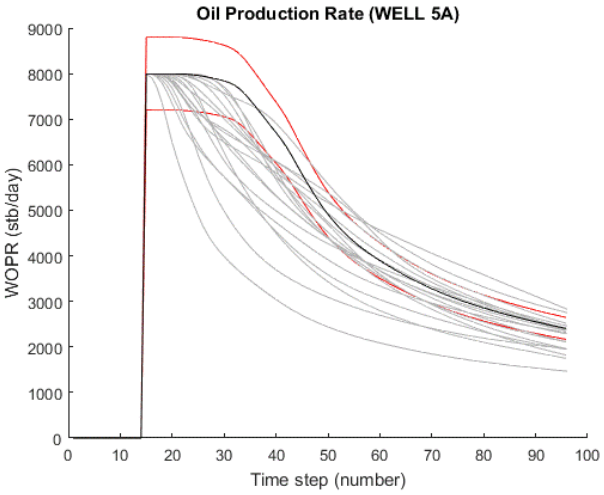
Oil Production Rate (WELL 5A)
WOPR (stb/day)
Time step (number)

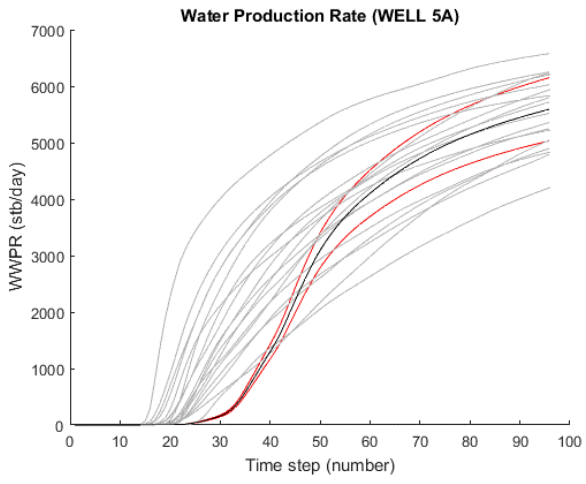
Water Production Rate (WELL 5A)
WWPR (stb/day)
Time step (number)

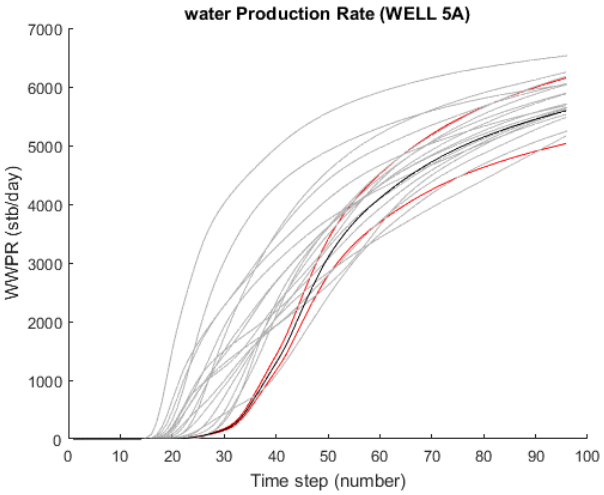
water Production Rate (WELL 5A)
WWPR (stb/day)
Time step (number)

WELL 6

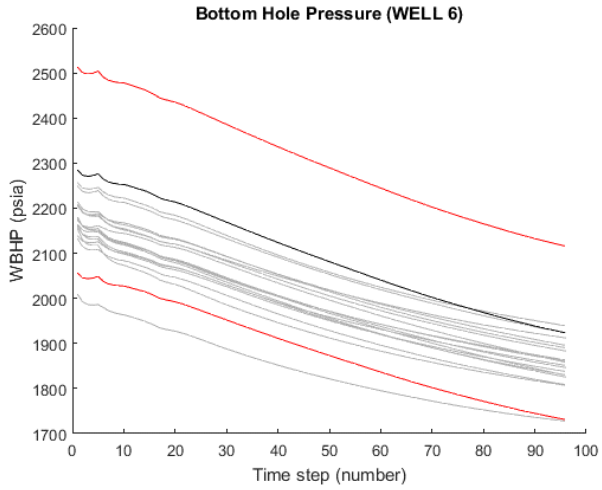
Bottom Hole Pressure (WELL 6)
WBHP (psia)
Time step (number)

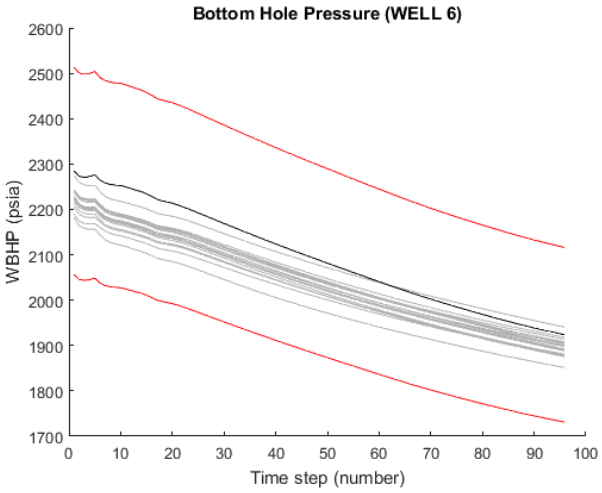
Bottom Hole Pressure (WELL 6)
WBHP (psia)
Time step (number)

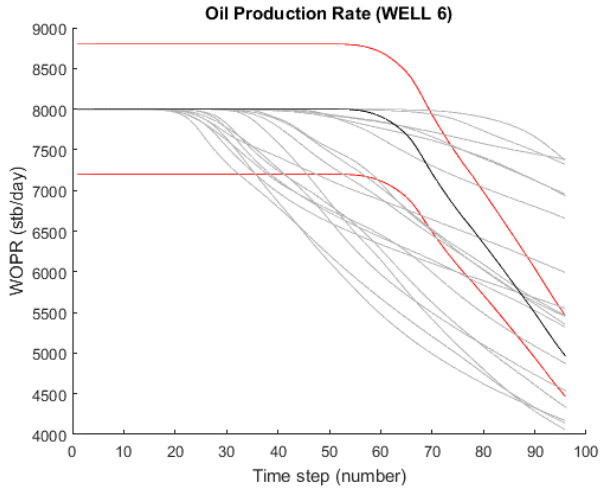
Oil Production Rate (WELL 6)
WOPR (stb/day)
Time step (number)

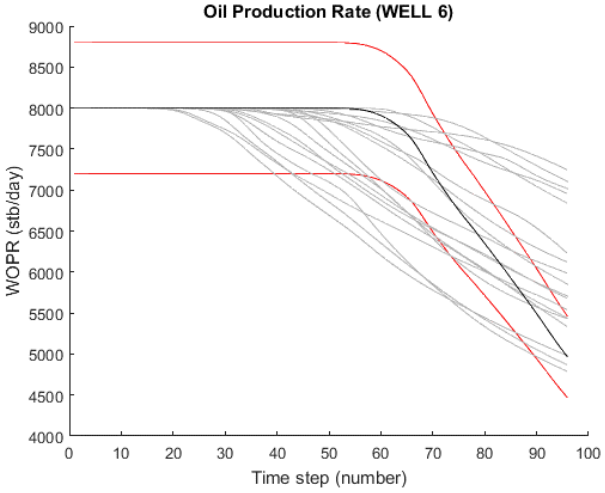
Oil Production Rate (WELL 6)
WOPR (stb/day)
Time step (number)

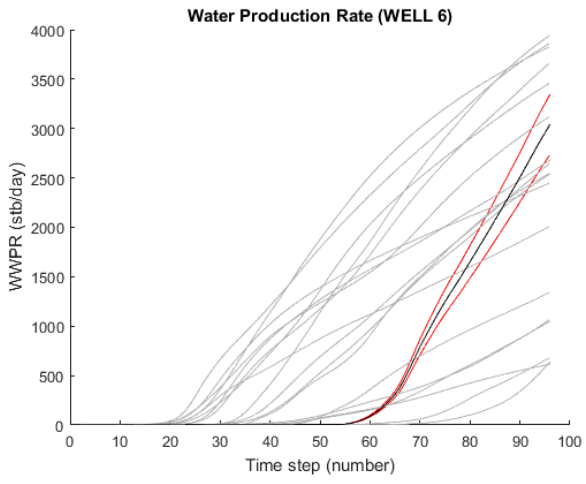
Water Production Rate (WELL 6)
WWPR (stb/day)
Time step (number)

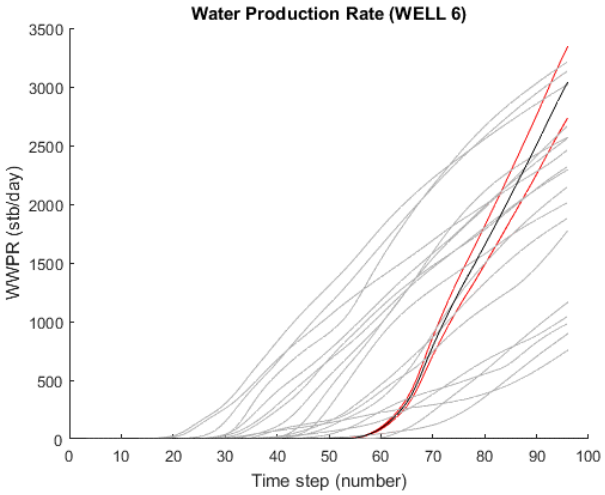
Water Production Rate (WELL 6)
WWPR (stb/day)
Time step (number)

WELL 7

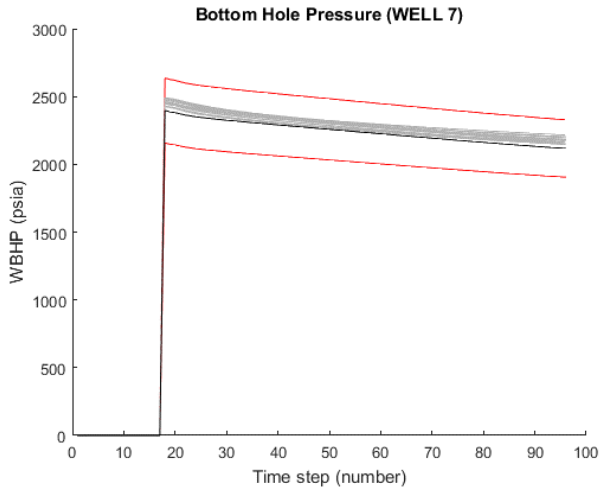
Bottom Hole Pressure (WELL 7)
WBHP (psia)
Time step (number)

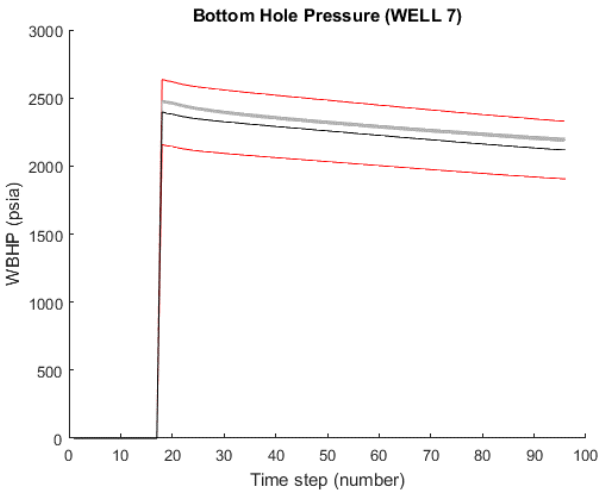
Bottom Hole Pressure (WELL 7)
WBHP (psia)
Time step (number)

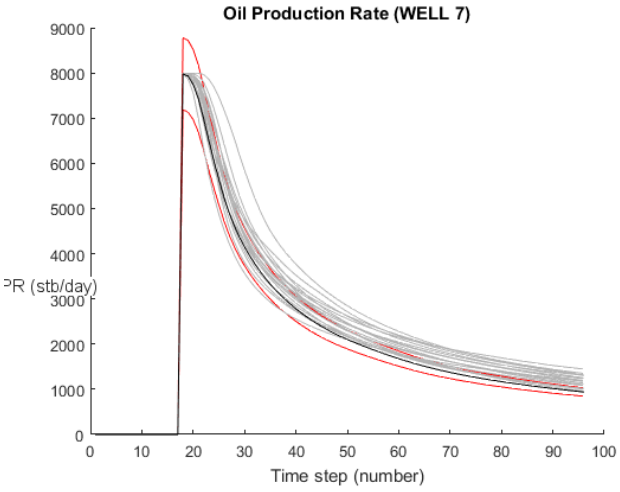
Oil Production Rate (WELL 7)
Time step (number)

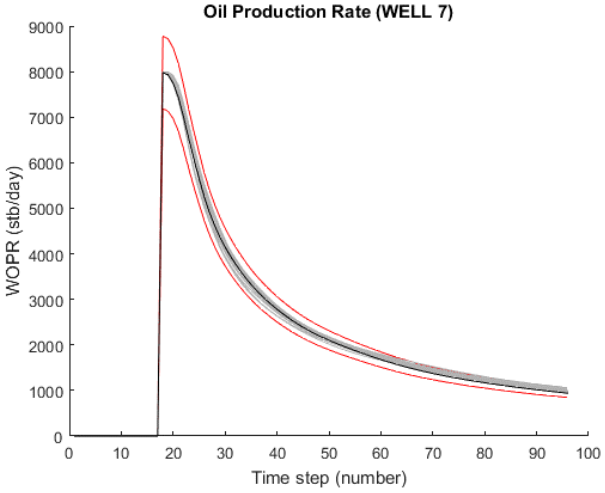
Oil Production Rate (WELL 7)
WOPR (stb/day)
Time step (number)

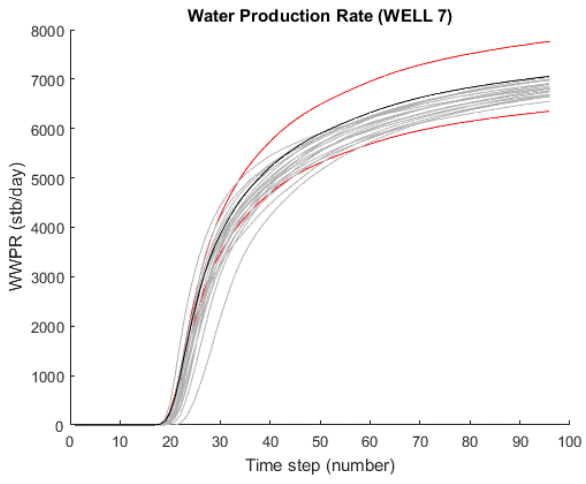
Water Production Rate (WELL 7)
WWPR (stb/day)
Time step (number)

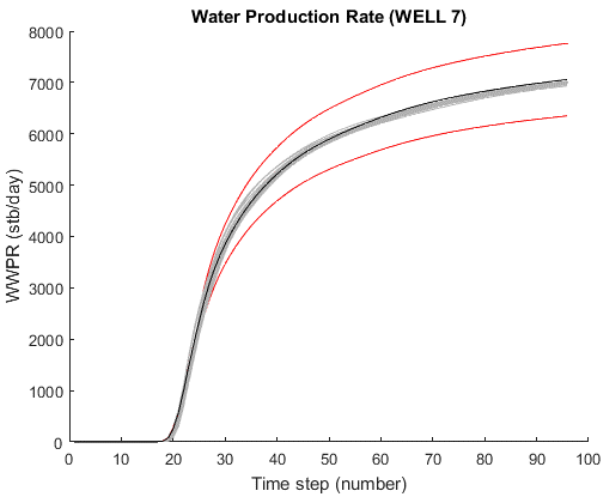
Water Production Rate (WELL 7)
WWPR (stb/day)
Time step (number)

WELL 8

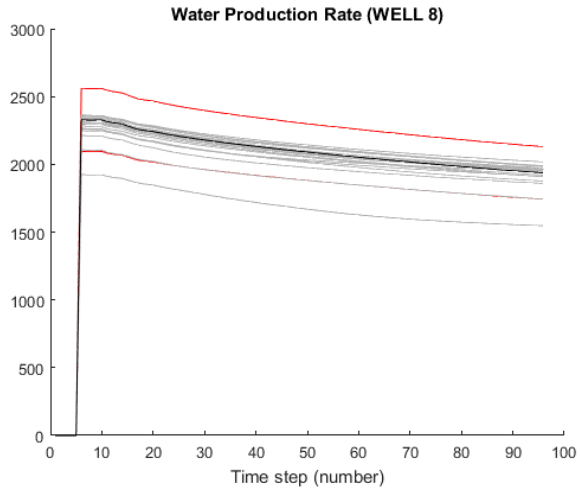
Water Production Rate (WELL 8)
Time step (number)

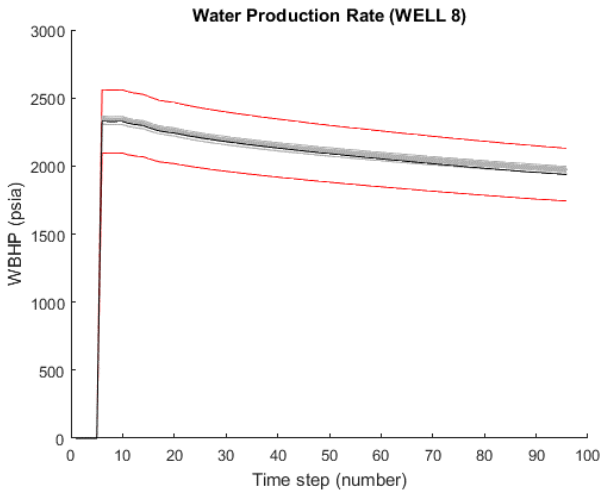
Water Production Rate (WELL 8)
WBHP (psia)
Time step (number)

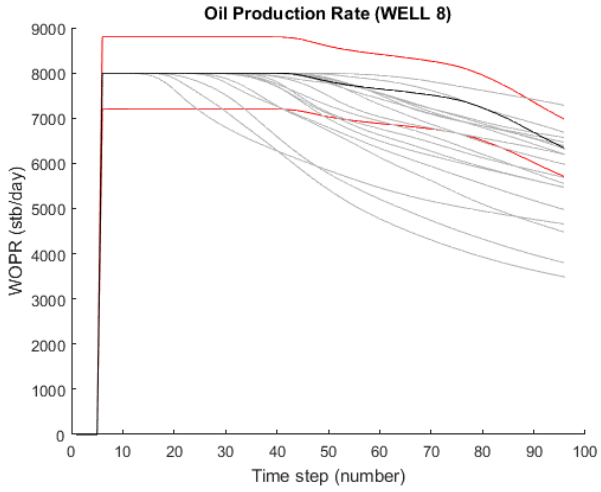
Oil Production Rate (WELL 8)
WOPR (stb/day)
Time step (number)

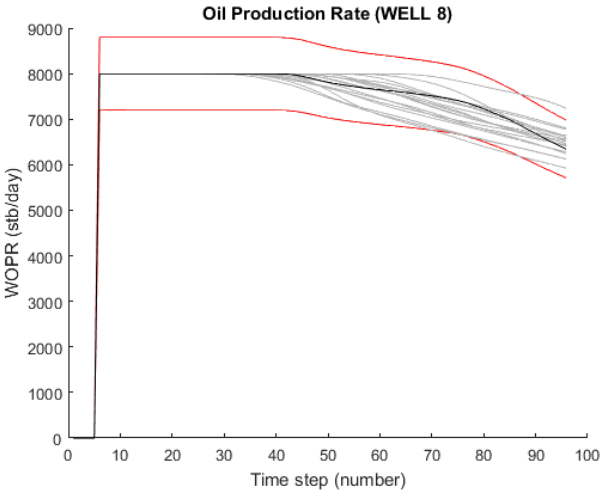
Oil Production Rate (WELL 8)
WOPR (stb/day)
Time step (number)

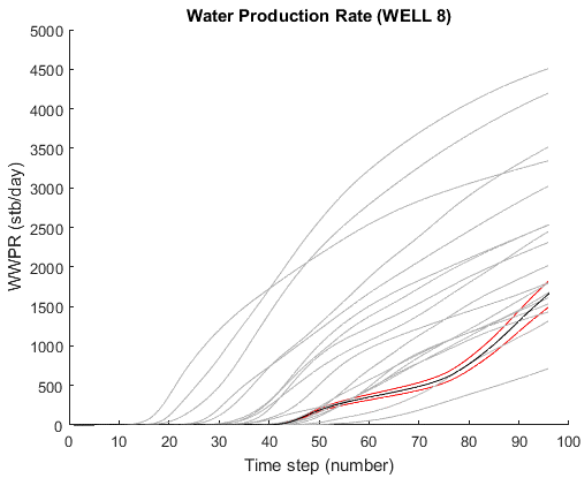
Water Production Rate (WELL 8)
WWPR (stb/day)
Time step (number)

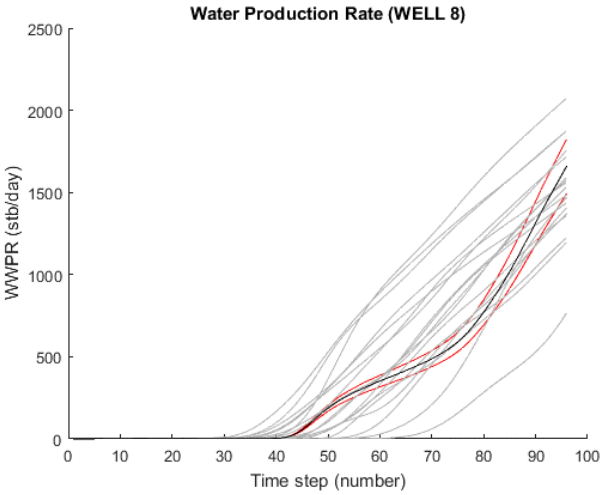
Water Production Rate (WELL 8)
WWPR (stb/day)
Time step (number)

WELL 9

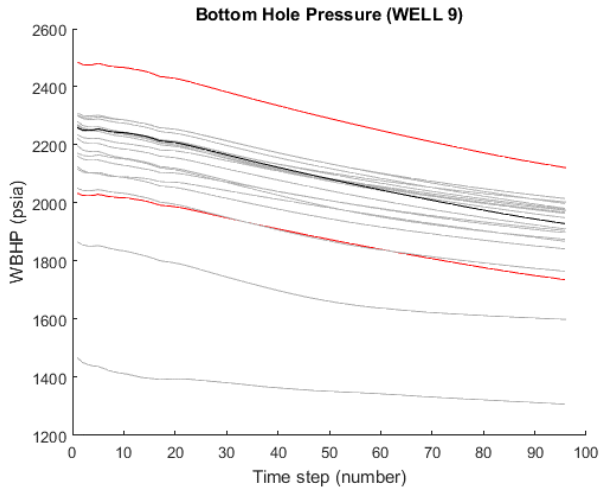
Bottom Hole Pressure (WELL 9)
WBHP (psia)
Time step (number)

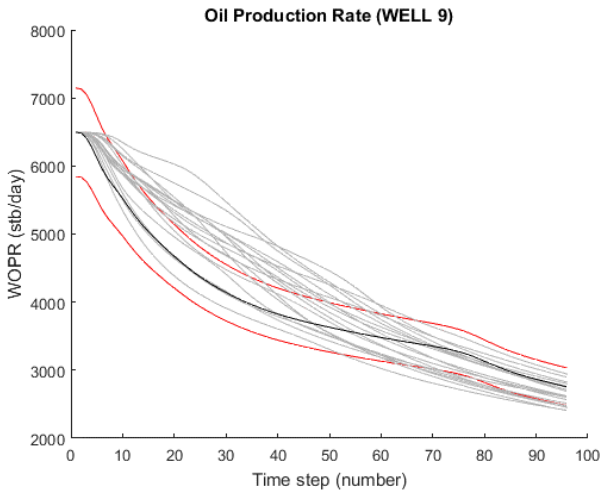
Oil Production Rate (WELL 9)
WOPR (stb/day)
Time step (number)

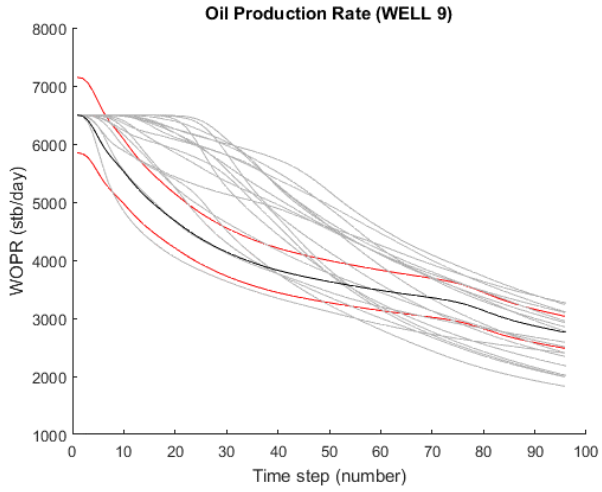
Oil Production Rate (WELL 9)
WOPR (stb/day)
Time step (number)

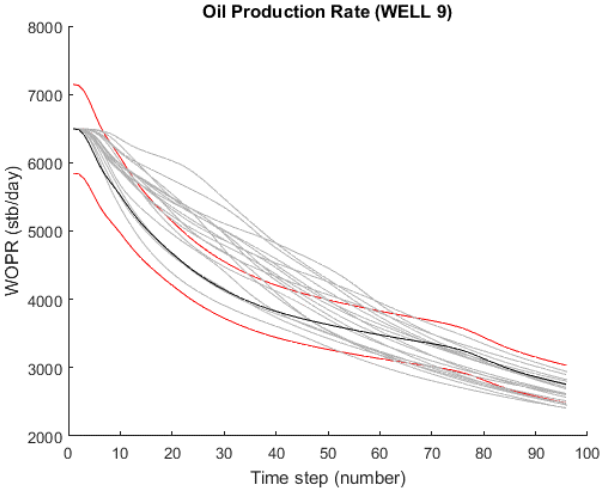
Oil Production Rate (WELL 9)
WOPR (stb/day)
Time step (number)

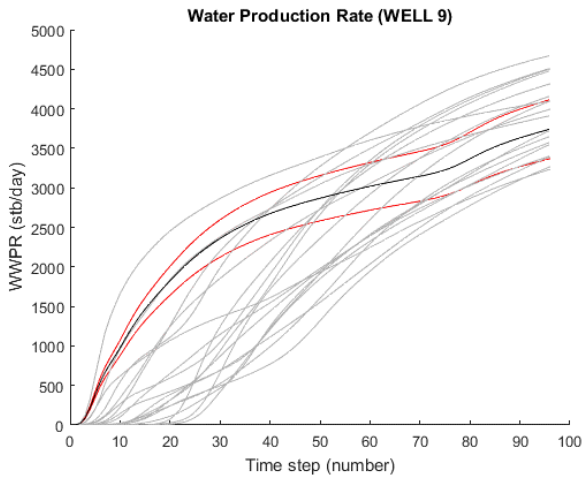
Water Production Rate (WELL 9)
WWPR (stb/day)
Time step (number)

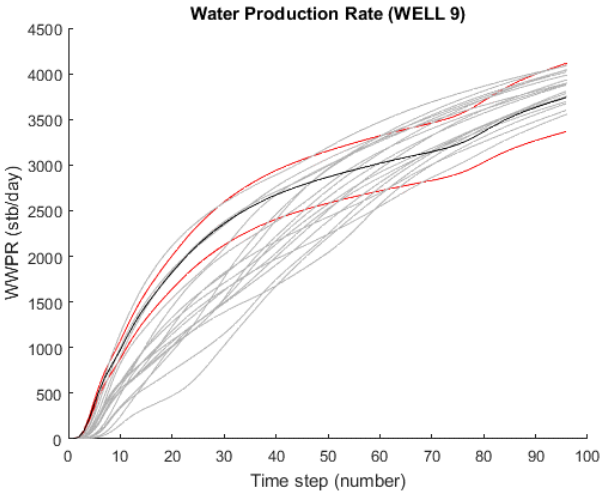
Water Production Rate (WELL 9)
WWPR (stb/day)
Time step (number)

WELL 10

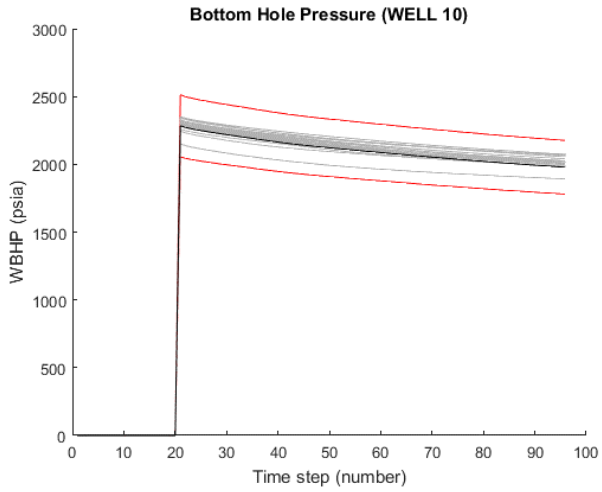
Bottom Hole Pressure (WELL 10)
WBHP (psia)
Time step (number)

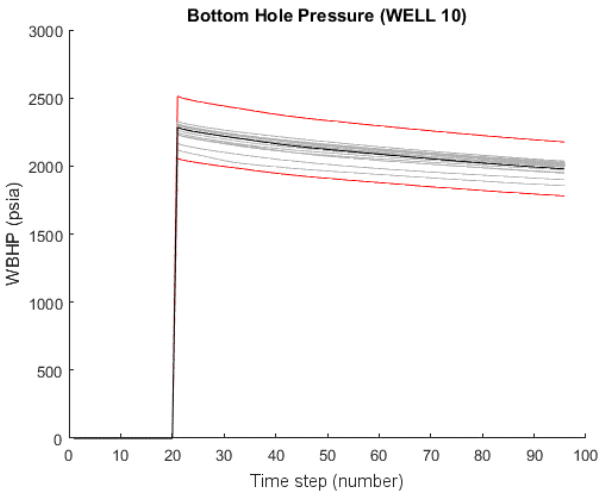
Bottom Hole Pressure (WELL 10)
WBHP (psia)
Time step (number)

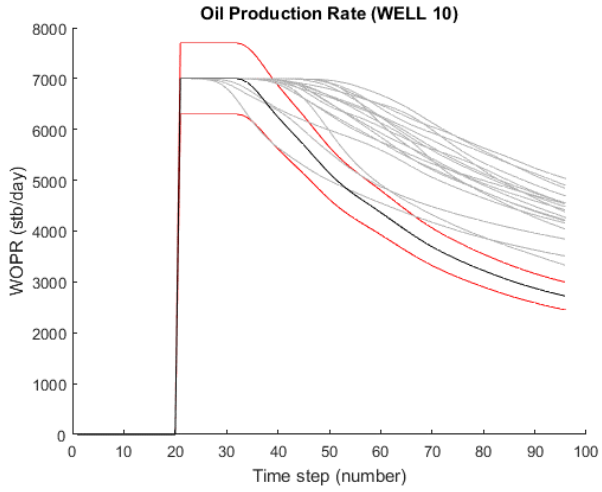
Oil Production Rate (WELL 10)
WOPR (stb/day)
Time step (number)

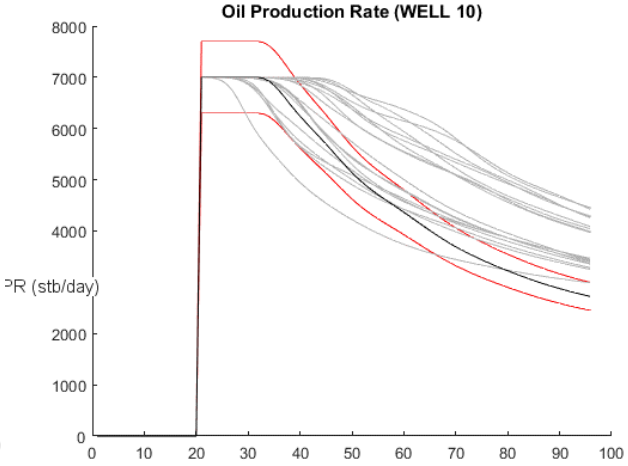
Oil Production Rate (WELL 10)
Time step (number)

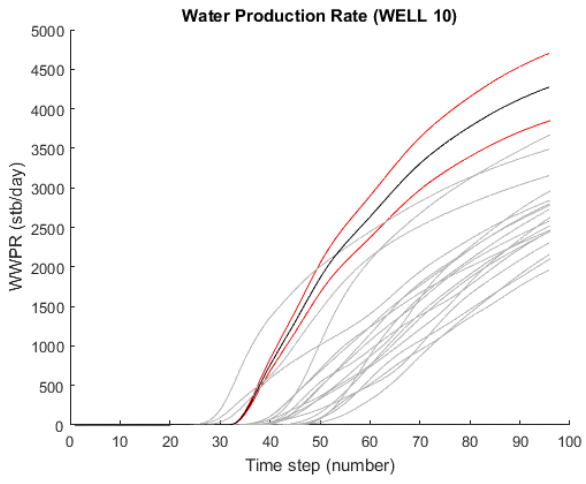
Water Production Rate (WELL 10)
WWPR (stb/day)
Time step (number)

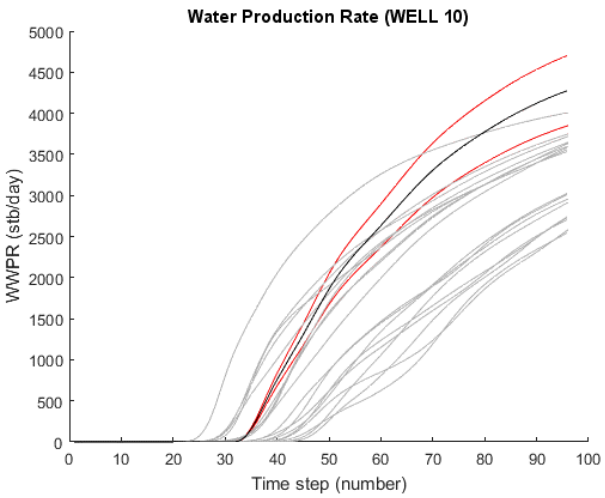
Water Production Rate (WELL 10)
WWPR (stb/day)
Time step (number)